MSc-thesis

Lessons learned from hydrological models for the improvement of climate model

Boyi Xie

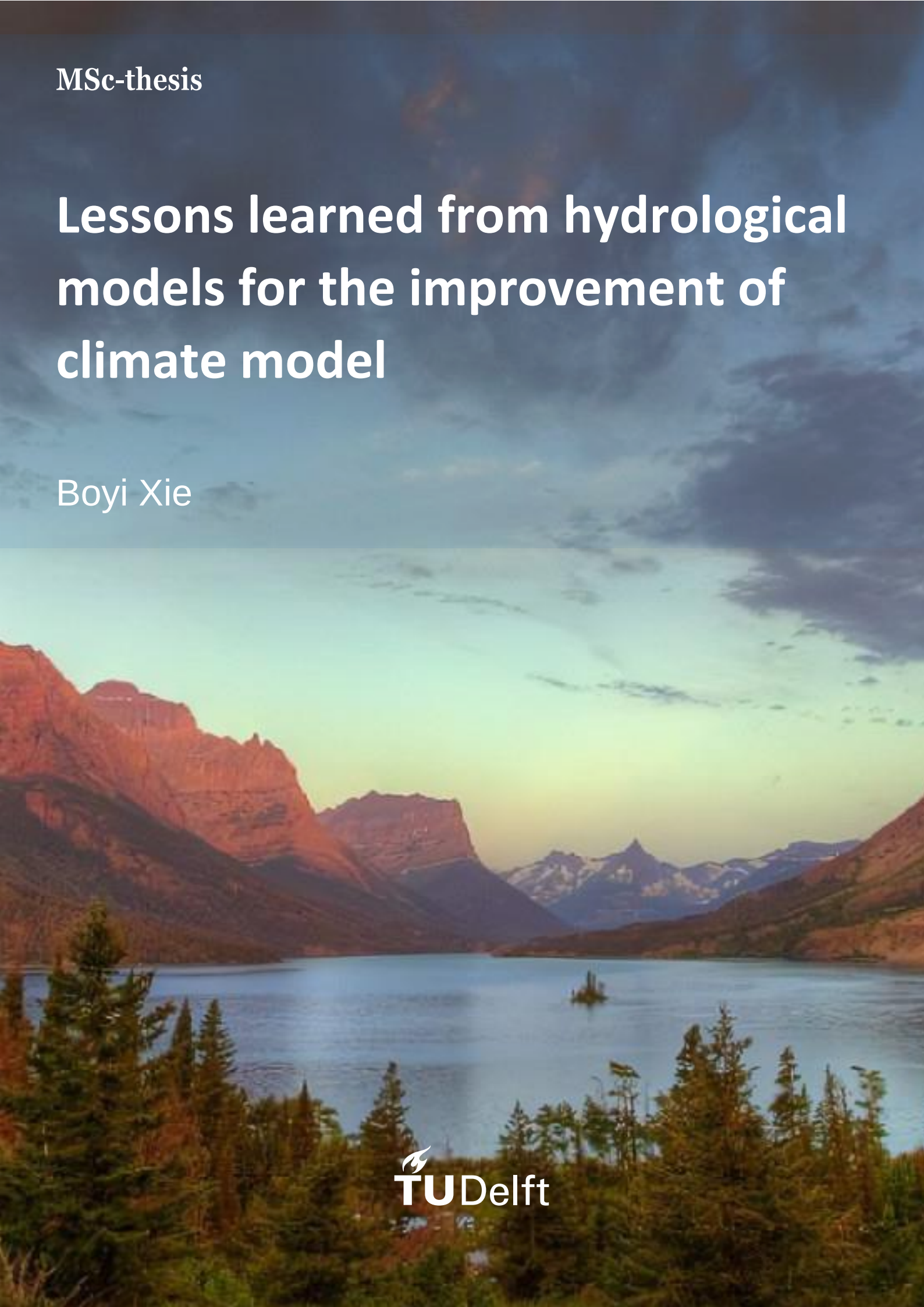

TU Delft

LESSONS LEARNED FROM HYDROLOGICAL MODELS FOR THE IMPROVEMENT OF CLIMATE MODEL

A thesis submitted to the Delft University of Technology
of the requirements for the degree of of

Master of Science

by

Boyi Xie

5087171

December, 7, 2021

Chairman:	Dr. ir. R.J.van der Ent	TU Delft
Thesis committee:	Ir. F.van Oorschot	TU Delft
	Dr. M.Hrachowitz	TU Delft
	Dr. ir. J.A.E.ten Veldhuis	TU Delft

TU Delft

SUMMARY

Hydrological models are designed to represent the interactions between the physical process and the water storage in short-term or long-term forecasting. The hydrological models in climate models (also know as Land Surface Models) aim to represent hydrological processes and interactions at a global scale. In this research, one Land Surface Model, HTESSEL is introduced. Previous studies have shown that HTESSEL is not reproducing hydrological fluxes well at a catchment scale. In this study, the problems in representing discharge in HTESSEL can be summarized in three aspects: mismatch in peaks, slower recession and the monthly delay. Thus, the aim of this research is to investigate the reasons of the poor performance in HTESSEL, and provide possible suggestions for a better fit. Therefore, the hydrological models HBV and GR4J (that operate on catchment scales) are introduced to identify the problems in HTESSEL by model comparison.

HTESSEL, HBV and GR4J models are used to simulate river discharge in 15 catchments are compared in terms of structure and parameterization. HTESSEL use tabulated parameter values, while HBV and GR4J are calibrated to match observations firstly. In order to investigate the influence of different model processes and parameters, a second calibration of the HBV and GR4J parameters is applied. Here, the model parameters are calibrated to the HTESSEL model output. Comparing the two calibration results, the parameter differences can be identified.

The results show that the soil column in HTESSEL is a key factor that influences the surface and subsurface runoff. On the one hand, HBV and GR4J can reproduce the slower falling limb in humid region by increasing their slow reservoirs. On the other hand, the top 50 cm of soil column is the effective depth that influences maximum infiltration rate. Thus, the changing of effective depth and the parameterization of orography variable b, which influences the fast runoff in HTESSEL, are necessary in temperate and mediterranean catchments.

According to this study, to solve the problem of mismatch in peaks this 50cm should be a spatial variable firstly. The increase of effective depth could overcome the overestimation in some places and the decrease of effective depth could overcome the underestimation of peaks in other places. In addition to effective depth, optimizing parameter b is also necessary, because it influences the fast runoff. Moreover, for the problem of slower recession and monthly delay, decreasing the size of soil column in HTESSEL is one way to get a better fit. Thus, in future, more study could focus on the interplay of the soil infiltration capacity and the fast runoff parameters. It might be helpful to improve the simulation.

CONTENTS

LIST OF FIGURES

LIST OF TABLES

1 INTRODUCTION

1.1 RESEARCH CONTEXT

Climate models play an important role in predictions of future temperatures, rainfall patterns, drought occurrence and flood events. As parts of climate models, Land surface models (LSMs) present hydrological processes and interactions between the subsurface, vegetation and the atmosphere. Besides this, Land surface models are also hydrological models with global scale.

In the short-term or long-term prediction, hydrological models are developed to simulate the interactions between the physical process and the water storage. The application of hydrological models can estimate how water moves in the catchment. Different hydrological models usually consist of similar functionalities of transmission, storage, and release of water in varying catchments (Fenicia et al. [2008]).

The Tiled ECMWF Scheme for Surface Exchanges over Land (TESSEL) was developed by Van Den Hurk et al. [2000]. TESSEL contains six land surface tiles, which includes low and high vegetation, bare ground, interception, shaded snow, and exposed snow. TESSEL chooses a single global soil texture to represent the real soil map. This leads to the deficient description of soil moisture and the runoff scheme (Balsamo et al. [2009]).

As one part of EC-EARTH climate simulations, the hydrology in the Tiled ECMWF Scheme for Surface Exchanges over Land(HTESSEL) is a revised model that overcomes the shortcoming of the identical soil texture and the lack of surface runoff in the simulation of hydrological process (Balsamo et al. [2009]).

While HTESSEL is not reproducing hydrological fluxes well, this is partly related to the representation of the root zone in this model (van Oorschot [2020]). Other parts of the hydrological cycle, e.g. the lack of groundwater representation, inappropriate parameterization could be a cause for the discrepancies between modeled and observed discharge. So, in this study, more research will be investigated in which aspects in HTESSEL need further attention, not only focus on the root zone.

In order to identify the errors of simulation in HTESSEL, catchment hydrological models GR4J and HBV are used. As a daily rainfall-runoff model, GR4J is one

of the soil moisture accounting models (Perrin et al. [2003]), which was also the last version of GR3J proposed by Michel [1989]. HBV model is the combination of routing routine of original HBV model with main buckets of FLEX model. Both of GR4J and HBV are popular lumped and widely used rainfall-runoff models (Perrin et al. [2003]).

Like HTESSEL, GR4J and HBV also show some similar structures or hydrological components, for example, the surface flow, subsurface flow, and root-zone storage. GR4J are based on four free parameters and two storages, while HBV works with eight free parameters and four storages, which representing different physical meaning. The identification of reasons of errors in hydrological model will be helpful to investigate what leads to the poor performance in HTESSEL. In this case, modeling comparison study is necessary and useful to explore the different causes of the errors in HTESSEL. The results of the HTESSEL model are affected by many factors, not only the model structures, but also its parameterization.

In this study, both land surface model and catchment hydrological models are hydrological models, the difference between them is that the former is at global scale, while the latter aims to predict at catchment scale.

1.2 RESEARCH QUESTIONS

The inadequate representation in HTESSEL shows some common problems in 15 catchments, when comparing with observation. In terms of the seasonality, there is a delay in rainy season in Tropical catchments and large bias in Mediterranean catchments. In terms of hydrograph, the main issues are smaller size of peaks and slower falling limb in HTESSEL. These problems usually lead to the missing or mismatch peaks in overall in HTESSEL.

To investigate the potential reasons of these problems in HTESSEL results, to find out what might be improved and to give the possible suggestions of the improvement, the results of GR4J and HBV could be a reference. Therefore, the main research question in this study is:

Which hydrological processes in HTESSEL could be improved to overcome poor performance of HTESSEL in modelling river discharge?

This overarching question can be split into other sub-questions.

- what aspects of the hydrographs are poorly represented by HTESSEL?
- HTESSEL, GR4J and HBV are all hydrological models. What are the differences in modelled discharge between HBV, GR4J and HTESSEL?

- Compared with observation data, what are the possible reasons that cause errors in HTESSEL?

2 METHODOLOGY

2.1 STUDY AREAS

The research focuses on 15 river catchments in Australia. These catchments are among different climatic regions. The vegetation coverage, soil moisture and root-zone storage also vary between different climate conditions. This is of interest for this study because modeling results usually will be significantly influenced by the climate and regions. Different but parallel study areas can compensate the modeling errors that caused by the lack of representation of climate.

These river catchments were selected based on three main standards (van Oorschot [2020]):

Size: The order of magnitude of the catchment area is of a gridpoint of 0.5° × 0.5° 2500 km2.

Location: The 15 catchments are distributed in different region with different soil type.

Streamflow:15 catchments keep the same length of time period, at least 25 years with no data gaps.

figure 2.1 is the map of 15 catchments. The main characteristics are in Table 2.1.

To investigate the relation between simulation results and model structure or parameterization, the 15 catchments could be mainly divided into 3 Tropical, Temperate and Mediterranean catchments, based on their climatic characteristics.

Tropical catchments contain catchments EA, EB, G, He, Mi, No and W. These catchments show the obvious rainfall seasonality. And their dry season are from May to October. Except G and EB, other catchments are covered with relative high vegetation. The soil types of catchments are mainly coarse, except G, Mi and W with median fine (van Oorschot [2020]).

Temperate catchments contain catchments A, D, Mu, Na and P. The seasonality in these 4 catchments is not obvious. Mediterranean catchments contain catchments K, R and Av.

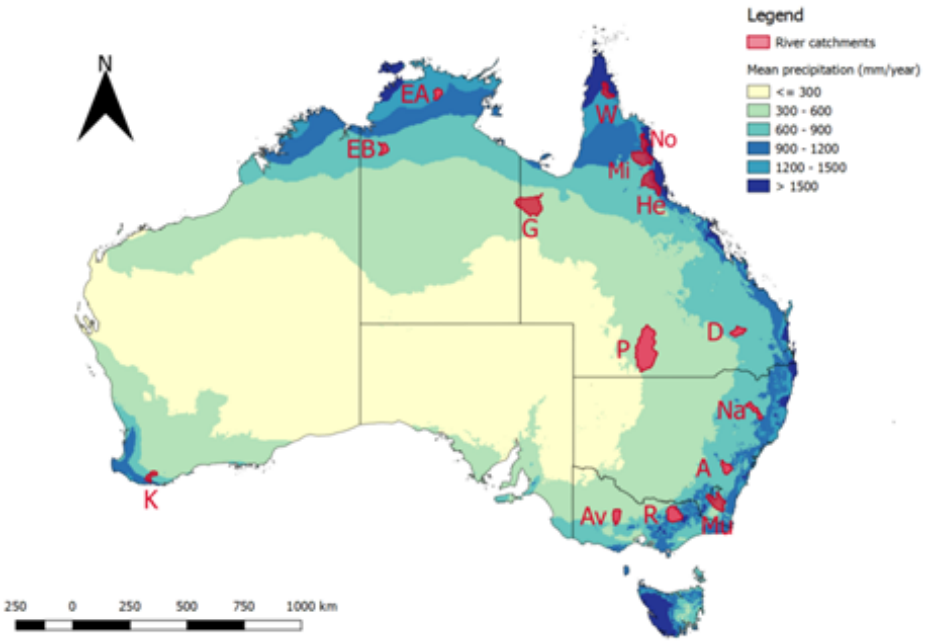

Figure 2.1: The annual mean precipitation in Australia (1961-1990) and the location of 15study catchments (van Oorschot [2020])

2.2 DATA

This study is based on the hydrological daily data in 15 catchments. The data mainly contains precipitation, potential evaporation, and discharge data and are implemented in three models. Other data, such as temperature, vegetation type and soil type are significant for the analysis of the modeling comparison.

The input precipitation data of hydrological models and temperature are collected from GSWP-3 dataset, representing the third phase of GSWP, which was established by Kim [2017]. Because there is no snow in study areas, the influence of snow data is limited and not taken into account. The vegetation data in Australia are collected from GLCC, the abbreviation of Global Land Cover Characteristics. The data of soil texture is obtained from FAO/UNESCO Digital Soil Map of the World (van Oorschot [2020]).

Potential evaporation data based on Hargreaves and Samani equation, which is derived from GSWP-3 temperature data. And the temperature data is based on the GSWP-3 dataset and radiation data at the top of atmosphere (ParisTech [2014], 2014). Actual evaporation is obtained from water balance.

Streamflow data is obtained from the Australian BoM (BoM [2015]). More detailed data could be downloaded from http://www.bom.gov.au/water/hrs/id=403221.

Catchment name	Catchment short name	Hydrological station	Coordinates	Climate	Area (km2)
Abercrombie River	A	412028	149.325°E, 33.955°S	Temperate	2631
Avoca River	Av	408200	143.299°E, 36.438°S	Mediterranean	2677
Dogwood Creek	D	422202B	150.179°E, 26.709°S	Temperate	2882
East Alligator River	EA	G8210010	133.332°E, 12.717°S	Tropical	2398
East Baines River	EB	G8110004	130.034°E, 15.766°S	Tropical	2443
Gregory River	G	912101A	139.252°E, 18.643°S	Tropical	12652
Herbert River	He	116006B	145.922°E, 18.491°S	Tropical	7487
Kent River	K	604053	117.087°E, 34.888°S	Mediterranean	1786
Mitchell River	Mi	919003A	144.290°E, 16.472°S	Tropical	7734
Murrumbidgee River	Mu	410761	149.101°E, 35.540°S	Temperate	5158
Namoi River	Na	419005	150.778°E, 30.678°S	Temperate	2532
Normanby River	No	105101A	144.839°E, 15.281°S	Tropical	2306
Paroo River	P	424201A	144.786°E, 28.689°S	Temperate	22885
Reedy Creek	R	403209A	146.345°E, 36.332°S	Mediterranean	5506
Wenlock River	W	925001A	142.638°E, 12.454°S	Tropical	3290

Table 2.1: Study catchments and geographical characteristics

2.2.1 Model overview

In this study, FLEX(HBV), GR4J, and HTESSEL are selected. Snow makes no contributions to the streamflow. And both of GR4J and new HBV are classical models that snow module is not active(Gaba et al. [2017]). This matches with the reality in Australia. Besides this, both of them are famous lumped models, which are same as HTESSEL. The implementation of HBV and GR4J can corresponds with the study areas of wide climate region. All of them are lumped models and have different free parameters that are used to determine the simulation result. The parametrization of real physical process summarizes and describes main features of flux. Apart from parameters, model structures are also significant to influeccne the simulated discharge. In this section, the main structure of models will be illustrated. According to Yang et al. [2020], Bouaziz et al. [2021], and Perrin et al. [2003], the comparison and main characteristics of three models are summarized and presented in figure 2.6.

HBV(FLEX)

This model is the combination of HBV and FLEX, hereinafter referred to as HBV. The main buckets of the model are FLEX-based model (Fenicia et al. [2008]). It has eight free parameters and four reservoirs. Unlike the various routines in original HBV model, this light model only retains the routing routine from HBV, which is the transformation function (Lindström et al. [1997]). The simulated discharge is routed at the outlet of the model. The snow module is not considered as well. figure 2.2 is the structure of this model. The description from Fenicia et al. [2008]

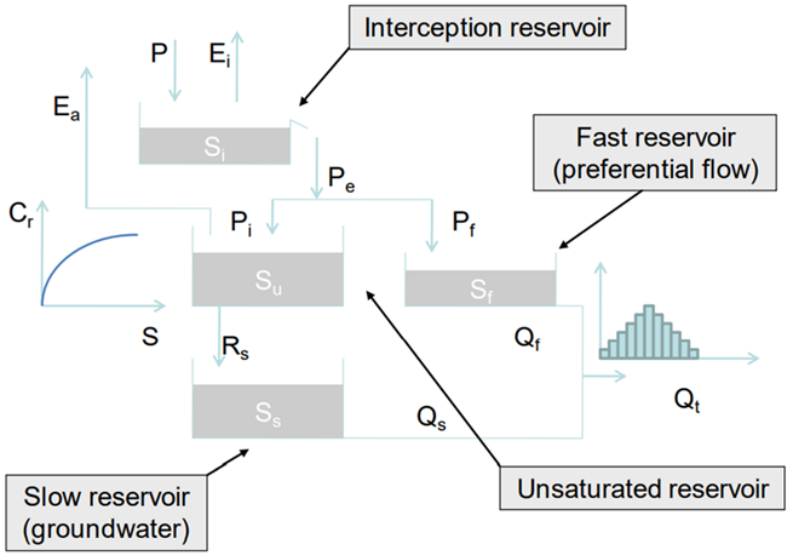

Figure 2.2: The main structure of FLEX(HBV) model

Parameter	Range	Unit	Description
Imax	(0, 10)	mm	Maximum interception capacity
Sumax	(40, 800)	mm	maximum soil moisture capacity in the root zone
Beta	(0.5, 10)	-	Shape factor of soil moisture function
Ce	(0.2, 20)	-	The fraction of transpiration on the soil moisture content.
Pmax	(0.001, 0.9)	mm/day	Maximum percolation capacity to the groundwater
Tlag	(0, 20)	days	Time lag
Kf	(0.001, 0.9)	days	Recession coefficient of fast reservoir
Ks	(0.0001, 0.9)	days	Recession coefficient of slow reservoir

Table 2.2: The range and description of parameters in HBV

and ranges of the parameters in this study are given in table 2.2.

GR4J

GR4J model is developed and improved by Perrin et al. [2003]. According to Wheater et al. [1993] or Young [2001], GR4J could be included in the hybrid metric-conceptual models. So the equation of GR4J are based on the empirical formula, and not all equations have clear physical meaning. figure 2.3 illustrates the GR4J model structures and parameters. Because snow is not considered in Australia, GR4J does not contain the snow module. The effective rainfall in routed via two branches with the fixed 90 percent and 10 percent, respectively. GR4J has 4 optimized parameters, 2 state variables and 2 reservoirs (Harlan et al. [2010]), of which the production store is the soil moisture accounting store. The range of parameters are given by Perrin et al. [2003] in table Table 2.3.

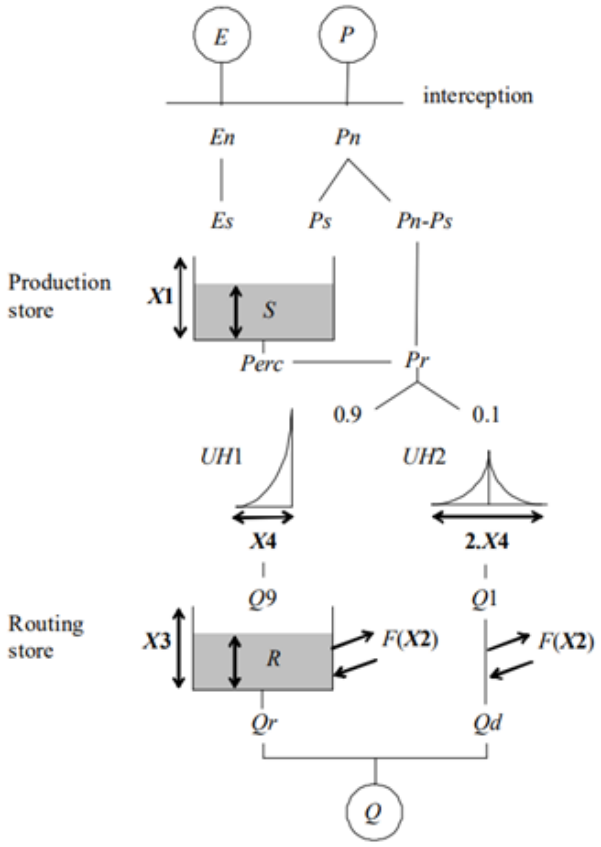

Figure 2.3: The GR4J model structure (Perrin et al. [2003])

	Property	Median value	80% Confidence interval	Unit	Description
X1	Parameter	350	(100, 1200)	mm	Maximum capacity of production store
X2	Parameter	0	(-5, 3)	mm/day	Ground water exchange coefficient
X3	Parameter	90	(20, 300)	mm/day	Maximum capacity of routing store of one day
X4	Parameter	1.7	(1.1, 2.9)	days	Time base of unit hydrograph UH1
S	State	-	-	mm	Production store level
R	State	-	-	mm	Routing store level

Table 2.3: The bounds of GR4J parameters and state variables

HTESSEL

HTESSEL land surface model is improved by Van Den Hurk et al. [2000] from TESSEL. figure 2.4 shows the main features of TESSEL and HTESSEL. HTESSEL is covered by 8 tiles: low vegetation, high vegetation, interception reservoir, bare ground, snow on groundlow vegetation, snow under high vegetation, open water and frozen water (ECMWF [2016]). Compared with TESSEL, HTESSEL introduce the infiltration and runoff schemes. HTESSEL contains 2 reservoirs, the interception reservoir and the root-zone reservoir. Not only the simulation of hydrological process will be included in this model, the influence of vegetation type, soil type, root distribution etc. are significant.

2.2.2 Model differences and similarities

This part will highlight and compare the main model structures in 3 hydrological models. Their differences and similarities will be described as below. According to the researches of Nijzink et al. [2016], Lindström et al. [1997], Perrin et al. [2003] and van Oorschot [2020], main characteristics and equations are summarized in figure 2.6. The symbols used are listed in table 2.4.

Model storage

HBV, GR4J and HTESSEL contain 4, 2 and 2 buckets respectively, representing their model storages. The simple scheme could be found in Figures 2.5. GR4J, HBV and HTESSEL have the interception module. But they show a different pattern. In GR4J, the interception storage is considered as zero capacity and it used in the determination of net precipitation (Pn) and net evapotranspiration capacity (En) (van den Brink [2018]). If the precipitation (P) is larger than the potential areal

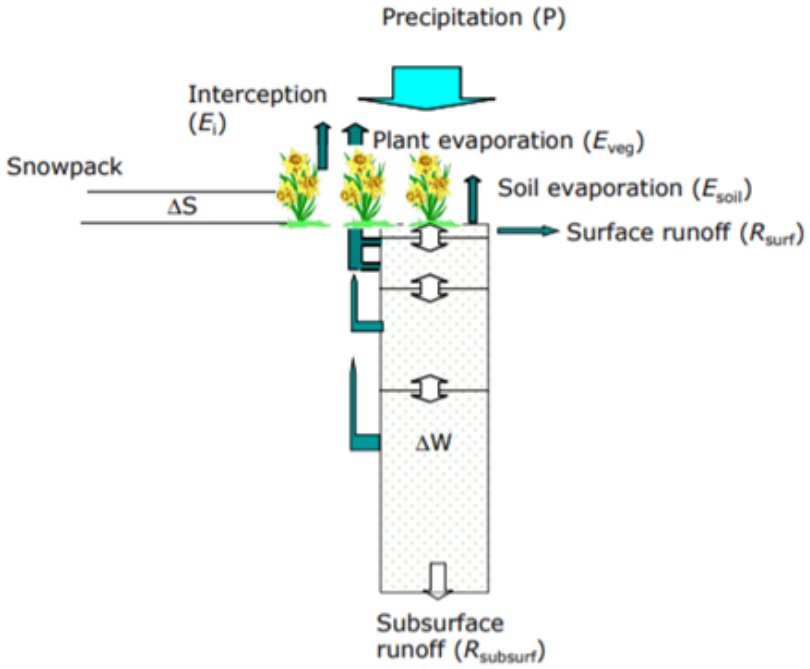

Figure 2.4: The land surface scheme HTESSEL (Wipfler et al. [2011])

evapotranspiration (E), net precipitation is computed as the subtraction of E from P, the equation is presented below in euqation 2.1:

$$\begin{aligned} If \quad & PE, then \quad P_n = P - E \quad and \quad E_n = 0 \\ & otherwise, P_n = 0 \quad and \quad E_n = E - P \end{aligned} \tag{2.1}$$

In HBV, the interception storage(equation 2.2) is determined by the interception evaporation (E_i) and effective rainfall (P_e). If rainfall is larger than 0, new interception reservoir need subtract the effective rainfall. If there is no rainfall, this is done by subtracting the interception evaporation.

$$\begin{aligned} &IfP > 0, S_i, new = S_i, old - P_e \\ &IfP > 0, S_i, new = S_i, old - E_i \end{aligned} \tag{2.2}$$

In HTESSEL, the interception reservoir is one of the tile coverages. It has a small capacity I_max, which is approximately 1 mm (ECMWF [2016]). When water flows in and out the storage, usually it represents the similar process in hydrological models. One of most important common storage is the rootzone water storage.

HBV model set calibrated parameter S_{umax} to limit the unsaturated storage, or the rootzone storage. However, this storage in GR4J was limited by one state variable, called production storage S (Perrin et al. [2003]). Like HBV, the water limit in GR4J could be adjusted during the simulation and calibration process, although the production storage is not the free parameter. Except the I_max and $S_{u,max}$, the

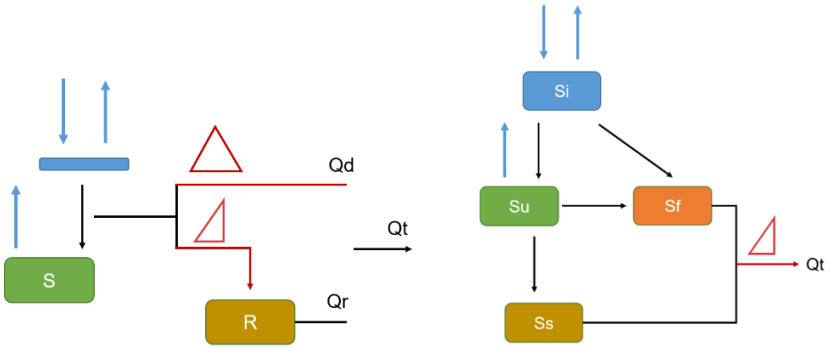

(a) The scheme of GR4J

(b) The scheme of HBV

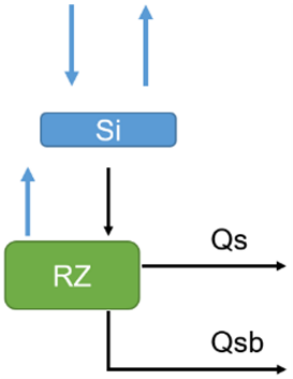

(c) The scheme of HTES-SEL

Figure 2.5: The scheme of 3 models.(The blue arrows mean the precipitation and evaporation. Black and red arrows represent the flow direction. Read triangles are the routing. Green box is the root-zone storage. Orange box is the fast reservoir. Brown box is the slow reservoir. Blue box is the interception reservoir.)

remaining reservoir are not controlled by the storage capacity in HBV.

The two stores in GR4J are non-linear stores (Perrin et al. [2003]), contrary to HBV, which apply linear reservoir. And these two stores are controlled by two parameters. Whether it's in GR4J or HBV, the root-zone storage of both model uses one parameter to limit the water content which could be stored in root-zone.

In HTESSEL, this capacity is SR, the rootzone storage capacity, which is not a calibrated parameter. It is the vegetation accessible water. The reservoir in HTESSEL is divided into four layers (Blondin [1991]). When the rainfall infiltrates and recharges the soil, the water above the field capacity will drain out. The rootzone storage capacity in HTESSEL is defined with then fixed modeling soil depth, which is 2.89m, times vegetation available water ($\theta cap - \theta pwp$) (ECMWF [2016]). θcap is the soil water content at field capacity, θpwp represent the wilting point in soil.

Model discharge

Most of time, rainfall will be routed to generate the discharge. In HBV, this process can be realized by the transfer function with the parameter Tlag. Routing process can reflect how quick the streamflow response to the precipitation. GR4J use the linear routing with unit hydrograph and split the effective rainfall Pr into 2 components with the fixed fraction: 90% of Pr is routed by unit hydrograph UH1 and used for the generation of subsurface flow, the remaining 10% of Pr is routed by unit hydrograph UH2 and used for the generation of surface flow (Perrin et al. [2003]). While in HTESSEL, the routing process is absent.

The internal flows in HBV show clear physical meaning, based on the flexible and apparent storage bucket. The total discharge mainly consists of the fast and slow flows. But this process separation is more abstract and ambitious in GR4J.

In HTESSEL, when the rate of surface flux is larger than the maximum infiltration rate in the soil, then surface runoff will be generated. Due to the only one bucket in HTESSEL, when water flux enters the soil and infiltrate downwards, water leaves the system from the fourth layer in the rootzone and generates the subsurface runoff. Apart from layer four, if the moisture exceeds the saturation in any layer, it can also generate the subsurface flow.

Symbol	Unit	Description
EP	mm/day	Potential evaporation
EI	mm/day	Interception evaporation
EA	mm/day	Total actual evaporation (sum of soil evaporation, transpiration, (separate) interception and, if applicable, sublimation
ET	mm/day	Transpiration and soil evaporation
PR	mm/day	Precipitation entering the root-zone storage (after snow and/or interception if present or fraction/total precipitation)
Pe	mm/day	effective precipitation
QR	mm/day	Flux from root zone to fast and/or slow runoff storage
QP	mm/day	Percolation flux from root-zone storage to slow runoff storage
ST	mm	Total storage
SI	mm	Interception storage
SR	mm	Root-zone storage
SF	mm	Fast runoff storage
SS	mm	Slow runoff storage
LP	-	Threshold of relative root-zone storage above which ER = EP
a	kgm^3	Air density
rc	sm^1	Canopy resistance
ra	sm^1	Air resistance
qL	-	Humidity
Q_s**at**	-	Saturated humidity
Tsk	centigrade	Tile skin temperature

Table 2.4: The description of symbols in HBV, GR4J and HTESSEL

	GR4J	HBV(FLEX)	HTESSEL
number of calibrated parameters	4	8	-
Represented catchment stores	2	4 All are linear storage	2
Represented flow component/routing mechanism	90% is routed by a UH and then a non-linear routing store, and 10% are routed by a single UH	Surface runoff, Interflow, Base flow; a single UH routing	Surface runoff, subsurface runoff; No routing
Lumped(L)/semi-Lumped(S)/ distributed(D)	L	L	L
interception storage	0	Linear reservoir	1 mm
Root-zone storage S_R			
Separate root-zone module with capacity $S_{R,max}$	√	√	√
Storage balance	$dS_R/dt = P_R - E_R - Q_R$	$dS_R/dt = P_R - E_R - Q_R - Q_P$	$dS_R/dt = P_R - E_R - Q_R$
	$S_T = S_R + S_S$	$S_T = S_I + S_R + S_F + S_S$	$S_T = S_R + S_I$
Main characteristics describing evaporation process			
Interception evaporation E_I	0	$E_I = \begin{cases} E_P, & \text{if } SI > 0. \\ 0, & \text{otherwise.} \end{cases}$	$E_I = \begin{cases} E_P, & \text{if } E_P dt < S_i. \\ \frac{S_i}{dt}, & \text{if } E_P dt \geq S_i \end{cases}$
Transpiration and soil evaporation ET	$E_T = E_P \cdot \frac{\bar{s}_R \cdot (2 - \bar{s}_R)}{1 + E_P / s_{R,max} \cdot (2 - \bar{s}_R)}$	$E_T = \begin{cases} (E_P - E_I) \cdot \frac{\bar{s}_R}{L_P}, & \text{if } \bar{s}_R < L_P. \\ E_P - E_I, & \text{otherwise.} \end{cases}$	$\overline{E}_T = \overline{P}_e - \overline{Q}$ $E_T = E_P \frac{\overline{E}_T}{\overline{E}_P}$
Total actual evaporation EA	$E_A = E_R + E_I$	$E_A = E_R + E_I$	$E_A = E_R + E_I$

Figure 2.6: Parameters and main characteristics, storage and balance equations inGR4J, HBV and HTESSEL

2.3 MODEL CALIBRATION AND MODEL TEST

Hydrological model is a simulation of the real hydrological process, so the modeling errors are inevitable. In this study, models are calibrated and validated on daily scale. Nash-Sutcliffe Efficiency is used as the objective function.

The adjustment of parameters on HTESSEL is restricted in this study. So the modeling comparison will be conducted in an indirect way. In the first step, three models make use of the same input data to create one set of outputs, mostly discharge, known as Q1. Model parameters in GR4J and HBV are calibrated to observations while HTESSEL uses tabulated parameter values. In the second step, the output discharge of HTESSEL is then used as the input streamflow in GR4J and HBV, and calibration based on the output discharge of HTESSEL generating in the first step. Anther group of outputs is produced, called Q2. During this process, all catchment utilize the same sampling method. Among 10,000 sets, only 50 best parameter set are selected for further comparison. Here, 50 best means the highest 50 NSE among 10,000 NSE values. NSE is used as an integrated value to evaluate the performance of hydrograph. However, in modeling comparison research, different parameter sets probably result in the similar outputs. So the ranking of NSE and selection of 50 best NSEs are reasonable, to reduce the problem of equifinality. The process is in table 2.5

	Based on observation	**Based on HTESSEL**
Model	GR4J, HBV	GR4J, HBV
Input	P, EP, $Q_{observation}$	P, EP, $Q_{HTESSEL}$
Monte Carlo Sampling	10,000 times	10,000 times
Output	Q1	Q2

Table 2.5: Two calibration approaches

Monte Carlo sampling is set to generate 10,000 parameter sets randomly both in GR4J and HBV. HTESSEL is uncalibrated. The threshold of sampling results is defined by NSE and is used as the objective function to evaluate the performance of 3 models. To keep the water balance and catchment closed, the water constrain is also introduced during the Monte Carlo sampling, see equation 2.3. WC means water constraints. It is the water deviation between the total amount of observed discharge and the modeled discharge. For instance, the WC could be set to 5% or 15% in Monte Carlo sampling. Here, 15% is selected. It indicates that the selected parameter set need to be larger than the threshold of NSE and lower than the water constraints. Only both requirements are satisfied, the current parameter set will be

retained. For example, the NSE is larger than 0.5 and the absolute value of errors of water constraints is smaller than 5%.

$$WC = \left| \frac{\sum_{i=1}^{n} Q_{s,i} - \sum_{i=1}^{n} Q_{o,i}}{\sum_{i=1}^{n} Q_{o,i}} \right| \tag{2.3}$$

The function of NSE is equation 2.4. Where Q_s, i refers to simulated discharge,Q_o, i is the observed discharge. $\overline{Q}_o, i$ is the average value of observed discharge.

$$NSE = 1 - \frac{\sum_{i=1}^{n} (Q_{s,i} - Q_{o,i})^2}{\sum_{i=1}^{n} (Q_{o,i} - \overline{Q}_{o,i})^2} \tag{2.4}$$

NSE provides the insight of high flow, while the logarithm of NSE capture more information at the low flow. See euqation 2.5

$$logNSE = 1 - \frac{\sum_{i=1}^{n} (logQ_{s,i} - logQ_{o,i})^2}{\sum_{i=1}^{n} (logQ_{o,i} - log\overline{Q}_{o,i})^2} \tag{2.5}$$

Other performance matrix are applied in the model to describe the errors from different aspects. PBIAS refers to the percentage of the simulated discharge below or above the observed discharge. For PBIAS value, the closer to zero, the more accurate of the simulation results. Positive PBIAS means the underestimation of the modeling results, while negative value indicates an overestimation of simulated values (Gupta et al. [2009]). The calculation follows the formula below:

$$PBIAS = \frac{\sum_{i=1}^{n} (Q_{O,i} - Q_{S,i})}{\sum_{i=1}^{n} (Q_{o,i})} \times 100 \tag{2.6}$$

RMSE represents the root mean squared error and n is the length of calibration or model test period. Like NSE, the RMSE also emphasize the performance in high flows(Clark et al. [2008]).

$$RMSE = \sqrt{\frac{1}{n} \sum_{i=1}^{n} (Q_{s,i} - Q_{o,i})^2} \tag{2.7}$$

R indicates the linear correlation coefficient, which is also known as Pearson's correlation coefficient. R reflects the bias of peaks or the degree of mismatch of peaks of the hydrograph. The range of R is from -1 to 1. When R=0, it means there is no relationship between observation and simulation; When R = -1, it represents the inverse relationship between observation and simulation. When σ_s and σ_o indicate the standard deviation of simulations and observations (Moriasi et al. [2007]).

$$R_{Q_o,Q_s} = \frac{cov(Q_o - Q_s)}{\sigma_o \sigma_s} \tag{2.8}$$

2.4 TIME AND SPATIAL RESOLUTION OF MODEL SIMULATIONS

All data are implemented in HTESSEL land surface model from 1973-2010. The output of HTESSEL is used to compare with the GR4J and HBV. Not only the discharge output of three models, but also the interflow output. Calibration is carried out in 15 catchments from 1973 to 2000, and the model test period(usually was called validation period) is selected from 2000-2010. Each catchment applies the Monte Carlo sampling mentioned in Section 2.3. Because the validation means the model can be proved if is a correct model or a wrong model. But actually it's impossible to prove it. So the words model test is more rigorous than validation.

3 RESULTS

3.1 HYDROLOGICAL MODEL PERFORMANCE IN 15 CATCHMENTS

In this research, the input data is performed in 3 models, but only GR4J and HBV are implemented. The performance matrix is presented and explained in this section. The bounds of the model parameters are given in Section 2.2.1.

3.1.1 Calibration

	Calibration			Model test		
	Tropical	**Temperate**	**Mediterranean**	**Tropical**	**Temperate**	**Mediterranean**
HBV	0.397	0.396	0.229	0.368	0.059	-0.544
GR4J	0.345	0.339	0.502	0.334	0.255	0.423
HTESSEL	-0.411	-2.052	-5.701	-0.112	-4.279	-7.215

Table 3.1: The average NSE of calibration(1973-2000) and model test(2000-2010) in HBV and GR4J, and the performance in HTESSEL

Calibration is a process that select the optimal parameter set automatically. In this section, the objective function is chosen NSE, which evaluates the model performance in an integrated value. On average, the calibration results are better than model test results. Table 3.1 shows the average performance evaluated by NSE in GR4J and HBV models. But here only GR4J and HBV are actually calibrated and validated. HTESSEL is chosen the same time series as GR4J or HBV, and make use of NSE and Log-NSE as model performance. The More calibrated discharge are presented in Section A.2.

3.1.2 Model test

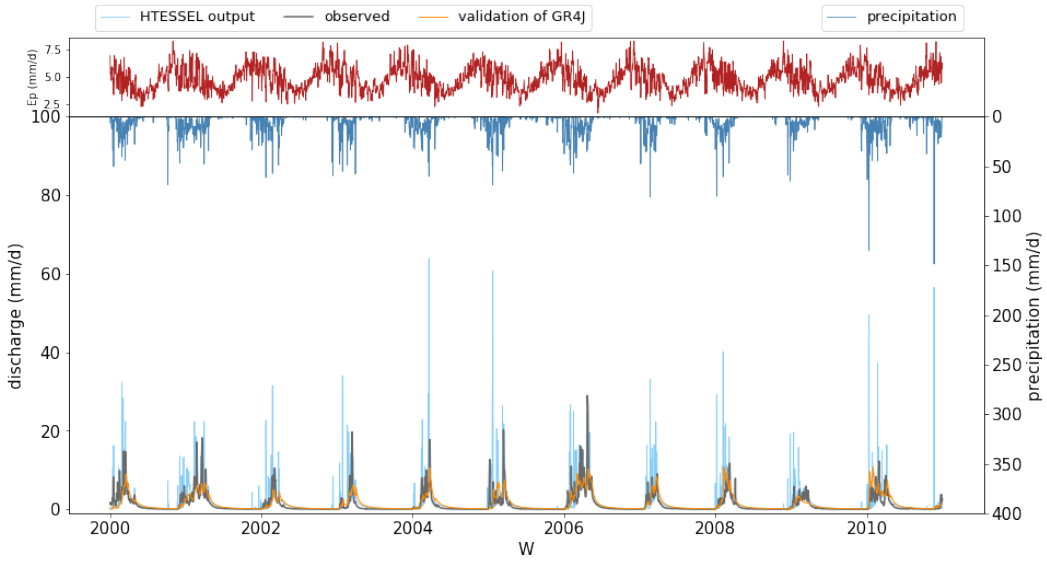

Figure 3.1: The simulation by GR4J and observed results in catchment W in model test period

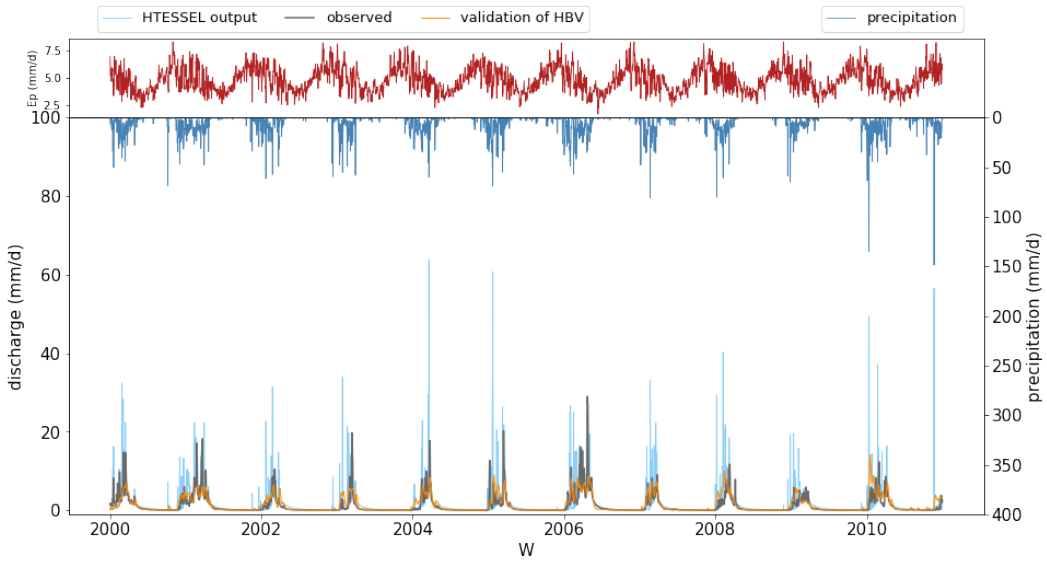

Figure 3.2: The simulation by HBV and observed results in catchment W in model test(validation) period

After calibration, the second step is model test. In this process, the time period is from 2000 to 2010. The input data with this length will be applied to test the accuracy of selected optimal parameters. Generally, the results of calibration are better than model test(validation). After 10,000 times Monte Carlo sampling, one optimal parameter set will be produced in the calibration period.

The model test(validation) results are presented in figure 3.1 and figure 3.2. After 10,000 times Monte Carlo sampling, one optimal parameter set will be produced in the calibration period. Based on optimal parameters, the hydrograph of GR4J and HBV can be visualized in the model test(validation) period. Here only catchment W is selected, the simulation results in model test period of rest 14 catchments are presented in Section A.3. In this catchment, it can be seen that compared with observation, GR4J and HBV, HTESSEL overestimates discharge too much.

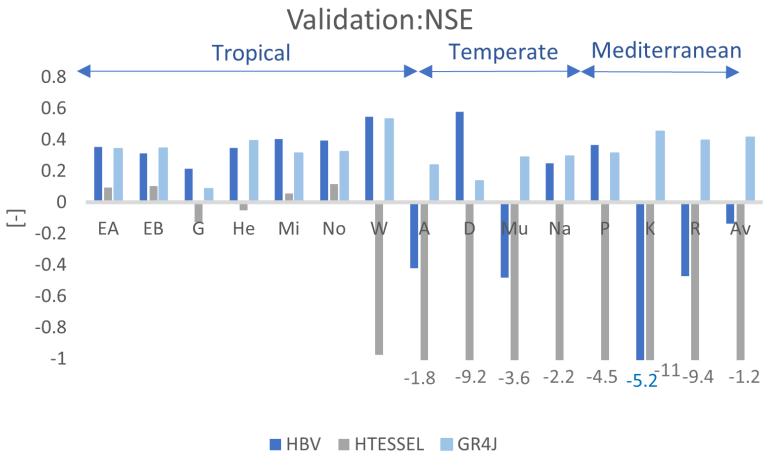

Figure 3.3: The NSE values of three models for each catchment in model test(validation) period

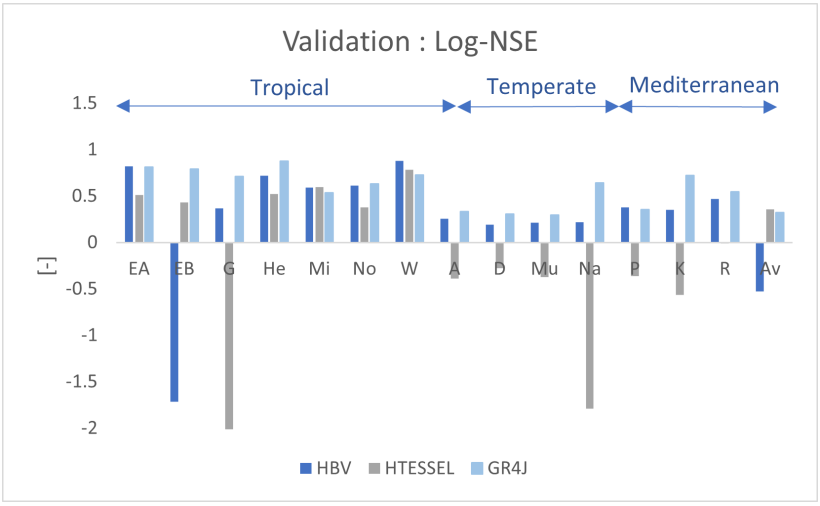

Figure 3.4: The NSE-log values of three models for each catchment in model test(validation) period

The performance metric is shown. Here GR4J and HBV are calibrated and validated via NSE, which is the objective function. The value of uncalibrated HT-

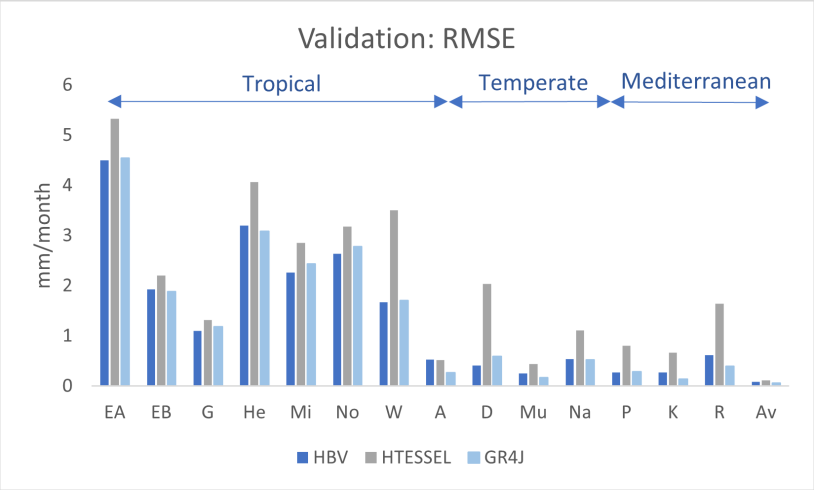

Figure 3.5: The RMSE values of three models for each catchment in model test(validation) period

ESSEL is just a score to evaluate the overall performance. Figures 3.3 and Figures 3.4 show that GR4J, HBV and HTESSEL all have a better performance in Tropical catchments, both in high flow and low flow compared with Temperate and Mediterranean catchments. While the overall performance of HTESSEL is worse than GR4J and HBV during the model test period. The negative NSE and NSE-Log that indicate HTESSEL can not simulate the discharge well and there are common factors that leads to bad performance of three models in Temperate and Mediterranean catchments.

The RMSE is also a general evaluation of the performance of hydrological models,see Figure 3.5. The higher the values, the worse simulation in high flow. GR4J and HBV have the similar scores in all catchments, while HTESSEL still under performs. In contrast to lower NSE in tropical catchments, RMSE ratings place a greater emphasis on high flows. It might mean that the impact of low-flow mistakes is greater than the impact of high-flow faults.

Both NSE and PBIAS may evaluate performance under high flows, but PBIAS specifically represents the bias of peaks in the hydrograph.In Figure 3.6 negative PBIAS implies that the simulated discharge has been overestimated. But the hydrograph also shows that, for example, in catchment K and No, the high absolute PBIAS is caused not only by overestimation, but also a slower recession or delay in the simulated discharge.

The results of correlation coefficient are presented in figure Figure 3.7. Correlation coefficient is an indicator that describes the relationship between two variables. The larger the value, the better the performance. General speaking, GR4J and HBV have the similar performance, while HTESSEL is worse, especially in Temperate and Mediterranean catchments.

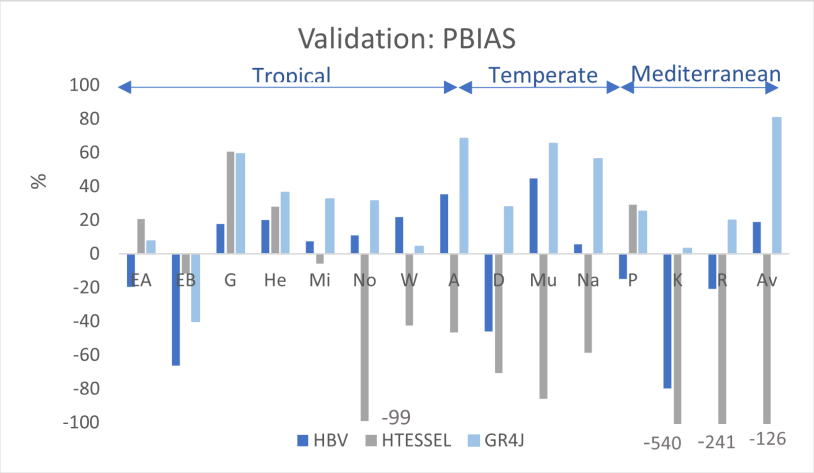

Figure 3.6: The PBIAS values of three models for each catchment in model test(validation) period

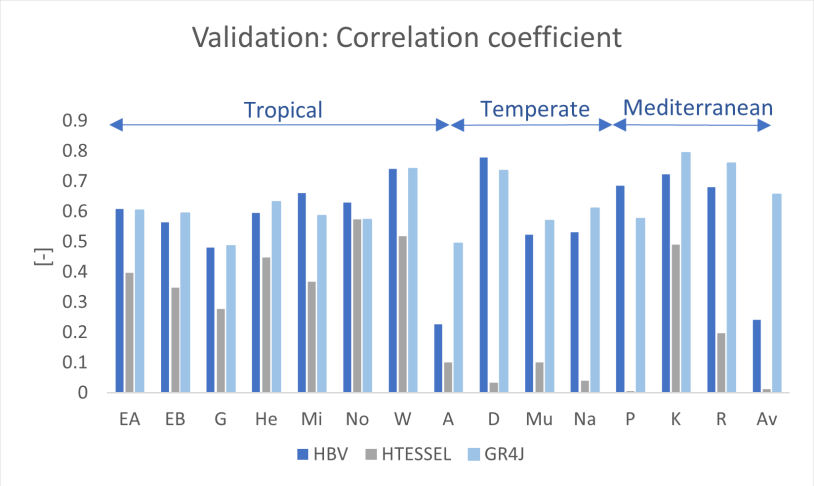

Figure 3.7: The Correlation coefficient values of three models for each catchment in model test(validation) period

Three kinds of catchments are marked with blue arrows on the top of figures. It was found that HTESSEL's tropical performance varies greatly comparing with temperate and mediterranean. This tropical difference displays some patterns in the monthly hydrograph. The falling limb of the hydrograph, for example, is much slower in catchment EB. Also delayed is the greatest monthly cumulative dischage.

The poor performance of HTESSEL thus far may be described in three ways: peak mismatch, slower decline in some catchments, and monthly delay.

3.2 THE PERFORMANCE OF HTESSEL

The previous section discusses the problem of catchment performance in terms of five different factors. On the one hand, when compared to HBV and GR4J, HTESSEL has a distinct pattern. The tropical catchments of HTESSEL, on the other hand, show a considerably different pattern than the temperate and mediterranean catchments.

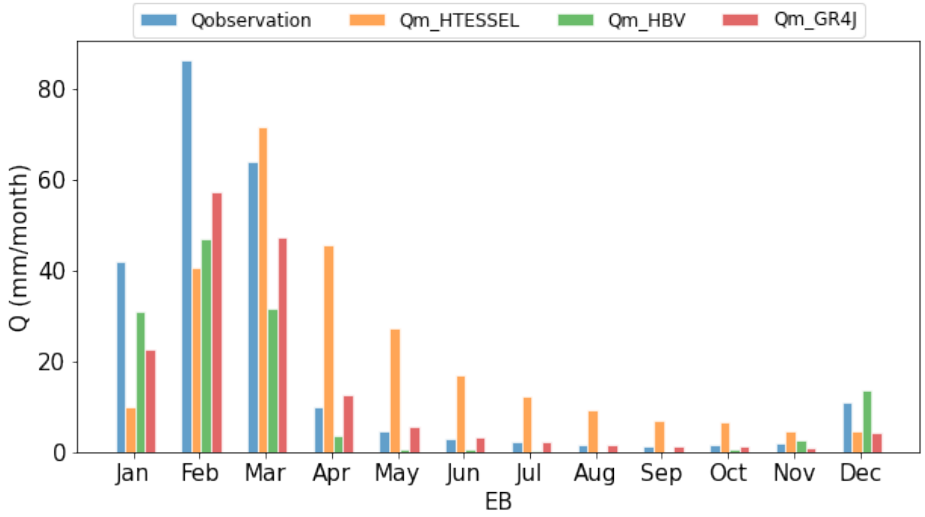

Figure 3.8: The delay of monthly rainfall in catchment EB.

Monthly delay

This section will describe what aspects of HTESSEL are poorly represented. The discharge is plotted in monthly and annually figures from 2000 to 2010. Take catchment EB for example. Figure 3.8 is the monthly histogram simulated in three models. It is obvious that the highest monthly discharge occurs in February in observation data, HBV output and GR4J output, which are represented by blue, green, and red bars. While the highest monthly discharge shows in Mar only in HTESSEL, one month delay comparing with other models. The monthly delay is also presented in catchments EA, Mi, No, K and R, besides EB. And catchments EA, EB, Mi, No are tropical catchments. The rest K and R are Mediterranean catchments.

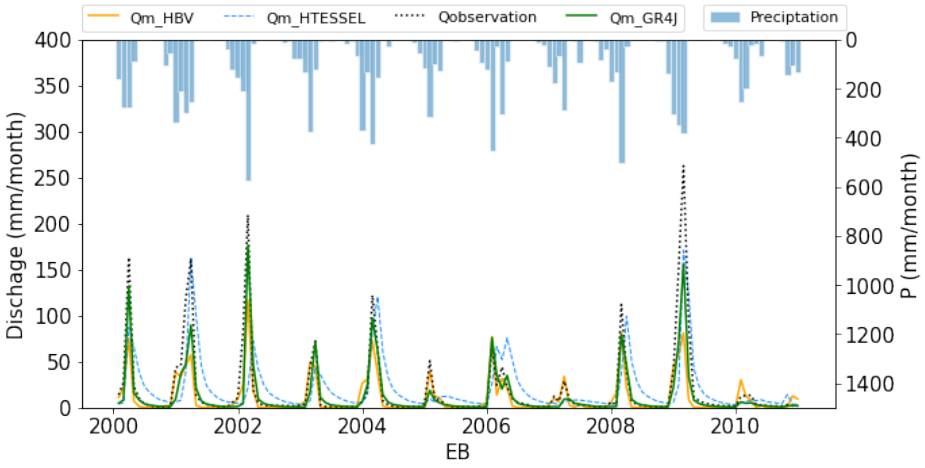

Figure 3.9: The monthly and annual plot of catchment EB

Slower falling limb

When look at the monthly line plots in Figure 3.9, the slower recession of hydrograph is presented in catchment EB. The blue dash line is the hydrograph of HTESSEL. It falls slower than observation (black dots), GR4J (green line), and HBV (orange line). The shape of recession limb usually consists of three components: base flow, surface flow and interflow at a specific catchment. The rising limb represents the increase of discharge in a hydrograph and the falling limb can represent the discharge return in a hydrograph. When comparing the recession of monthly observed streamflow and the modeling outputs, Tropical catchments EA, EB, No and Mediterranean catchments K, R show the different degrees of slower recession. More figures are presented in Section A.1.

Mismatch in peaks

Mismatch in peaks includes overestimation and underestimation of hydrograph. This occurs in almost all catchments, which are simulated by HTESSEL. Some peaks are too large and some peaks are too small. Both in daily plots and monthly plots of HTESSEL show this characteristic. Figures are presented in Section A.1.

3.3 INTERNAL MODEL STATES

In the Monte Carlo sampling, all catchments have generated 10,000 parameter sets. The only optimal parameter is limited to represent all aspects of modeling performance. So it makes more sense to choose a range or band of parameters. In this section, 50 best parameter sets are selected based on the 50 highest NSE values among the 10,000 generated NSE. The range of parameters can reflect the uncertainties and describe the performance better.

3.3.1 Soil storage and root-zone soil moisture

Root-zone storage is the water that vegetation can access. In one catchment, if the soil is close to saturated state, then less water could be stored when starting precipitation. The water that cannot be stored will lead to the fast runoff.

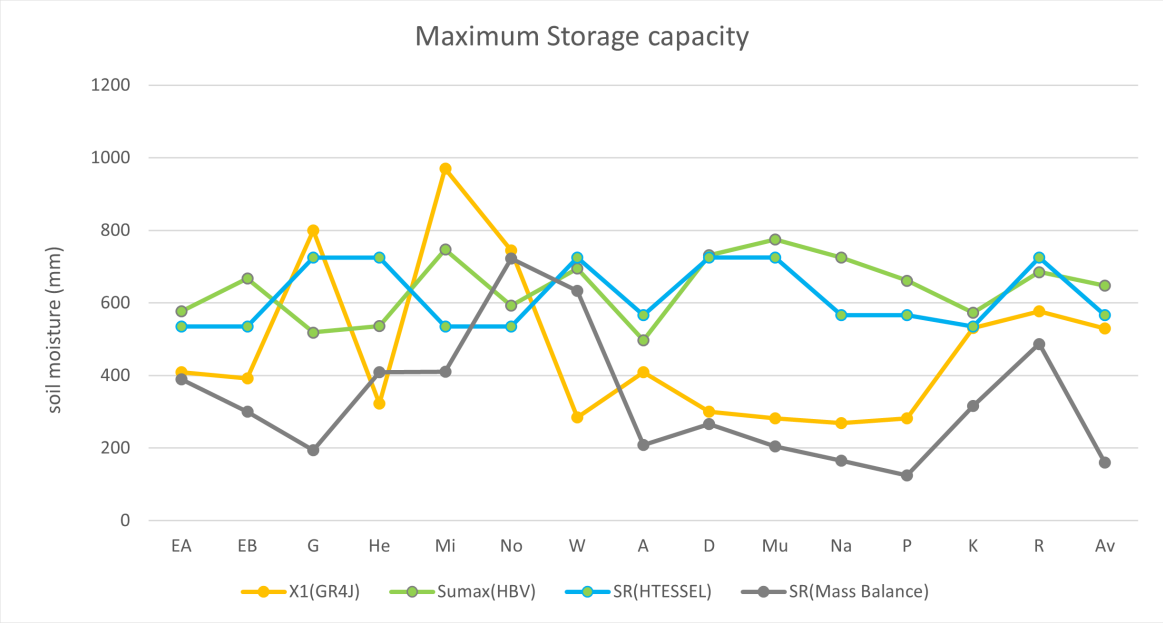

Figure 3.10: The median values of maximum storage capacity in 3 models

In figure 3.10, SR(Mass Balance) is the root-zone storage capacity based on the mass balance method, which is the maximum value of the storage deficit. So, it could be considered as a reference value that is based on observational data instead of model calibration. SR(HTESSEL) is the estimated root-zone storage capacity estimated by HTESSEL. Similarly, the X1 is the capacity of the production store in GR4J and S_{umax} is the average storage capacity, based on reformulated HBV model. The Figure 3.11, 3.12, 3.13, presents the soil moisture estimated in 3 models. Soil moisture always change due to the seasonality. The soil moisture shows huge difference in wet and dry season. So in order to show the general trend in soil moisture, the median output in 50 best results is selected and is visualized in boxplots. The boxplots can represent the variation of soil moisture along time series. It's easier to compare the lower or upper bound and the range of soil moisture in different season and different catchment. The soil moisture in HTESSEL need subtract the water content at wilting point, while the results of GR4J and HBV are obtained from the median soil moisture. When comparing three models, the soil moisture found in HTESSEL is higher than HBV and GR4J. The lower bound of the water stored in root-zone is always larger in HTESSEL, which indicates that the vegetation accessible water does not dry out. Soil is saturated quickly and can produce fast flow easily, which always influences the peaks of hydrograph. This probably one of reasons that the overestimated discharge in HTESSEL. While the performance of soil moisture is constant in GR4J and HBV.

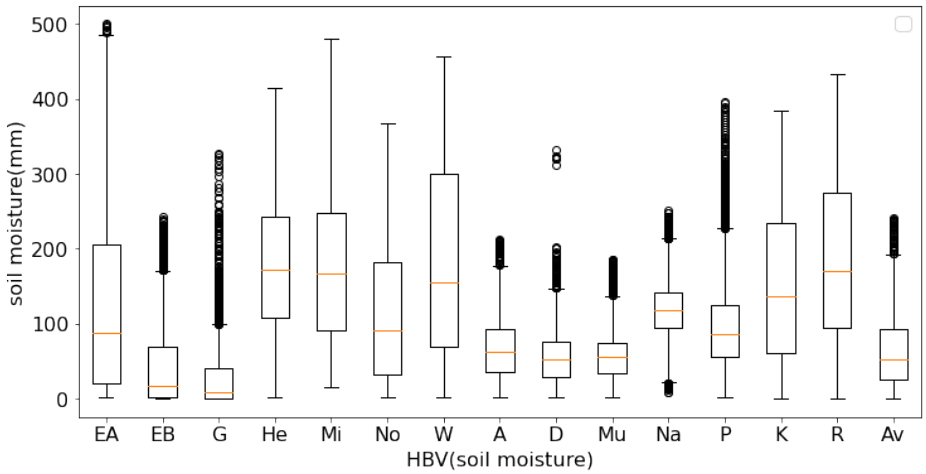

Figure 3.11: The soil moisture in HBV along the time series.

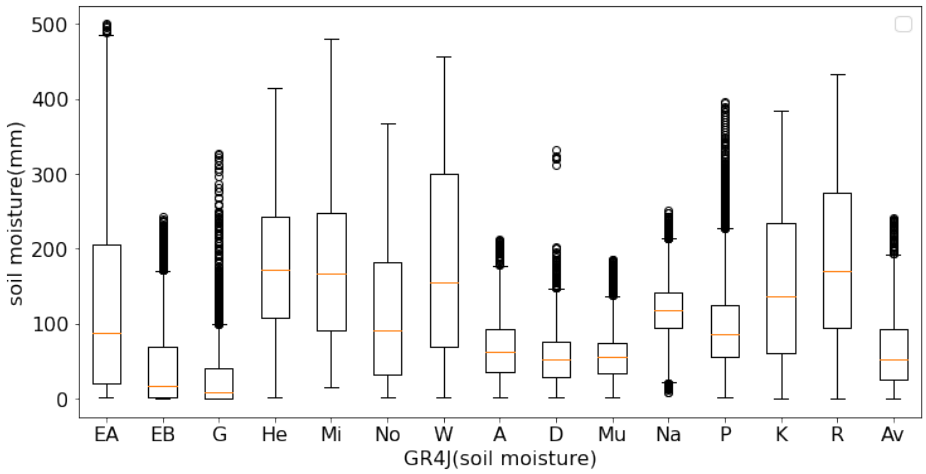

Figure 3.12: The soil moisture in GR4J along the time series.

3.3.2 Calibration based on HTESSEL outputs

In order to investigate further the cause of different performance in HTESSEL and other two models, the HBV and GR4J are calibrated based on HTESSEL outputs. The calibration approach is discussed in Section 2.3. In the first group, HBV and GR4J are calibrated to observation data, while HTESSEL uses tabulated parameter values. In another group, HBV and GR4J are calibrated to HTESSEL outcomes. The optimal results of GR4J and HBV are presented respectively in Figure 3.14. Here take the catchment W for example.

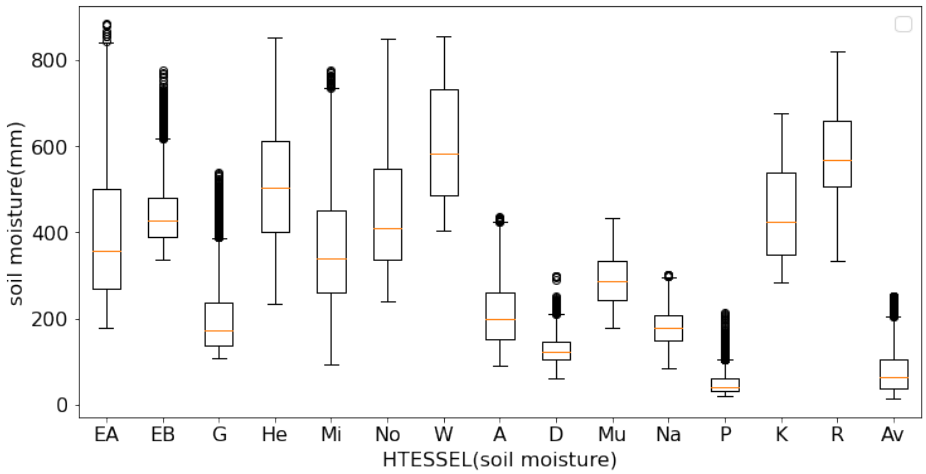

Figure 3.13: The soil moisture in HTESSEL along the time series.

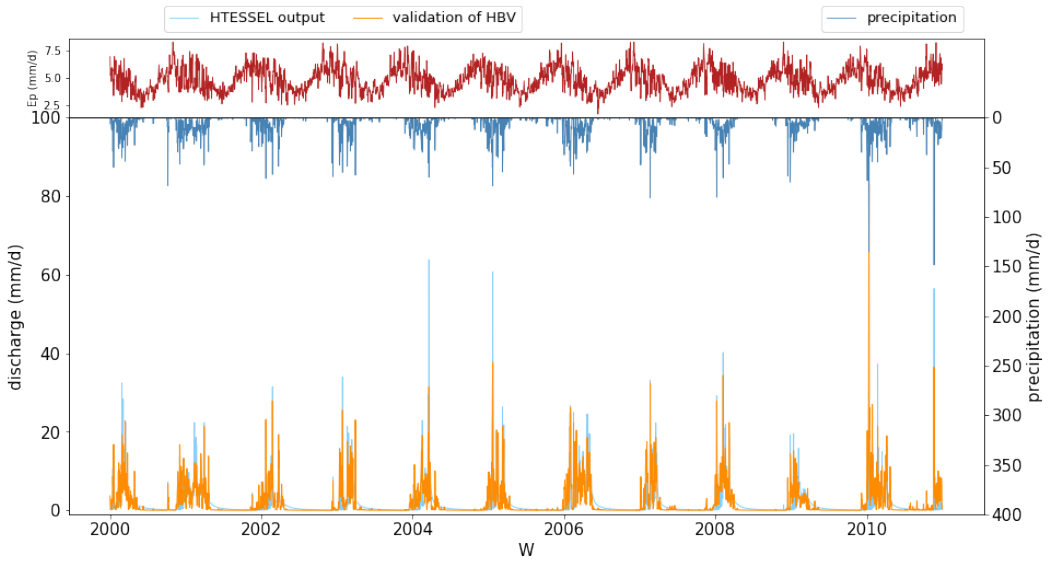

(a)

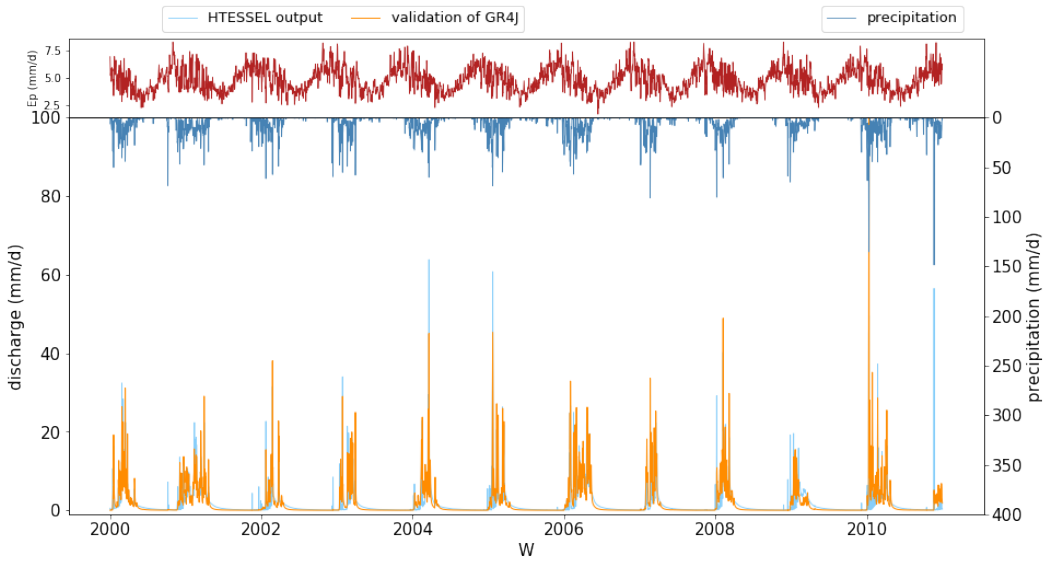

(b)

Figure 3.14: The model test(validation) results of HBV(a) and GR4J(b) when calibrated from HTESSEL in catchment W

The range of parameters in 15 catchments is shown from figure 3.15 to figure 3.21. The orange box is the range that calibrated from the original observed data, and the grey box is the value in GR4J that calibrated from HTESSEL. They represent the parameter ranges before change(Q1) and after change(Q2), which is discussed in table 2.5. Similarly, the grey box of second group is obtained from HTESSEL, the blue box is the range that calibrated from the original observed data in HBV. The label of x-axis represents individual parameter in GR4J or HBV. In GR4J, four parameters, X1, X2, X3, and X4 show apparent differences in two calibration strategy. According to the single unit hydrograph equation:

$$SH1 = (\frac{t}{X_4})^{\frac{5}{2}}$$
$$SH2 = \frac{1}{2}(\frac{t}{X_4})^{\frac{5}{2}} \tag{3.1}$$

Smaller X4 will increase the ordinates of unit hydrograph. Routing store could be

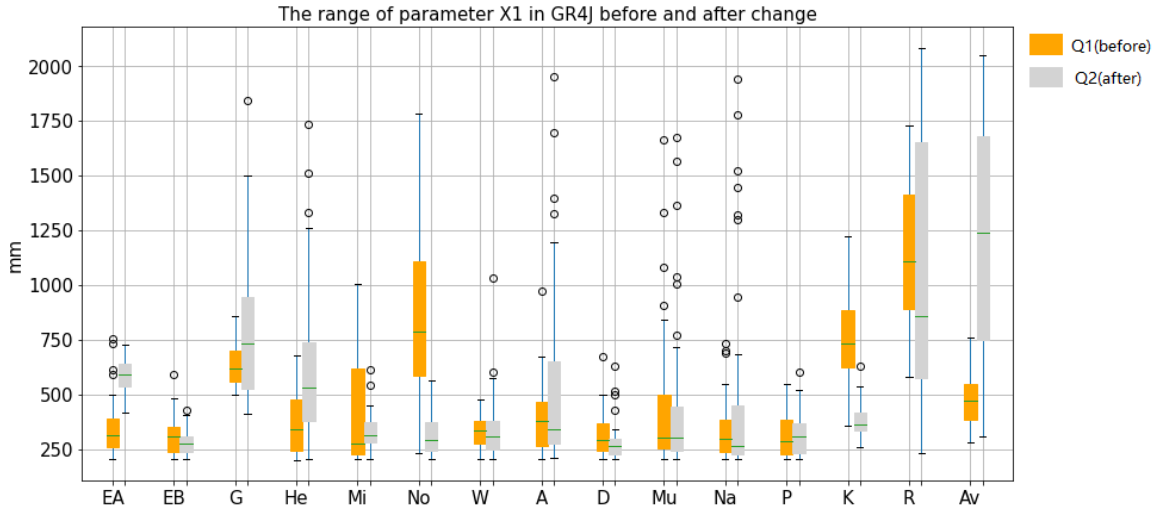

Figure 3.15: The range of parameter X1 in GR4J before and after changes. Orange box is the original range of parameters. Grey box is the new range that calibrated from HTESSEL.

easily influenced by X2. Increased X2 leads to more water entering into the aquifer from groundwater. The increase of X3 also means larger maximum capacity of routing reservoir, which cause longer streamflow recession. See figure Figure 3.16 and Figure 3.17.

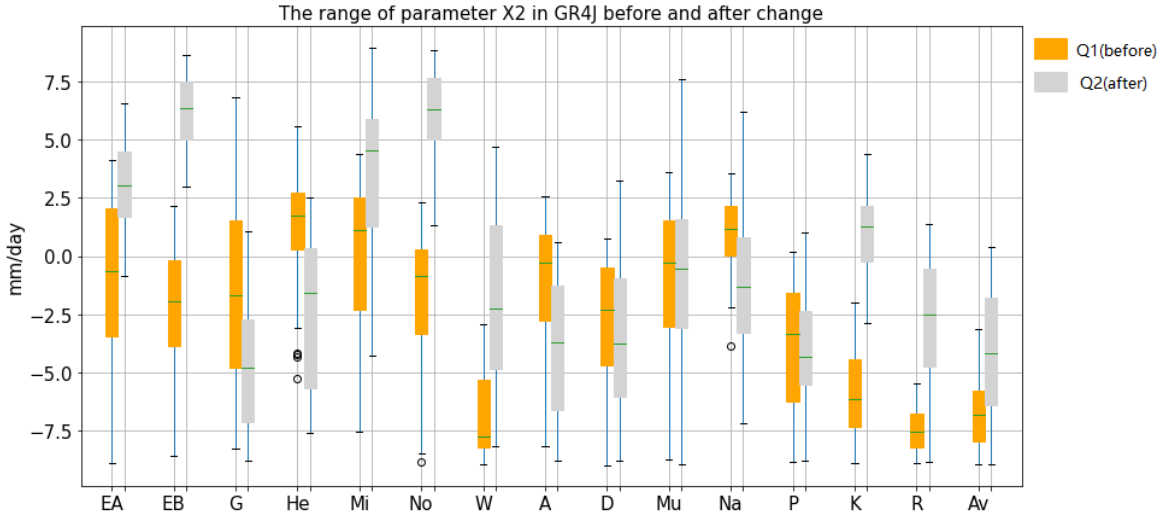

Figure 3.16: The range of parameter X2 in GR4J before and after changes. Orange box is the original range of parameters. Grey box is the new range that calibrated from HTESSEL.

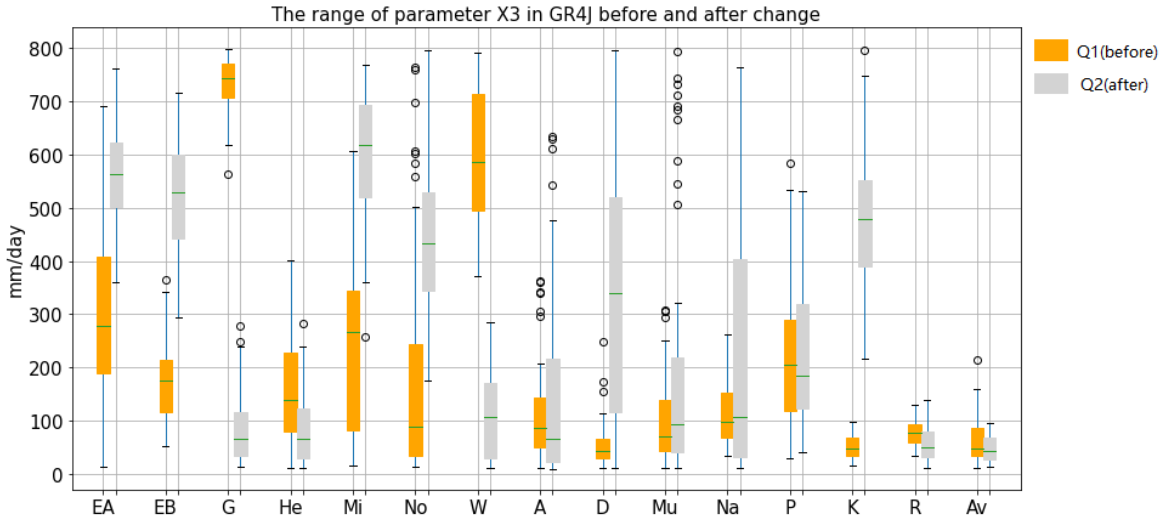

Figure 3.17: The range of parameter X3 in GR4J before and after changes. Orange box is the original range of parameters. Grey box is the new range that calibrated from HTESSEL.

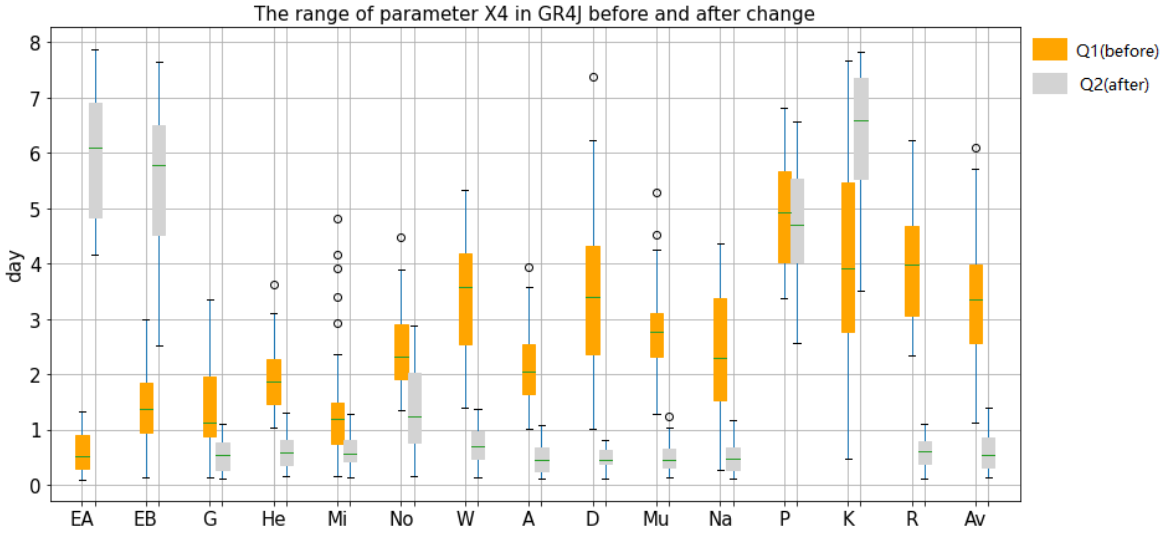

Figure 3.18: The range of parameter X4 in GR4J before and after changes. Orange box is the original range of parameters. Grey box is the new range that calibrated from HTESSEL.

Generally, the common trend shows in GR4J is the increase of routing reservoir and higher UH ordinates, while in HTESSEL, there is no routing. While in HBV, it is obvious that the parameter I_{max}, P_{max} and K_s are not sensitive to the change. It indicates they contribute less to the difference of hydrograph between HBV and HTESSEL.

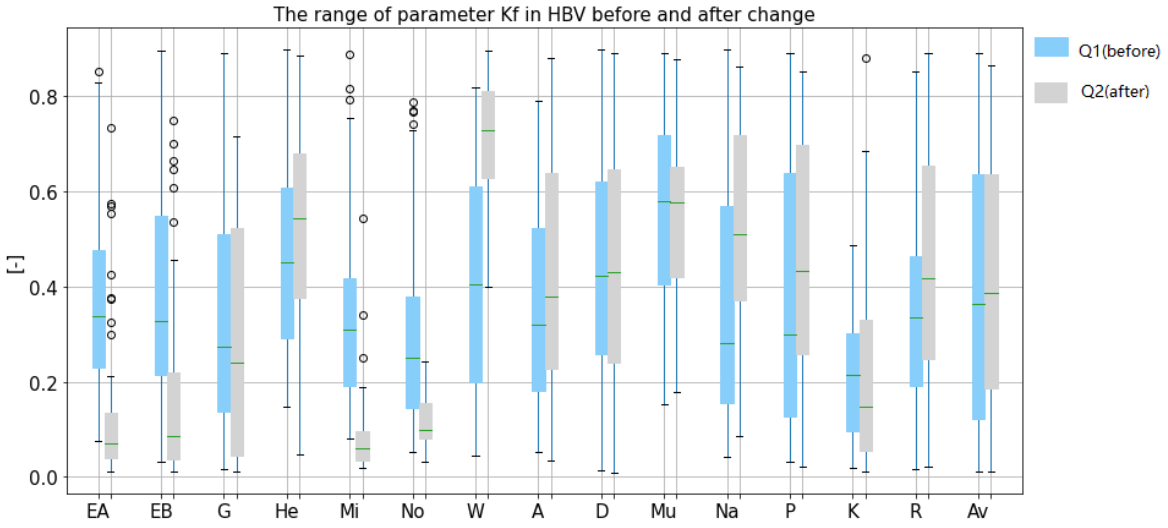

Figure 3.19: The range of parameter $K_f$in HBV before and after changes. Blue box:the original range of parameters. Grey box is the new range that calibrated from HTESSEL.

At most of catchments, new strategy has lower S_{umax}. Root-zone storage provides the buffer to a rainfall, which is related to the fast components in hydrograph (Ngo-Duc et al. [2007]). Smaller S_{umax} means less water can be stored in

root-zone, and more water will drain as fast flow, increasing the peaks. This trend corresponds with the higher K_f in new strategy for temperate and mediterranean catchments, also leading to higher surface runoff, while the subsurface remains relatively constant. But for part of tropical catchment where the slower recession occurs, K_f is decreased, for instance catchment EA, EB, Mi, No, K. Higher T_{lag} means longer time lag. So the common decrease in T_{lag} of new strategy could represent the shorter routing time, which could simulate the lack of routing in HTESSEL. The change of K_f and K_s sre presented in Figure 3.19 and Figure 3.20.

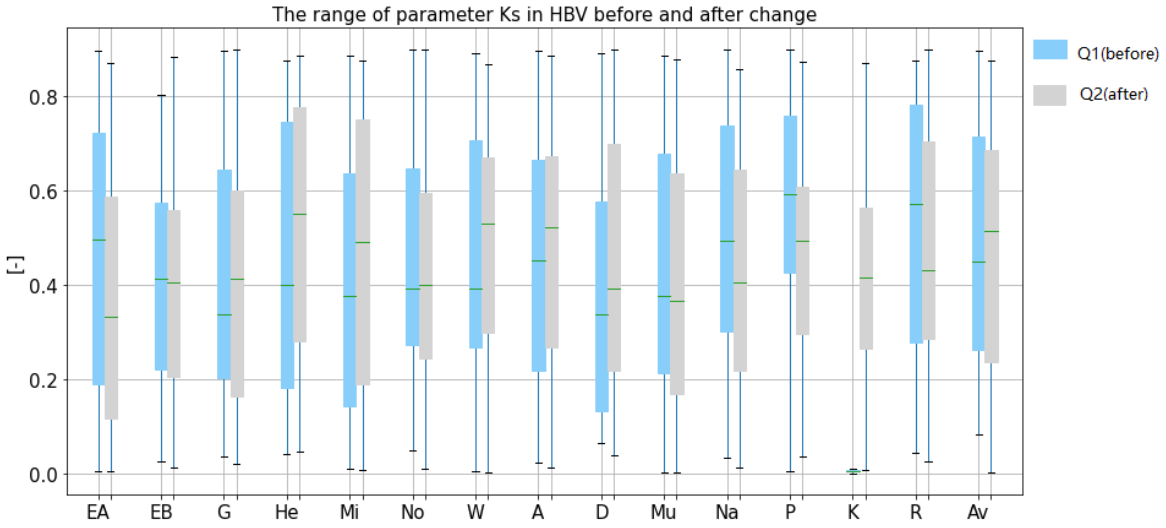

Figure 3.20: The range of parameter $K_s$in HBV before and after changes. Blue box:the original range of parameters. Grey box: the new range that calibrated from HTESSEL.

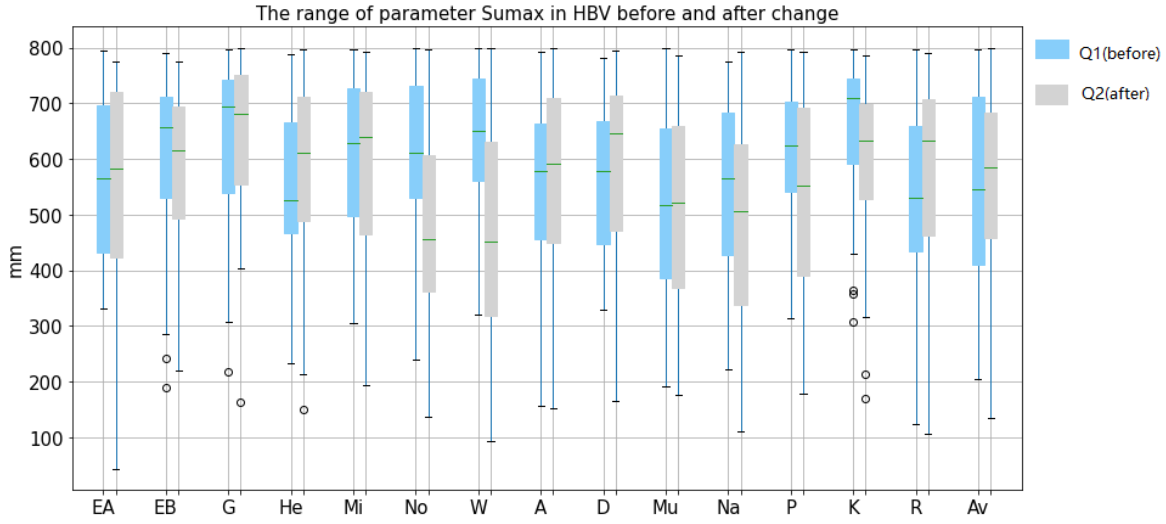

Figure 3.21: The range of parameter S_{umax}in HBV before and after changes. Blue box:the original range of parameters. Grey box: the new range that calibrated from HTESSEL.

In HTESSEL, the interception is approximately 1 mm, and in GR4J it is zero capacity. And in HBV, the I_{max} also shows non-sensitivity. It means, the parametrization of interception in HTESSEL is not the main reason that cause mismatch in hydrograph.

By the describing the change of 4 parameters, it is found that X1, X2, X3, X4 in GR4J are sensitive, whereas I_{max}, P_{max}, S_{umax}, and Beta, K_S are not sensitive in HBV. It means during the process of simulating HTESSEL, these parameters do not play important roles. And the variables Kf, $Tlag$, and Ce are quite sensitive.

3.4 THE INFLUENCE OF ROUTING

One of most differences in HTESSEL with other two models would be the lack of routing part.So, it is reasonable to analyze the influence of routing part in the first step.

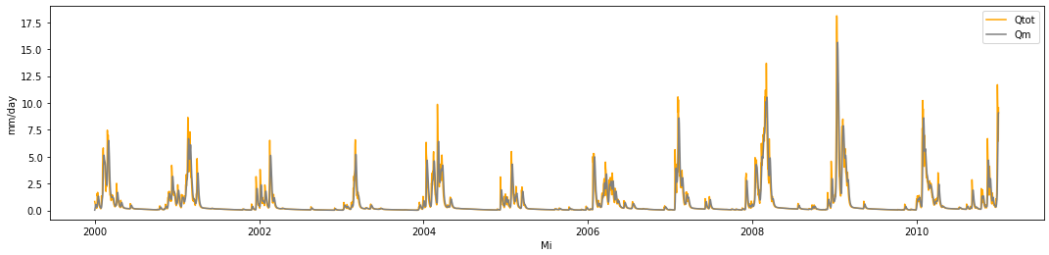

Figure 3.22: Qm and Qtot in HBV(catchment Mi)

HBV

In HBV, the last step of simulation is routing. In order to investigate the influence of routing in HBV, the model without transfer function is tested. Figure 3.22 is the simulated discharge with routing, named Q_m and without routing, named Q_{tot} of catchment Mi. It is obvious that Q_m and Q_{tot} have the similar rising limbs, falling limbs and timing of peaks except their value of peaks.

In all catchments, the addition of routing part only influences the peaks of hydrograph instead of the recession. Look back to the boxplots of the changes of different parameters in Section A.4, the lag time in HBV has more significant influence than the addition of whole routing part with respect to the produce of slower falling limb.

GR4J

In GR4J, 90 % of tot quantity of water will be routed by the single unit hydro-

graph UH1 before entering into reservoirs, and the rest 10% is routed by single unit hydrograph UH2. The equations of unit hydrograph are in 3.2:

$$\begin{aligned} UH1 &= SH1(j) - SH1(j-1) \\ UH2 &= SH2(j) - SH2(j-1) \end{aligned} \tag{3.2}$$

The unit hydrographs are determined by time delay parameter X4. And according to Pushpalatha et al. [2011], the addition of one parameter X5 in the groundwater exchange equation, called GR5J, or the addition of one routing store in GR4J in parallel to the existing ones of GR4J, reaches a higher performance,especially yielding better low flow.

But the addition of lag-function between reservoirs is less efficiency and do not lead to an improvement in low flow. It means the change within routing part does not lead to a better performance, instead the addition of one more routing reservoir has more important influence on low flow.

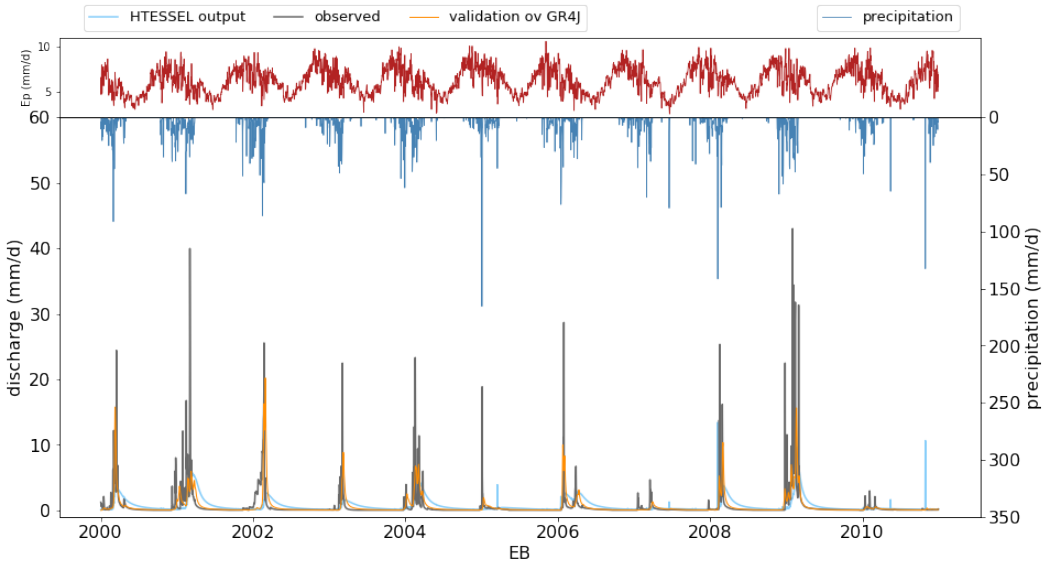

Figure 3.23: The observation, HTESSEL output and the modeling result calibrated from HTESSEL with only X4-free in GR4J(X4 = 7.9)

This can be supported by the boxplots of parameter changes, take the catchment EB for example again. X4 is the only parameter that related to routing. Although in figure 3.18 the X4 varies a lot when calibrated from HTESSEL, this is the result that all four parameters working together. In order to figure out the role of X4, parameter X1, X2, X3 are fixed, using the optimal parameter set, only X4 is freely calibrated. X4 varies within the parameter range which is presented in table 2.3. Make GR4J to simulate the performance of HTESSEL output, the result shows that it's easy to perform like HTESSEL. When X1, X2 and X3 keep constant, X4 is sensitive, but it has more influence on peaks as well, instead of the recession. Different

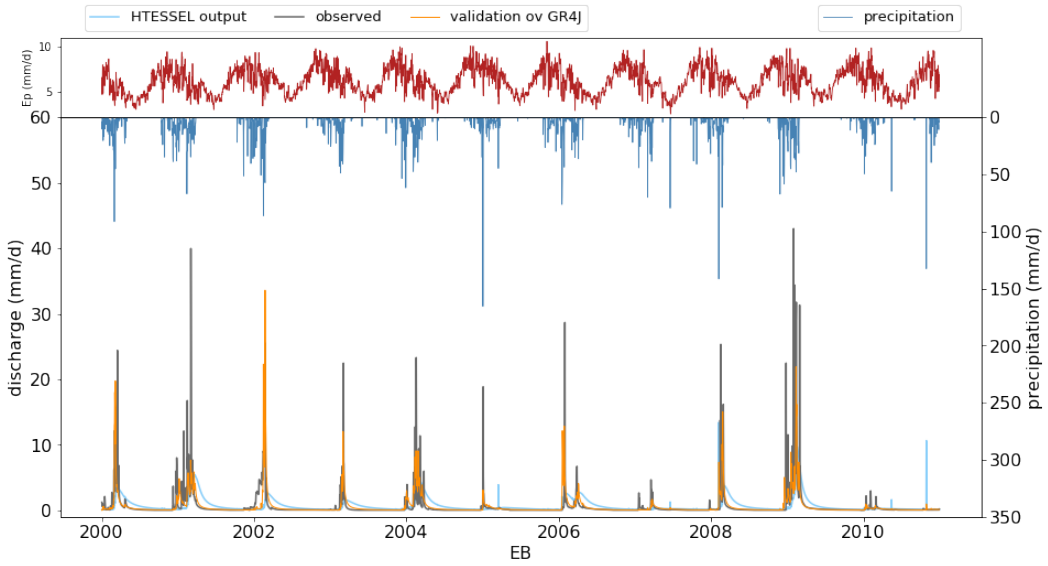

Figure 3.24: The observation, HTESSEL output and the modeling result calibrated from HTESSEL with only X4-free in GR4J(X4 = 0.9)

X4 values can get similar performance. The change of routing itself, here means X4, may adjust the peaks of hydrograph and yields different high flow, but it is not strong enough to make the falling limb of hydrograph slower or faster. The low flow remains at the same efficiency. This process is tested in figure 3.23, figure 3.24 and figure 3.25. For example, for the catchment EB, the orange hydrograph is the simulation, they looks quite similar when applying different X4.

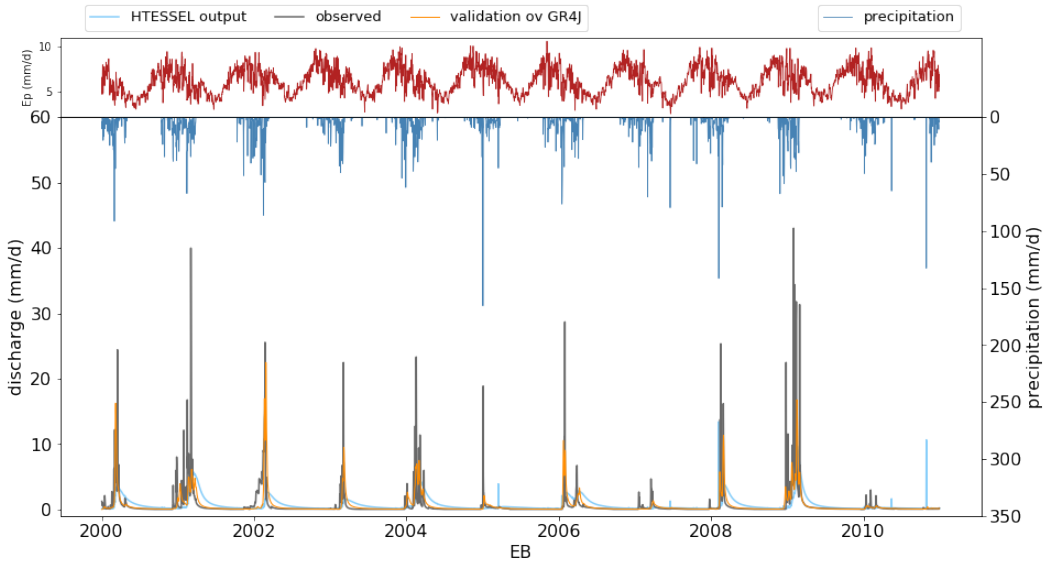

Figure 3.25: The observation, HTESSEL output and the modeling result calibrated from HTESSEL with optimal parameter set in GR4J(all freely calibrated, X4=5.53)

Applying the same method on parameter X1, keep other three parameters constant. Take the catchment EB for example again. The adjustment of X1 impacts

the peaks of hydrograph, see figure 3.26 and 3.27.Based on the performance of boxplots, current tests can be brought to one conclusion: The slower recession might be drawn from the change of X2 and X3. X1 and X4 have higher efficiency in impacting high flows.

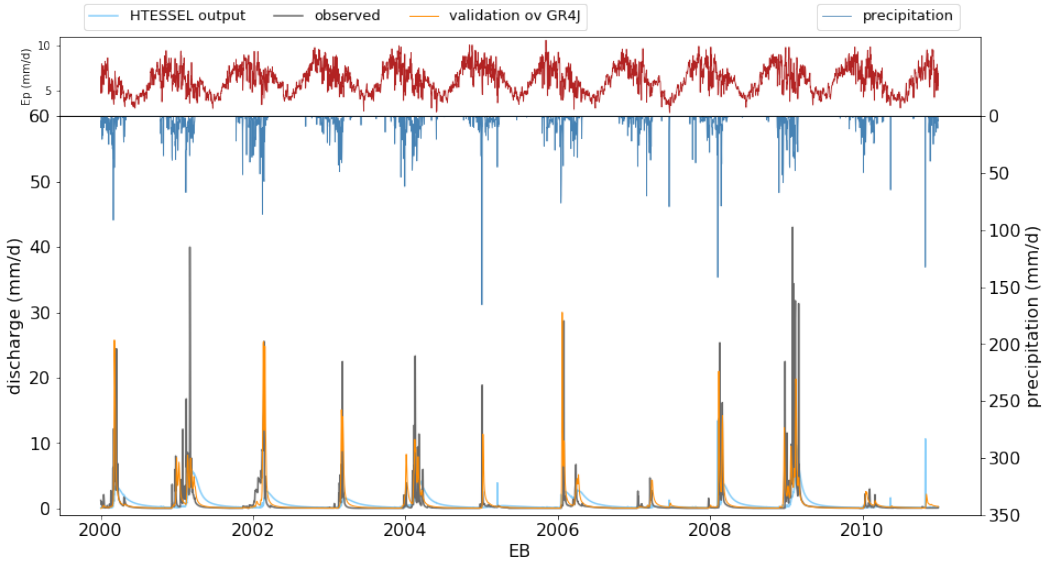

Figure 3.26: The observation, HTESSEL output and the modeling result calibrated from HTESSEL with only X4-free in GR4J(X1=100)

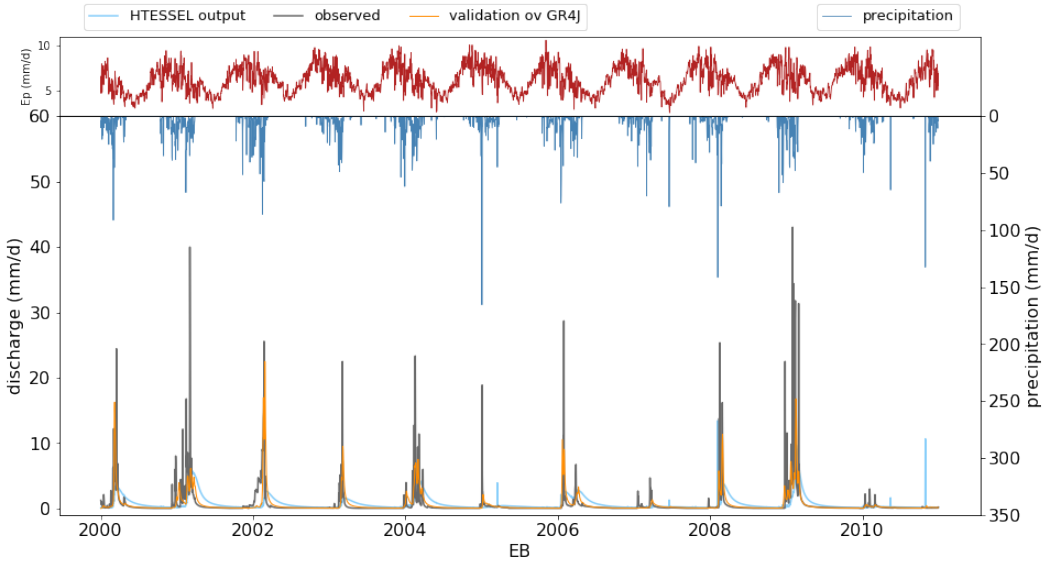

Figure 3.27: The observation, HTESSEL output and the modeling result calibrated from HTESSEL with only X4-free in GR4J(X1=226)

In figure of parameter changes, although all of four parameters are sensitive parameters, the influence of X1 and X4 on recession can be excluded, then the rest parameters are the key parameters in GR4J. Because according to the definition

of X2 and X3, both of X2 and X3 are related to the routing reservoir.Increased X2 leads to more water entering into the aquifer from groundwater, reaching a larger routing reservoir. The increase of X3 also means larger maximum capacity of routing reservoir. This conclusion corresponds with previous research results found by Pushpalatha et al. [2011], that if one more reservoir store could be added into model, the performance will increase, but the lag function between reservoirs do not improve the performance dramatically.

It was verified low flows are more sensitive to the size of routing reservoir in GR4J. The addition/increase of routing store has more influences on low-flow. In other words, the size of routing store is more significant. If utilizing GR4J to perform as HTESSEL, the size of key reservoirs need to be increased.

In this way, by analyzing the existing of routing part in HBV and GR4J and their results with or without routing part, this can inspire the analysis of HTESSEL. Maybe the lack of routing part is not the reason that induces the occurrence of slower recession in HTESSEL in some catchments.

HTESSEL

The impact of routing part in HTESSEL is verified in Pappenberger et al. [2010]. TRIP2 river routing model (Ngo-Duc et al. [2007]) is introduced, which is an individual runoff routing component and compensate the deficiency of routing in HTESSEL. Figure 3.28 shows the schematic of coupled model. It was found the groundwater delay parameter (GTM) in TRIP2 was very sensitive. But the coupled model still produces significant uncertainties in runoff predictions. The research results indicate that the uncertainties are derived from hydrological model HTESSEL or observation data, not from the routing part.

Combine the previous discussion on HBV and GR4J with this coupled model, the conclusion is clear now: The lack of routing part in HTESSEL is not the main reason that could cause slower recession or delay. The structure of HTESSEL itself need to be improved to get a better output.

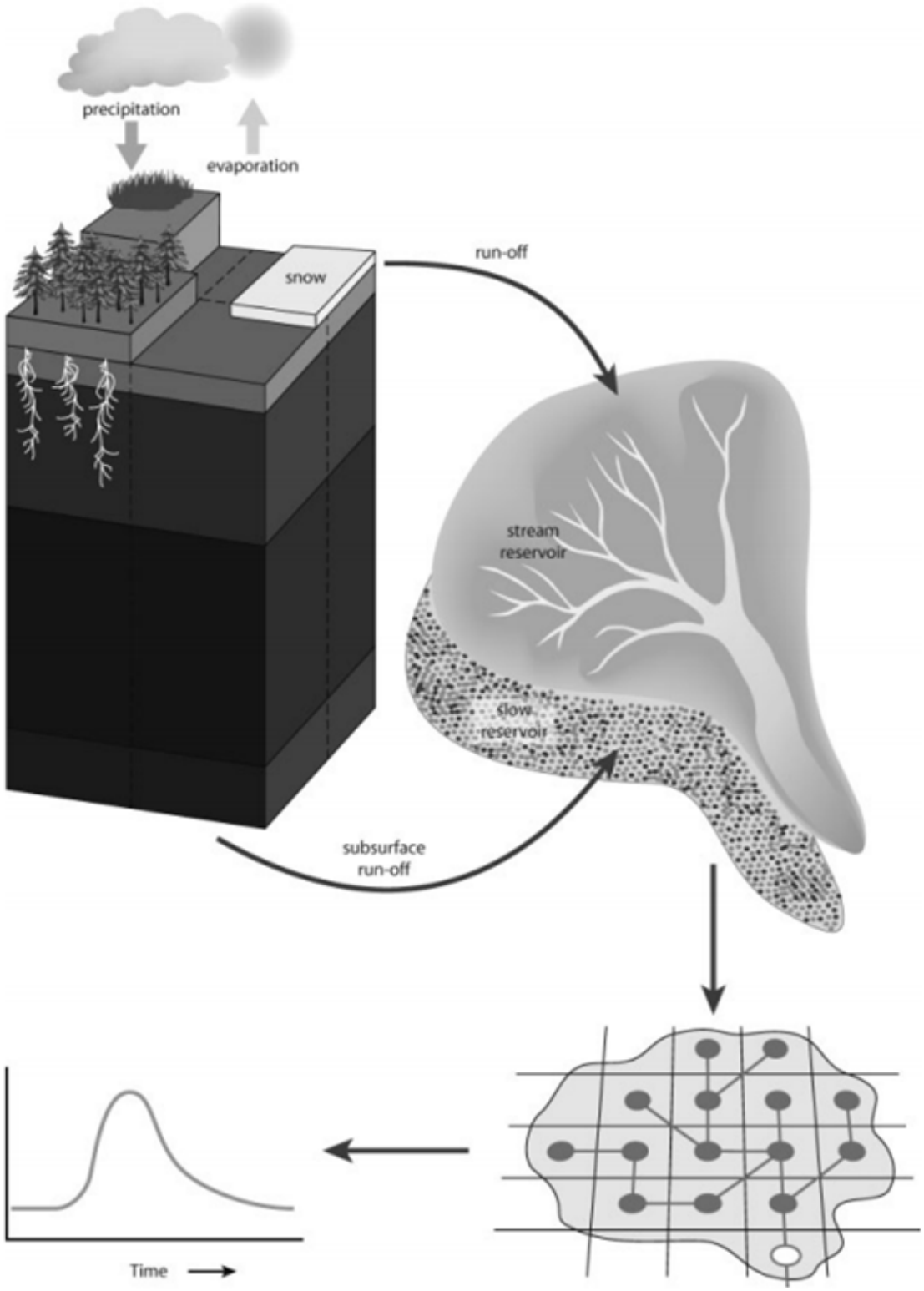

Figure 3.28: Scheme of coupled HTESSEL-TRIP2 model(Pappenberger et al. [2010])

3.5 INTERNAL FLOWS

Previous section discusses the role of routing part in three models, it was expected routing part is a significant factor that leads to the slower recession, but results prove that the internal structure of models could act as an important role resulting in poor performance of simulation. Therefore, more studies should focus on the interflow of models. In this section, the variation of internal flows will be discussed when using the calibrated results based on observation and calibrated results based on HTESSEL output respectively.

Fast flow

Usually, the fast-responding components will be affected by root-zone storage(Nijzink et al. [2016]), here which is unsaturated sotrage Su. S_{umax} represents the maximum sotrage capacity. High S_{umax} indicates high capability to store water in root zone. The high storage can buffer more water and reduce the recharge to the groundwater, then the peaks are decreased.

In HBV, fast runoff is directly calculated by equation 3.3. S_f is the fast reservoir.

$$Q_f = S_f * K_f \tag{3.3}$$

In HTESSEL, fast runoff is directly generated by the top 50cm. Thus the top 50cm and the fast reservoir in HBV play as the similar role in modeling. Section 3.3.2 comparing the parameter changes, it was found that for catchment where slower recession occurs, K_f decreased when calibrated to HTESSEL. And in temperate and Mediterranean catchments, K_f always increased. In HTESSEL, the top 50cm depends on the maximum infiltration rate I_{max} (ECMWF [2016]). The maximum infiltration rate is a function of vertically integrated soil water contents(W), precipation(T), and parameter b and it is simplified by the function 3.4 :

$$I_{max} = f(W, T, b) \tag{3.4}$$

The soil moisture and preciptation are fixed at a certain place. Thus the I_{max} is depended on variable b, which is related to the orography. It means, like K_f impacting the fast runoff in HBV, parameter b could be the key parameter that impacts the surface runoff in HTESSEL. In HBV, higher K_f means higher fast runoff. HBV is trying to reproduce the discharge in HTESSEL by increasing K_f from the boxplot of change of parameter. According to ECMWF [2016], surface runoff generation has a positive relationship with parameter b. The higher the b, the larger the surface runoff generation rate. In this case, the decrease in parameter b or the increase of this 50cm are possible to lower the peaks of hydrograph and improve the performance of HTESSEL.

Besides the different pattern in discharge, the soil moisture also shows some pattern. The soil moisture in HTESSEL is bounded by wilting point, which is always

keep high level compared with other two models in figure 3.11. Rootzone storage capacity is considered as maximum storage deficit. In humid area, the soil moisture deficit is not large(Zhao et al. [1995]). In HTESSEL, the bucket in rootzone divided into four layers, which means the modeled surface runoff (Q_s) is directly affected by absolute moisture(van Oorschot et al. [2021]). And the soil moisture in HTESSEL depends on the soil depth (z), see equation 3.5. When rainfall enters soil, it's easier to saturate top 50 cm and produce fast runoff.

$$S_r = z(\theta_{cap} - \theta_{pwp}) \tag{3.5}$$

On the one hand,this answers the question why the overestimation of peaks or mismatch in peaks are quite common in three kind of catchments of HTESSEL: fast flow obtains from high soil moisture. This corresponding with the lower NSE of HTESSEL. On the other hand, tropical catchment with higher soil moisture does not generate overestimation in peaks very often, comparing with temperate and mediterranean catchments. For example, tropical catchments have higher value in PBIAS.

In GR4J, like the discussion mentioned in previous section, the parameter X1 could influence the direct flow, also called surface flow. But due to the fixed percentage in the separation of routed and direct flows, the X1 and production store can impose limited impact on the direct flow. Figure 3.29 shows the case of Qd and Qr on catchment EB. The larger Qr, the larger impact on flows.

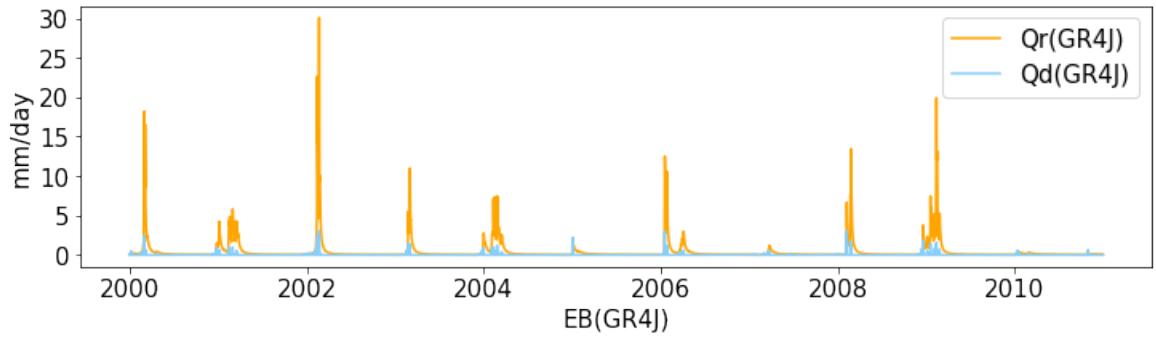

Figure 3.29: Fast reservoirs and slow reservoirs based on two calibration method of HBV in catchment EB

Slow flow

In HTESSEL, the slower recession mainly comes from subsurface runoff (Q_{sb}), figure 3.30 and Section A.6 shows the relation between Q_s and Q_{sb}. For almost all catchment where slower recession occurs, such as EA, EB, No, W, K, R, groundwater or Q_{sb} are the dominated runoff in HTESSEL. While in other catchments, the Q_s simulated by HTESSEL is the main streamflow.

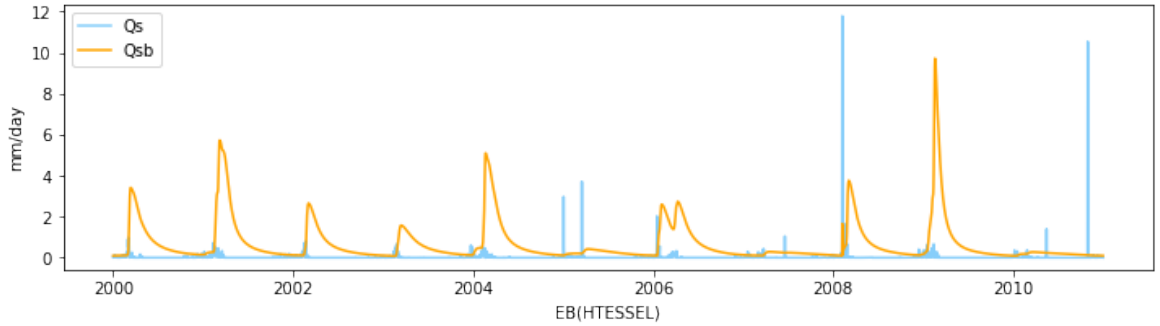

Figure 3.30: The surface flow(Q_s) and subsurface flow (Q_{sb}) in HTESSEL(catchment EB)

Figure 3.31 shows the variation of reservoirs with two methods of HBV. In HBV, soil moisture stored in unsaturated reservoir, when the effective rainfall exceeds the threshold of this bucket, the water will flow to fast reservoir and infiltrate into slow reservoir.

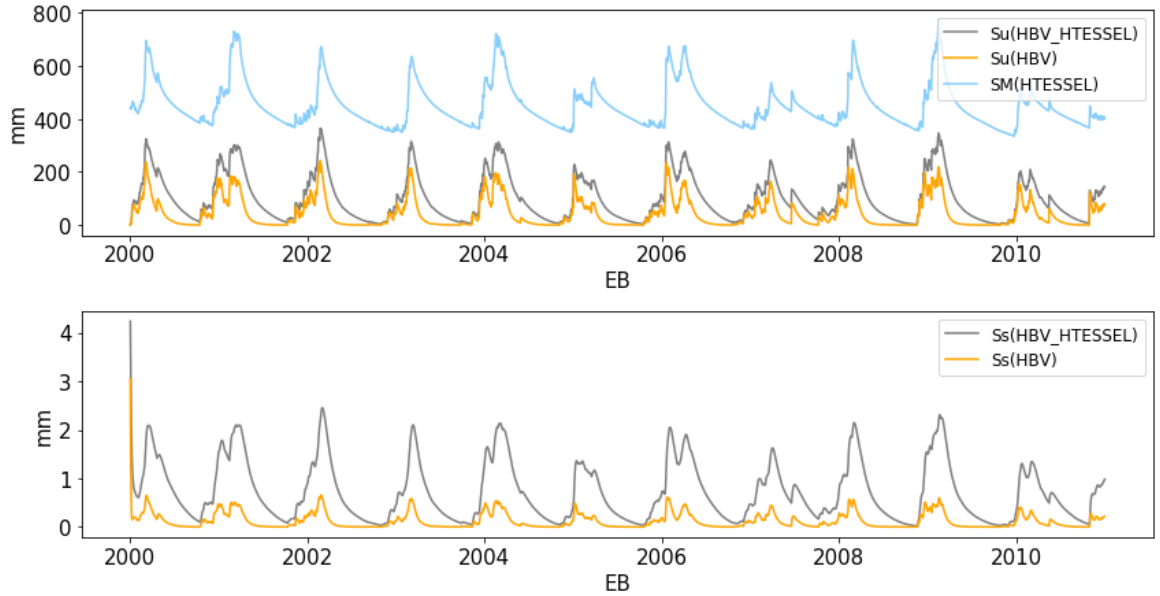

Figure 3.31: Unsaturated reservoirs and slow reservoirs based on two calibration method of HBV in catchment EB

For catchments slower recession occurs, particularly in catchment EA, EB, No, K and R, the size of unsaturated reservoir and slow reservoir both alter dramatically and their falling limbs usually become more flat or longer. And the change of slow reservoir can influence the slow flow directly, in figure 3.32, the slow flow of HBV is trying to act like the subsurface flow in HTESSEL. Besides HBV, GR4J also shows similar performance in figure 3.33, the routing store also increases the size and has a longer recession process after the change. This change matches the variation in the boxplot of X2 and X3. The boxplot clearly shows that in figure 3.16 and figure 3.17, the value of X2 and X3 indeed increases a lot after the change in catchment EA, EB, No, K and R.

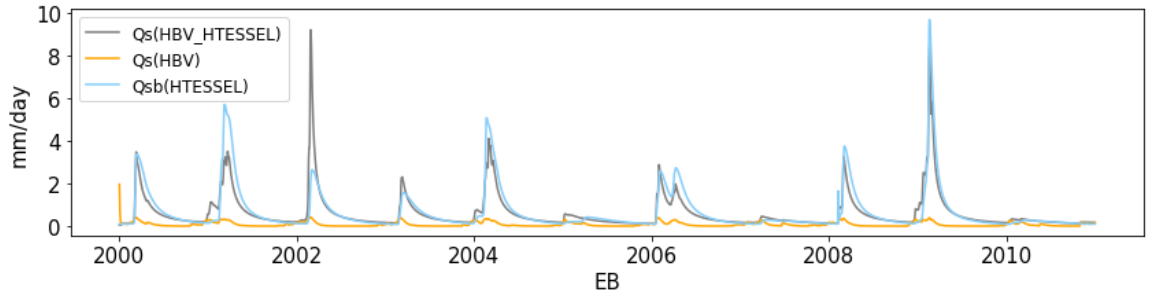

Figure 3.32: Slow flows based on two calibration method of HBV and subsurface flow in HTESSEL in catchment EB

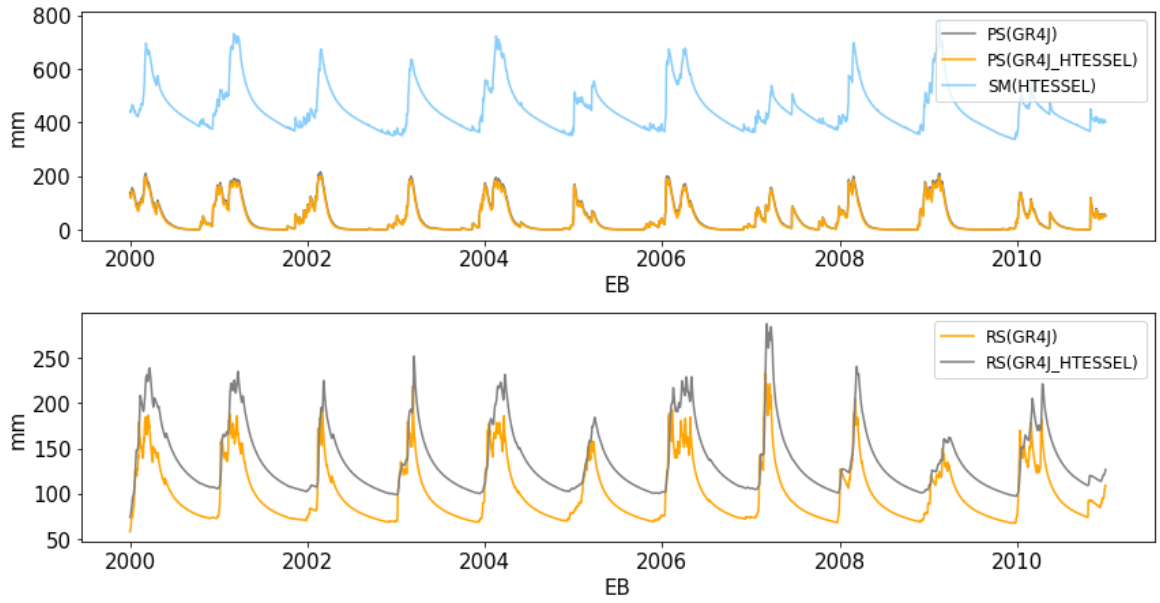

Figure 3.33: The production store(PS) and routing store (RS) in GR4J(catchment EB)

Although in HBV, the K_s is not as sensitive as K_f during the application of two methods, the change of slow reservoir (S_s) is larger than fast reservoir (S_f), so that they can compensate each other to produce slower falling limb. More figures are presented in Section A.6. Based on the discussion before, the enlarged size of unsaturated and slow reservoirs in HBV, or the increased production store and routing store in GR4J, could simulate the large size of storage in HTESSEL. So the large soil column of HTESSEL maybe a significant cause that leads to the slower recession in some catchments. The total soil depth is set to 2.89m in HTESSEL, of which the top 50 cm of HTESSEL make contributions to the fast flow and rising limb of hydrograph, but the remaining large soil column could impact the slow flow. Or in other words, the large size of soil clomun in HTESSEL could be considered as the key component and slower recession probably derives from it.

The transpiration could be one influential factor in the deeper soil as well. On the one hand, the whole soil column can keep a high level of soil moisture. For

HTESSEL, although the root depth is set to 2.89m of soil, but the effective depth which generates surface runoff is limited to top 50 cm. It takes a longer time to transpire the water stored in subsurface (van Oorschot [2020].

The simulated evaporation among 15 catchments do not vary significantly, ranging from 0 to 10mm/day, but the amount of annual precipitation and soil moisture have a huge difference, see figure 3.13. In wet region, like part of tropical catchments, the low evaporation, low exchange rate and high soil moisture in HTESSEL compared with temperate and Mediterranean catchments, could lead to the slower recession limb of hydrograph. Catchment K and R have a higher soil moisture and annual precipitation (Section A.1) than any other temperate or Mediterranean catchments, so they generate slower falling limbs as well. Huang et al. [2008] developed a new subsurface flow formulation and introduces the special change of recharge and topography in HTESSEL. The results show that no matter implementing with spatial variability of recharge alone or implementing with the combination of recharge and topography, both two factors are important for the mean subsurface flow.

From the point of review of describing better performance, reservoir is the main factor that control the modeled recession limbs of hydrograph(Fenicia et al. [2006]. Q_f and Q_s as the outflows are the linear function of S_f and S_s.Four bucket in HBV are linear storage. Besides, the transfer function is linear transformation as well, used to describe outflows. While in GR4J, the power function with parameter X4 is applied. In HTESSEL, the outflow Q_s and Q_{sb} are depended on soil depth and soil storage capacity, without a power function. According to the study of Van Esse et al. [2013], the complexity of structure of conceptual model will not necessarily improve the output, but the power function can achieve a better mean performance than the model using linear function. This can explain why GR4J has a better mean performance than HBV. The average NSE of GR4J are higher than HBV in mediterranean and temperate catchments. In tropical, their average values are quite similar, GR4J with 0.334 and HBV with 0.368.

So, in GR4J, the main variability of parameters contributed to the increase of routing store when simulating performance of HTESSEL output. And in HBV, the larger S_s and sensitive S_f also try to imitate the large storage in HTESSEL to produce slower recession. The large storage in HTESSEL, imposes the slower falling limbs.

3.6 MONTHLY DELAY

The soil column in HTESSEL makes the simulated storage large enough, causing the slower falling limb. It means the recession will be slower and delayed. The peaks of hydrograph attenuate with a lower rate. The largest monthly accumu-

lated precipitation occurs slower due to the soil moisture memory. This is the direct reason that leads to monthly delay in Section A.1. So it is apparent that the slower recession always occurs with the appearance of monthly delay simultaneously. For instance, catchment EA, EB, No, K and R. So when the input is calibrated to HTESSEL,the highest bar occurs one month later for HBV and GR4J as well (see figure 3.34), compared with the original plot in figure 3.8. It indicates the soil moisture indeed impose impact on monthly delay.

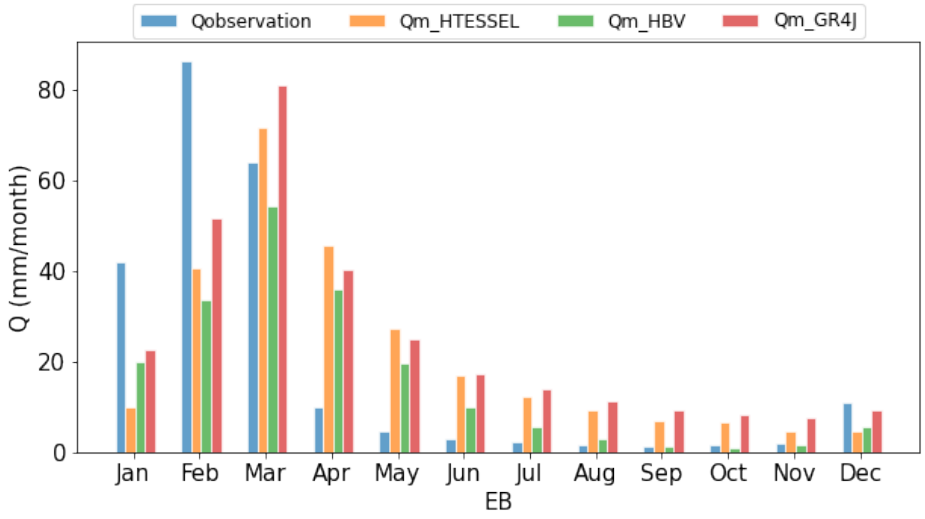

Figure 3.34: The delay of monthly rainfall when calibrated to HTESSEL in catchment EB

4 DISCUSSION

Previous chapter describes the possible reasons of slower recession, overestimation in peaks and delay. Hydrological models are also known as simulations and representations of reality. HTESSEL, HBV and GR4J all are lumped models. So the oversimplification in model is inevitable sometimes. And during this process, all catchments are assumed to be at water balance. Thus there would be some limitations inside and outside of models. They are worthy to be discussed.

4.1 LATERAL WATER EXCHANGE

Section 2.3 has mentioned that water constrain the parameter sampling process is set to meet the requirement of water balance. But in reality, there still exist a little bit lateral water exchange in groundwater.For instance, the lateral water distribution of precipitation is not allowed in HTESSEL. The exchange between each grid cells (Wipfler et al. [2011]) is not taken into account in this research. Thus, the influence outside the model is not considered.

4.2 PARALLEL AND SERIAL STRUCTURE

Figure 2.5 is the scheme of 3 models. So another large difference between HTESSEL and HBV, GR4J is the model structure. Both of HBV and GR4J have parallel and serial reservoirs, but HTESSEL is serial connection only. In the literature, the effects of parallel or serial model structure have been studied. Fenicia et al. [2014] and Van Esse et al. [2013] found that the introduction of parallel reservoirs improve the performance considerably, particularly in groundwater component dominated catchment. But for lateral subsurface flow dominated catchment, the addition of parallel structure could deteriorate the performance. This corroborates the first limitation in previous section. The horizontal behaviors between catchments in lumped model indeed influence the predictive discharge.

GR4J has a typical parallel structure, of which parameter X2 is groundwater exchange coefficient. For all catchment slower recession occurs, the X2 has increased. It indicates more water enter into aquifer from groundwater. It shows the change

of groundwater component. But in this study, the discussion of absence of parallel in HTESSEL is poor.

5 CONCLUSION

This research investigates the reasons of poor performance in HTESSEL. Considering the similar basic hydrological modules, GR4J and HBV are introduced to identify the errors. NSE is used as the objective function to evaluate the performance of three models. The main conclusions for each sub-questions are summarized as follows:

- *What aspects of the hydrographs are poorly represented by HTESSEL?*

  Based on analysis of their final streamflow, internal flows and model structure in Section 3.2, it was found that the poor performance could be separated into three aspects: the overestimation in peaks, slower falling limbs of hydrograph (figure 3.9 and the monthly delay in accumulated monthly plots (figure 3.9).

- *HTESSEL, GR4J and HBV are all hydrological models. What are the differences in modelled discharge between HBV, GR4J and HTESSEL?*

  On average, both GR4J and HBV have better performance matrix than HTESSEL (see Section 3.1.2), which is obvious as the model parameters in GR4J and HBV are calibrated to observations while HTESSEL uses tabulated parameter values. From the point of describing three aspects, the performance of tropical catchment in HTESSEL shows different pattern than other two kind of catchments. Tropical catchment, also including catchment K and R, concentrate the phenomena of slower recession in HTESSEL. Tropical catchment also perform better in GR4J and HBV. This could be verified from the visible NSE, Log-NSE, PBIAS, RMSE and correlation coefficient. Overestimation in peaks mainly occurs in temperate and mediterranean catchments in HTESSEL modeling. For GR4J and HBV, they fail to simulate the peaks of observed discharge as well.

- *Compared with observation data, what are the possible reasons that cause errors in HTESSEL?*

  The performance shows different pattern in different catchments. Thus the possible reasons could be answered in three aspects. More studies focus on the internal flows and structure of HTESSEL.

Slower recession. By analyzing the components of flows of Section 3.5, the slower recession mainly comes from the subsurface flow Q_{sb} in HTESSEL (see figure 3.30). In temperate and mediterranean catchments which are less humid, the precipitation produce fast runoff directly, but less water fluxes percolate into deeper soil, meaning fewer attenuation on hydrograph. This is why the slower recession always occurs in wet regions, like part of tropical catchment and catchment K and R, instead of in temperate catchments. Therefore, in other words, the lack of routing is not the main reason that causes the slower falling limbs. The key component that controls the predicted recession limbs of the hydrograph is the reservoir(Fenicia et al. [2006]). And it could be learned from the comparison of parameters in Section 3.3.2 that the decrease of size of soil column in HTESSEL is a possible way to lower the occurrence of slower recession, particularly in tropical catchments. For temperate and mediterranean catchment, their problems are more focus on the fast runoff.

Mismatch in peaks. The soil moisture in HTESSEL is always higher than HBV and GR4J (see figure 3.13). Therefore, precipitation can easily exceed the top 50 cm of soil column in HTESSEL and produces surface runoff. If the catchment is relatively dry, for instance, temperate catchment and mediterranean catchment, less water fluxes go downwards. The whole soil column is set to 2.89m in HTESSEL. Only the top 50cm, less than one in five of soil depth is related to fast runoff. The remaining deeper soil column are mainly utilized to store water content. The mismatch in peaks in HBV and GR4J can be reproduced when calibrating to HTESSEL. This makes sense to answer the question why the slower recession always occurs in humid area, such as part of tropical catchments, while the overestimation or mismatch in peaks are more often in temperate and mediterranean catchments, although tropical has a higher soil moisture in the soil moisture figure 3.13.

Section 3.5 also compared the equation of fast runoff in HBV and HTESSEL, it could be learned that the parameterization of first 50cm in HTESSEL is a key factor to influence the peaks and fast surface runoff, of which orography parameter b is more than significant than other parameters. So it is possible to achieve a better fit of hydrograph in temperate or mediterrenean catchments by changing parameter b, or increasing the top 50cm to other values. This need further study in the future. In humid region, deeper soil column, more than four fifths of all column, shows stronger control over the performance of hydrograph and leads to slower recession. While in less humid region, top 50 cm of soil column has more control over the hydrograph and results in mismatch in peaks.

Monthly delay. Delay is linked to the slower falling limbs directly. The highest accumulated discharge delay with the slower attenuation of hydro-

graph. During this process, the soil moisture is involved. The soil column in HTESSEL causes the slower falling limb by making the simulated store large enough. As a result, it's clear that the slower recession invariably coincides with the emergence of a monthly delay, such as Catchment EA, EB, No, K, and R. Learning from the experiments in Section 3.3.2, Section 3.6 reproduces the delay again in catchment EB when calibrated to HTESSEL. It means the delay is caused by slower recession. It further illustrates the size of soil column in HTESSEL has close relationship with the delay, not only the recession.

By doing the modeling comparison, the main research question *"Which hydrological processes in HTESSEL could be improved to overcome poor performance of HTESSEL in modelling river discharge?"* can be answered now. Firstly, the analysis of both parameter changes and internal flows shows that if we utilize GR4J and HBV to simulate the discharge modelled by HTESSEL, their slow reservoirs usually increase. Therefore, HTESSEL needs to decrease the size of large soil column to get a better performance on falling limbs. Secondly, for improving the fast runoff, the effective depth should be a spatial variable. By increasing the value, this variable could overcome the overestimation in some places and get a smaller fast runoff, similarly, by decreasing the value, this variable could overcome underestimation of peaks in other places. Moreover, variable b, which is orography related parameter and could influence the fast runoff, should be optimized. Thus, more study could focus on the interplay of the soil infiltration capacity (determined by the effective depth) and the fast runoff parameters (which is parameter b).

This research contributes to the improvement of land surface model HTESSEL. In future, further studies could investigate a greater study on the parameterization in top 50cm in HTESSEL. In addition to this, the introduction of lateral exchange outside HTESSEL and the addition of parallel structure are worthwhile.

BIBLIOGRAPHY

Balsamo, G., Beljaars, A., Scipal, K., Viterbo, P., van den Hurk, B., Hirschi, M., and Betts, A. K. (2009). A revised hydrology for the ecmwf model: Verification from field site to terrestrial water storage and impact in the integrated forecast system. *Journal of hydrometeorology*, 10(3):623–643.

Blondin, C. (1991). Parameterization of land-surface processes in numerical weather prediction. In *Land Surface Evaporation*, pages 31–54. Springer.

BoM (2015). Hydrologic reference stations.

Bouaziz, L. J., Fenicia, F., Thirel, G., de Boer-Euser, T., Buitink, J., Brauer, C. C., De Niel, J., Dewals, B. J., Drogue, G., Grelier, B., et al. (2021). Behind the scenes of streamflow model performance. *Hydrology and Earth System Sciences*, 25(2):1069–1095.

Clark, M. P., Slater, A. G., Rupp, D. E., Woods, R. A., Vrugt, J. A., Gupta, H. V., Wagener, T., and Hay, L. E. (2008). Framework for understanding structural errors (fuse): A modular framework to diagnose differences between hydrological models. *Water Resources Research*, 44(12).

ECMWF (2016). Ifs documentation cycle cy34r1. *Digital soil map of the world (dsmw)*, epart iv.

Fenicia, F., Kavetski, D., Savenije, H. H., Clark, M. P., Schoups, G., Pfister, L., and Freer, J. (2014). Catchment properties, function, and conceptual model representation: is there a correspondence? *Hydrological Processes*, 28(4):2451–2467.

Fenicia, F., Savenije, H., Matgen, P., and Pfister, L. (2006). Is the groundwater reservoir linear? learning from data in hydrological modelling. *Hydrology and Earth System Sciences*, 10(1):139–150.

Fenicia, F., Savenije, H. H., Matgen, P., and Pfister, L. (2008). Understanding catchment behavior through stepwise model concept improvement. *Water Resources Research*, 44(1).

Gaba, C., Alamou, E., Afouda, A., and Diekkrüger, B. (2017). Improvement and comparative assessment of a hydrological modelling approach on 20 catchments of various sizes under different climate conditions. *Hydrological Sciences Journal*, 62(9):1499–1516.

Gupta, H. V., Kling, H., Yilmaz, K. K., and Martinez, G. F. (2009). Decomposition of the mean squared error and nse performance criteria: Implications for improving hydrological modelling. *Journal of hydrology*, 377(1-2):80–91.

Harlan, D., Wangsadipura, M., and Munajat, C. M. (2010). Rainfall-runoff modeling of citarum hulu river basin by using gr4j. In *Proceedings of the world congress on engineering*, volume 2, pages 1607–1611.

Huang, M., Liang, X., and Leung, L. R. (2008). A generalized subsurface flow parameterization considering subgrid spatial variability of recharge and topography. *Journal of Hydrometeorology*, 9(6):1151–1171.

Kim, H. (2017). Global soil wetness project phase 3 atmospheric boundary conditions. experiment 1.

Lindström, G., Johansson, B., Persson, M., Gardelin, M., and Bergström, S. (1997). Development and test of the distributed hbv-96 hydrological model. *Journal of hydrology*, 201(1-4):272–288.

Michel, C. (1989). Un modèle pluie-débit journalier à trois paramètres. *La Houille Blanche*, (2):113–122.

Moriasi, D. N., Arnold, J. G., Van Liew, M. W., Bingner, R. L., Harmel, R. D., and Veith, T. L. (2007). Model evaluation guidelines for systematic quantification of accuracy in watershed simulations. *Transactions of the ASABE*, 50(3):885–900.

Ngo-Duc, T., Oki, T., and Kanae, S. (2007). A variable streamflow velocity method for global river routing model: model description and preliminary results. *Hydrology and Earth System Sciences Discussions*, 4(6):4389–4414.

Nijzink, R., Hutton, C., Pechlivanidis, I., Capell, R., Arheimer, B., Freer, J., Han, D., Wagener, T., McGuire, K., Savenije, H., et al. (2016). The evolution of root-zone moisture capacities after deforestation: a step towards hydrological predictions under change? *Hydrology and Earth System Sciences*, 20(12):4775–4799.

Pappenberger, F., Cloke, H., Balsamo, G., Ngo-Duc, T., and Oki, T. (2010). Global runoff routing with the hydrological component of the ecmwf nwp system. *International Journal of Climatology*, 30(14):2155–2174.

ParisTech, M. (2014). Radiation data.

Perrin, C., Michel, C., and Andréassian, V. (2003). Improvement of a parsimonious model for streamflow simulation. *Journal of hydrology*, 279(1-4):275–289.

Pushpalatha, R., Perrin, C., Le Moine, N., Mathevet, T., and Andréassian, V. (2011). A downward structural sensitivity analysis of hydrological models to improve low-flow simulation. *Journal of hydrology*, 411(1-2):66–76.

van den Brink, N. (2018). Influence of hydrological model structures on extreme high flow simulations in the meuse basin.

Van Den Hurk, B., Viterbo, P., Beljaars, A., and Betts, A. (2000). Offline validation of the era40 surface scheme, ecmwf techmemo 295. *Reading, UK*.

Van Esse, W., Perrin, C., Booij, M. J., Augustijn, D. C., Fenicia, F., Kavetski, D., and Lobligeois, F. (2013). The influence of conceptual model structure on model performance: a comparative study for 237 french catchments. *Hydrology and Earth System Sciences*, 17(10):4227–4239.

van Oorschot, F. (2020). The hydrologically active rootzone in climate models.

van Oorschot, F., van der Ent, R. J., Hrachowitz, M., and Alessandri, A. (2021). Climate-controlled root zone parameters show potential to improve water flux simulations by land surface models. *Earth System Dynamics*, 12(2):725–743.

Wheater, H., Jakeman, A., and Beven, K. (1993). Progress and directions in rainfall-runoff modelling.

Wipfler, E., Metselaar, K., Van Dam, J., Feddes, R., Meijgaard, E. v., Van Ulft, L., Hurk, B., Zwart, S., and Bastiaanssen, W. (2011). Seasonal evaluation of the land surface scheme htessel against remote sensing derived energy fluxes of the transdanubian region in hungary. *Hydrology and earth system sciences*, 15(4):1257–1271.

Yang, W., Chen, H., Xu, C.-Y., Huo, R., Chen, J., and Guo, S. (2020). Temporal and spatial transferabilities of hydrological models under different climates and underlying surface conditions. *Journal of Hydrology*, 591:125276.

Young, P. (2001). Data-based mechanistic modelling and validation of rainfall-flow processes. *Model validation: perspectives in hydrological science*, pages 117–161.

Zhao, R., Liu, X., et al. (1995). The xinanjiang model. *Computer models of watershed hydrology.*, pages 215–232.

A | APPENDIX

A.1 THE MONTHLY AND ANNUAL PLOTS OF GR4J, HBV AND HTESSEL

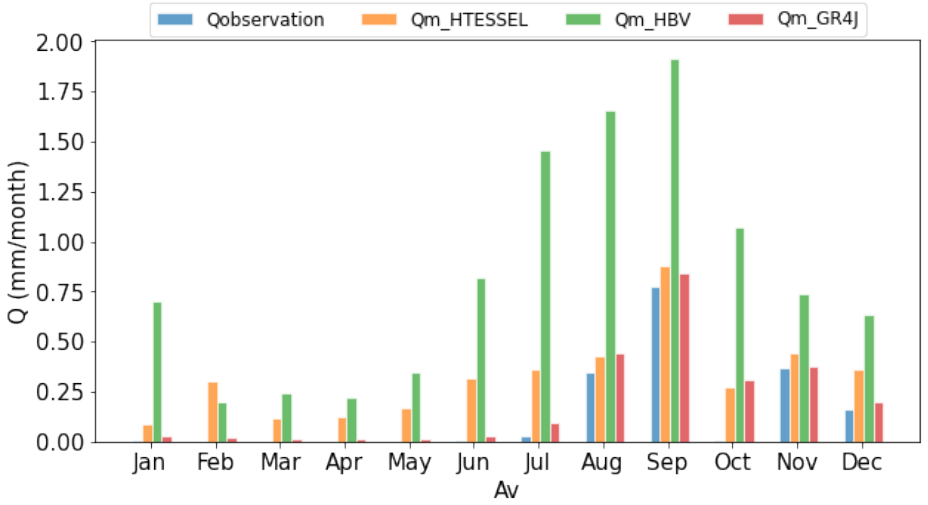
Qobservation
Qm_HTESSEL
Qm_HBV
Qm_GR4J
Q (mm/month)
2.00
1.75
1.50
1.25
1.00
0.75
0.50
0.25
0.00
Jan
Feb
Mar
Apr
May
Jun
Jul
Aug
Sep
Oct
Nov
Dec
Av

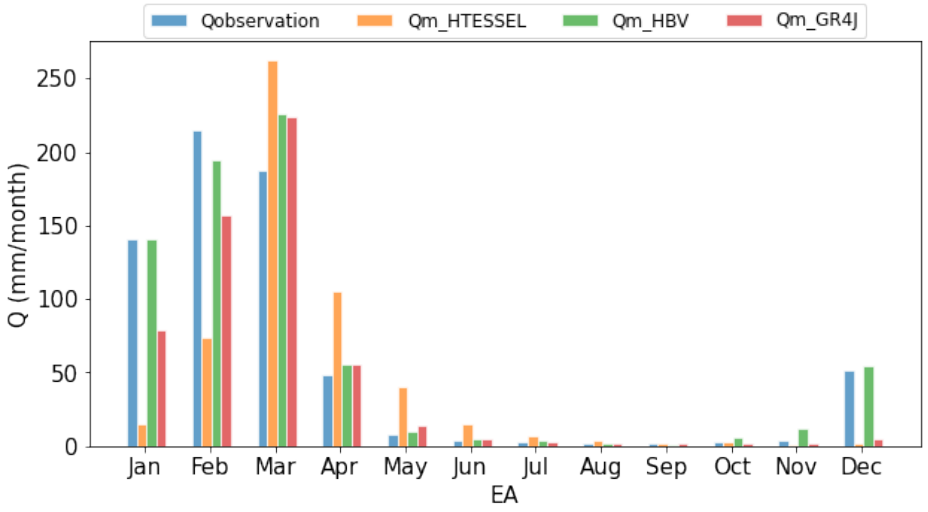
Qobservation
Qm_HTESSEL
Qm_HBV
Qm_GR4J
Q (mm/month)
250
200
150
100
50
0
Jan
Feb
Mar
Apr
May
Jun
Jul
Aug
Sep
Oct
Nov
Dec
EA

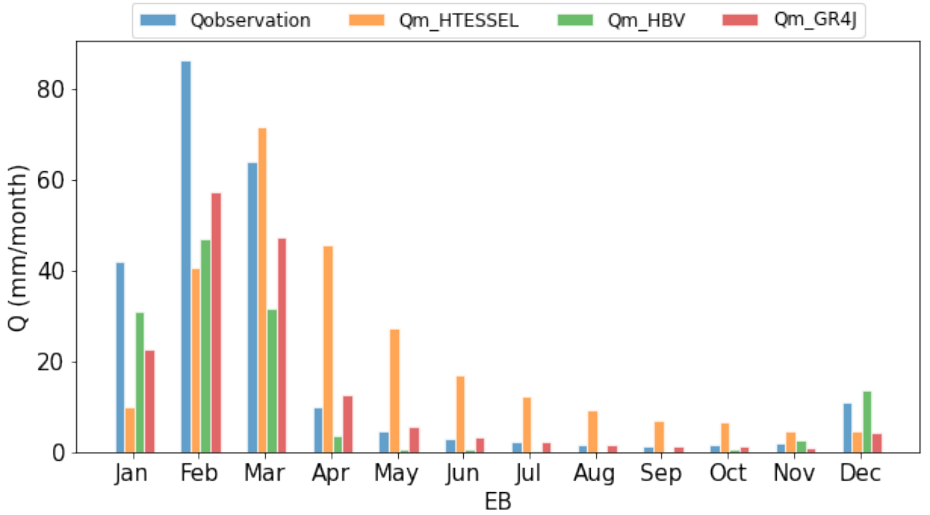
Qobservation
Qm_HTESSEL
Qm_HBV
Qm_GR4J
Q (mm/month)
80
60
40
20
0
Jan
Feb
Mar
Apr
May
Jun
Jul
Aug
Sep
Oct
Nov
Dec
EB

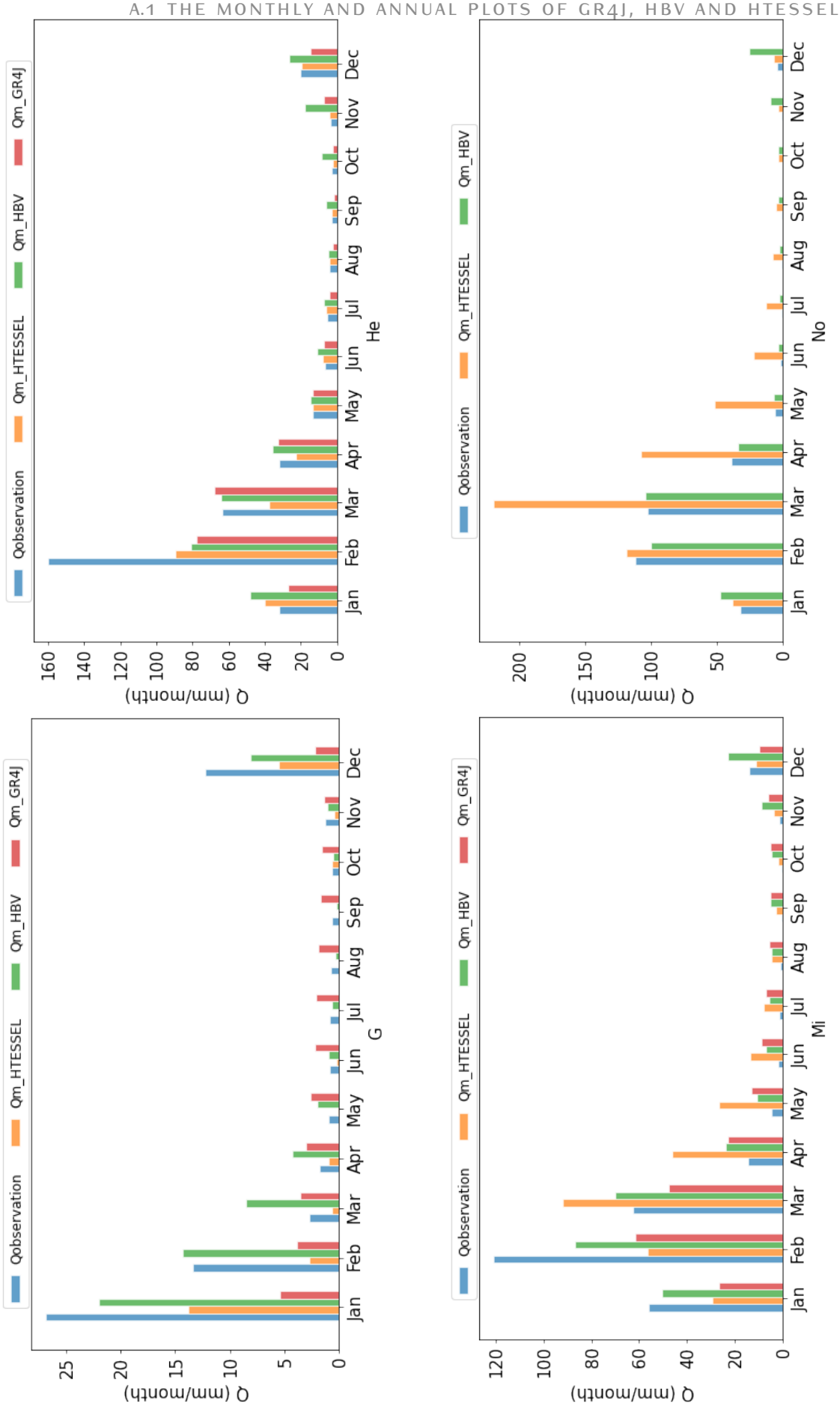
Qobservation
Qm_HTESSEL
Qm_HBV
Qm_GR4J
Q (mm/month)
Jan
Feb
Mar
Apr
May
Jun
Jul
Aug
Sep
Oct
Nov
Dec
He
No
G
Mi

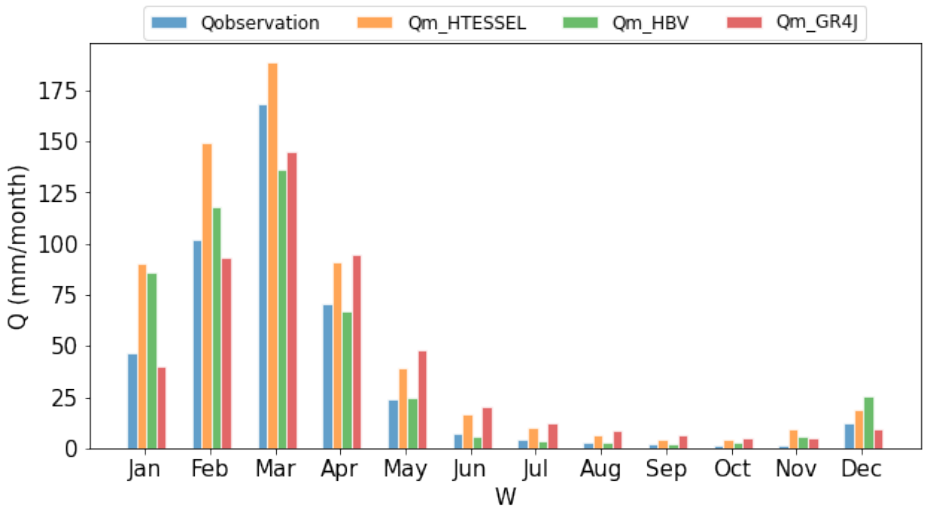
Qobservation
Qm_HTESSEL
Qm_HBV
Qm_GR4J
Q (mm/month)
0
25
50
75
100
125
150
175
Jan
Feb
Mar
Apr
May
Jun
Jul
Aug
Sep
Oct
Nov
Dec
W

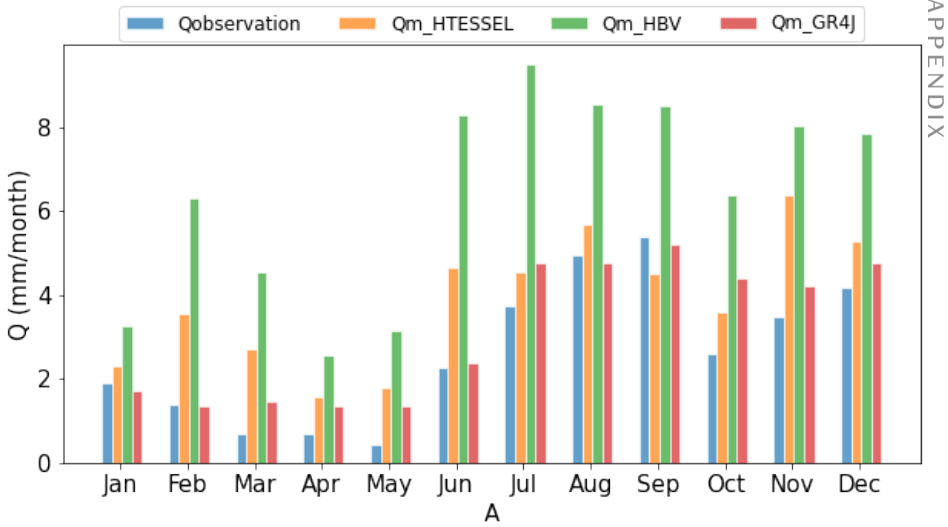
Qobservation
Qm_HTESSEL
Qm_HBV
Qm_GR4J
Q (mm/month)
0
2
4
6
8
Jan
Feb
Mar
Apr
May
Jun
Jul
Aug
Sep
Oct
Nov
Dec
A

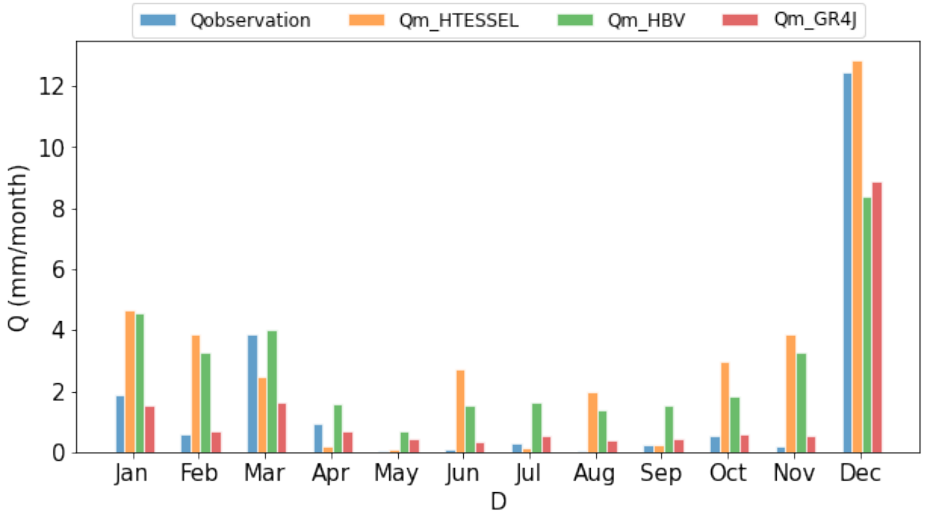
Qobservation
Qm_HTESSEL
Qm_HBV
Qm_GR4J
Q (mm/month)
0
2
4
6
8
10
12
Jan
Feb
Mar
Apr
May
Jun
Jul
Aug
Sep
Oct
Nov
Dec
D

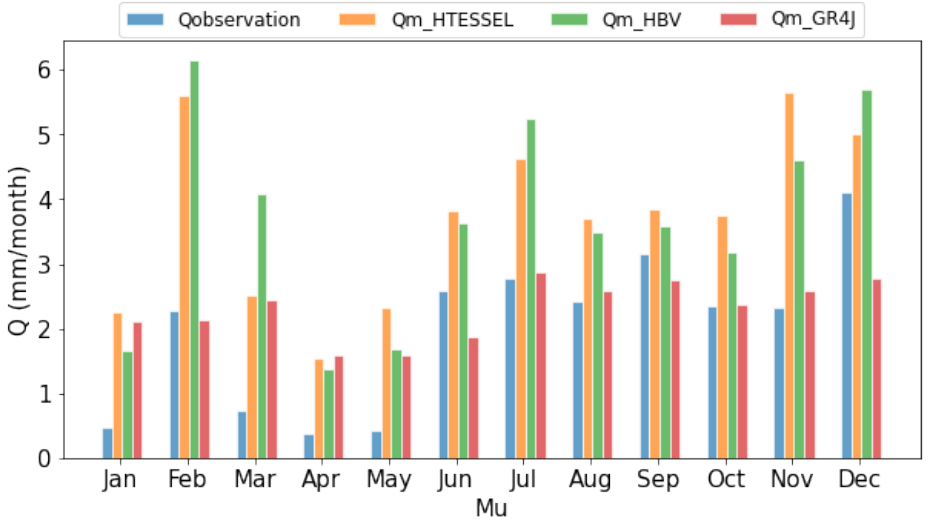
Qobservation
Qm_HTESSEL
Qm_HBV
Qm_GR4J
Q (mm/month)
0
1
2
3
4
5
6
Jan
Feb
Mar
Apr
May
Jun
Jul
Aug
Sep
Oct
Nov
Dec
Mu

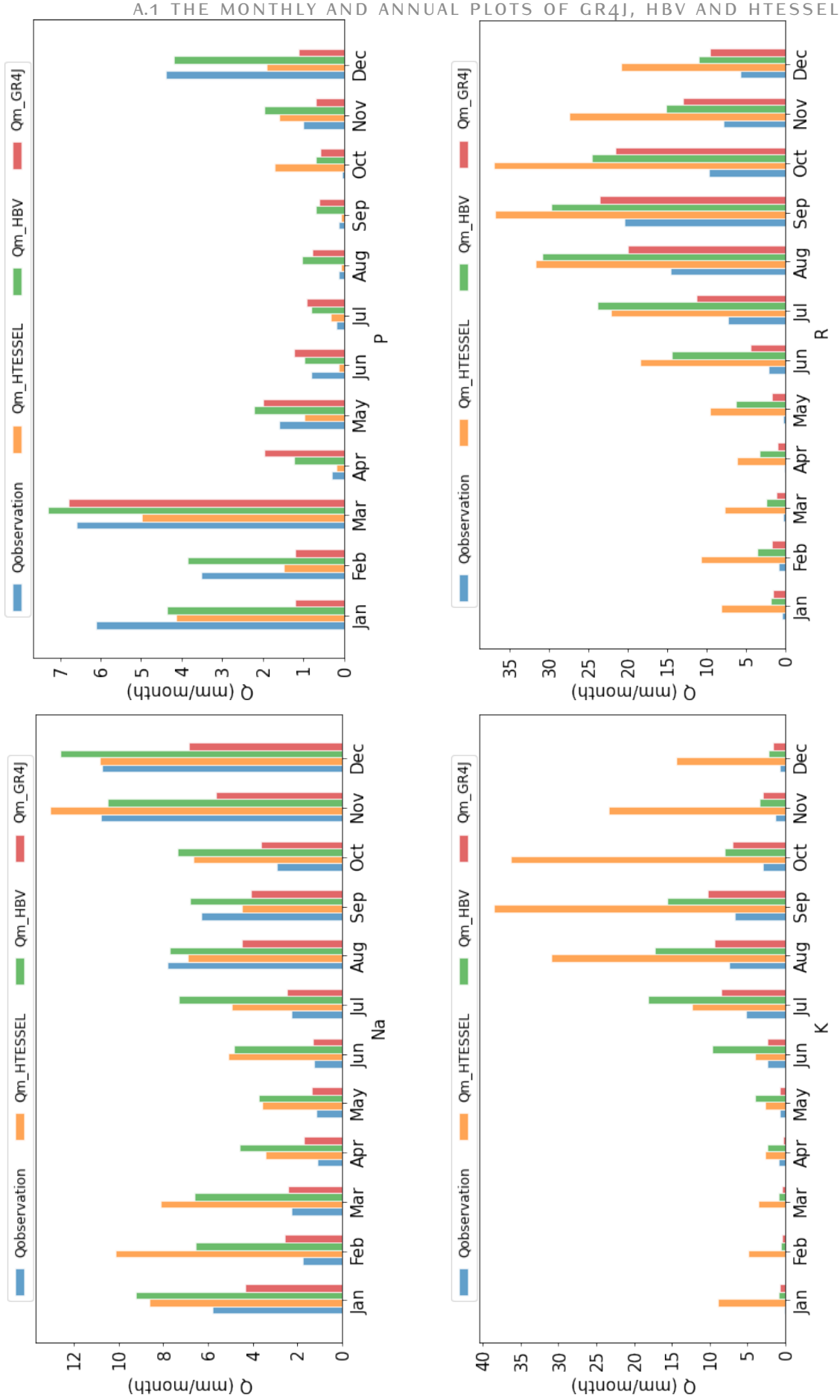
Qobservation
Qm_HTESSEL
Qm_HBV
Qm_GR4J
Jan
Feb
Mar
Apr
May
Jun
Jul
Aug
Sep
Oct
Nov
Dec
Q (mm/month)
P
R
Na
K

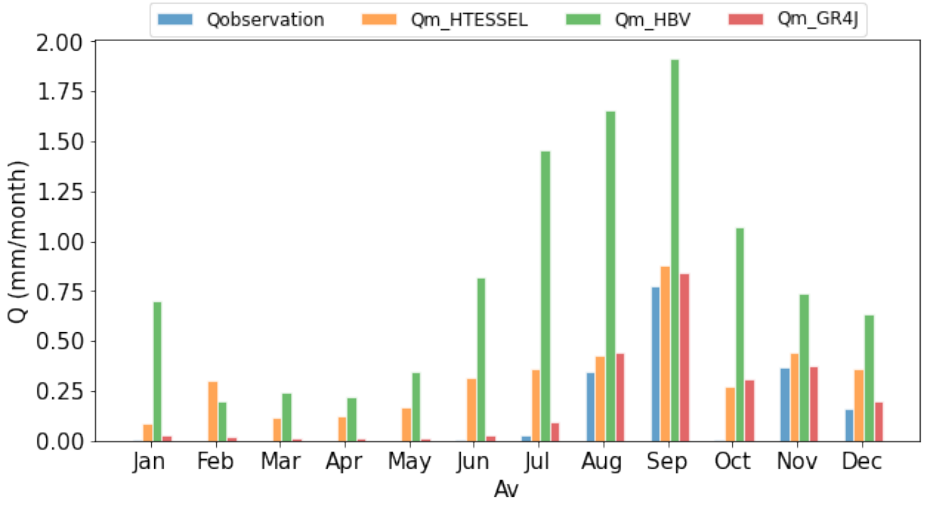
Qobservation
Qm_HTESSEL
Qm_HBV
Qm_GR4J
Q (mm/month)
2.00
1.75
1.50
1.25
1.00
0.75
0.50
0.25
0.00
Jan
Feb
Mar
Apr
May
Jun
Jul
Aug
Sep
Oct
Nov
Dec
Av

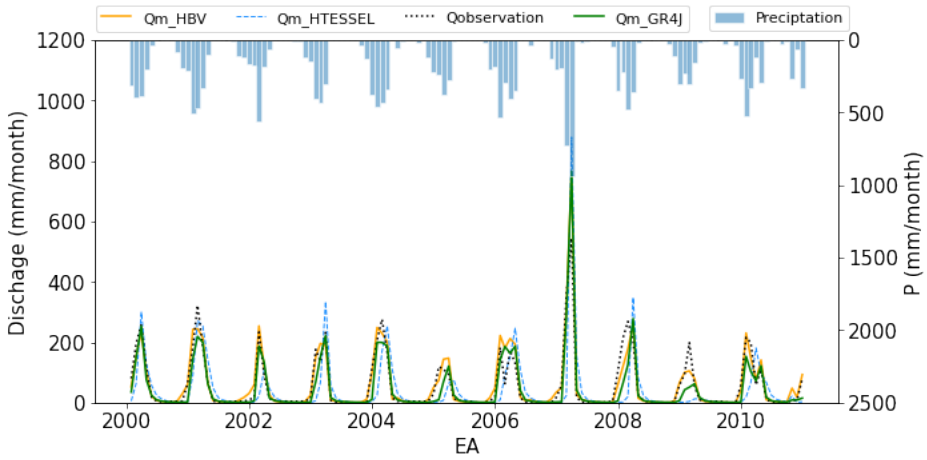
Qm_HBV
Qm_HTESSEL
Qobservation
Qm_GR4J
Preciptation
Dischage (mm/month)
P (mm/month)
1200
1000
800
600
400
200
0
0
500
1000
1500
2000
2500
2000
2002
2004
2006
2008
2010
EA

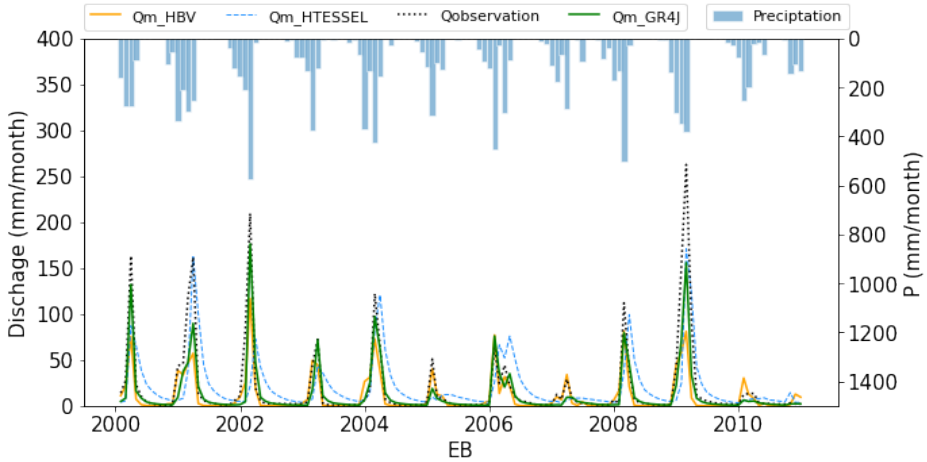
Qm_HBV
Qm_HTESSEL
Qobservation
Qm_GR4J
Preciptation
Dischage (mm/month)
P (mm/month)
400
350
300
250
200
150
100
50
0
0
200
400
600
800
1000
1200
1400
2000
2002
2004
2006
2008
2010
EB

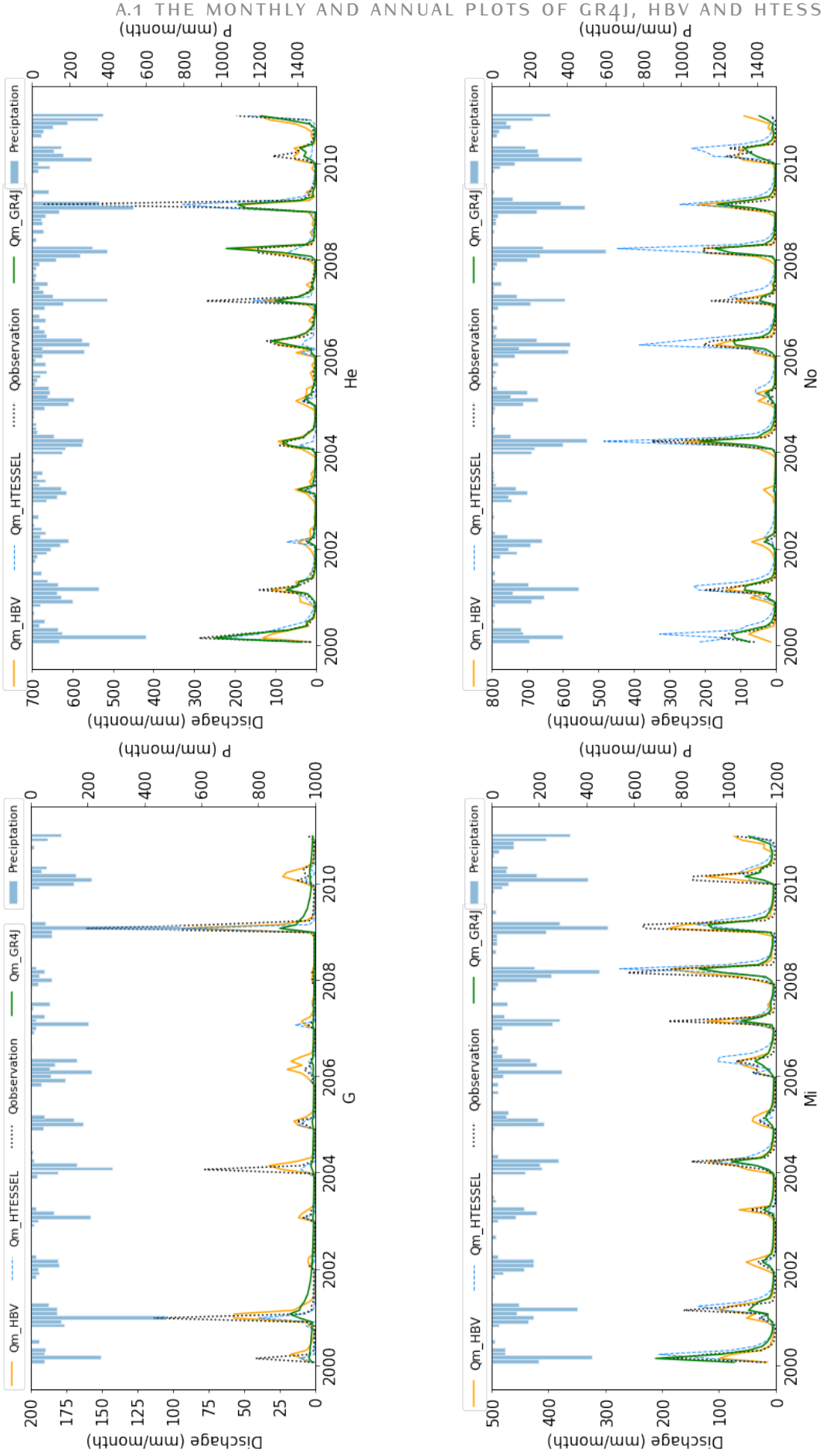
Qm_HBV
Qm_HTESSEL
Qobservation
Qm_GR4J
Preciptation
Discharge (mm/month)
P (mm/month)
He
No
G
Mi

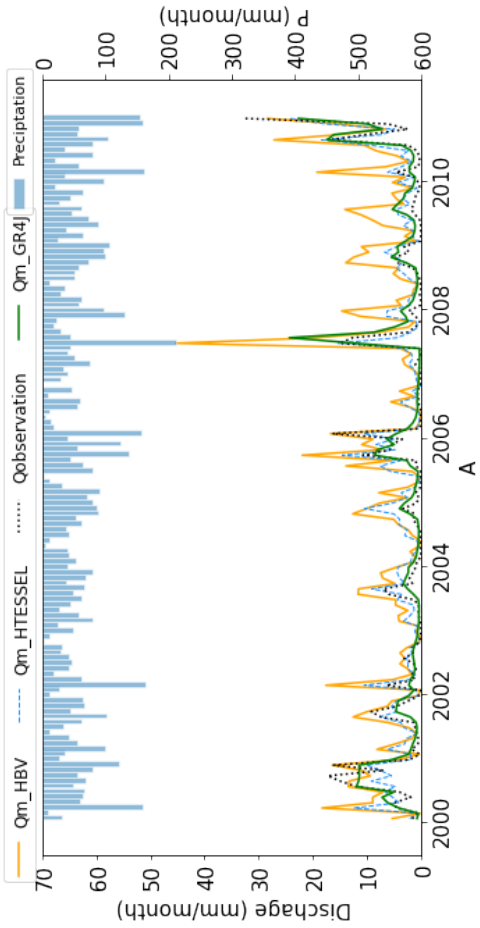
A
Discharge (mm/month)
P (mm/month)
Qm_HBV
Qm_HTESSEL
Qobservation
Qm_GR4J
Preciptation

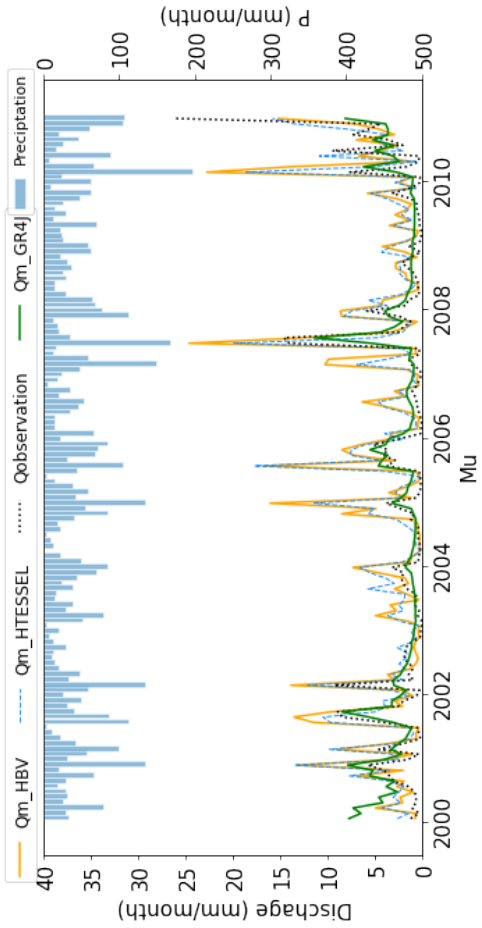
Mu
Discharge (mm/month)
P (mm/month)
Qm_HBV
Qm_HTESSEL
Qobservation
Qm_GR4J
Preciptation

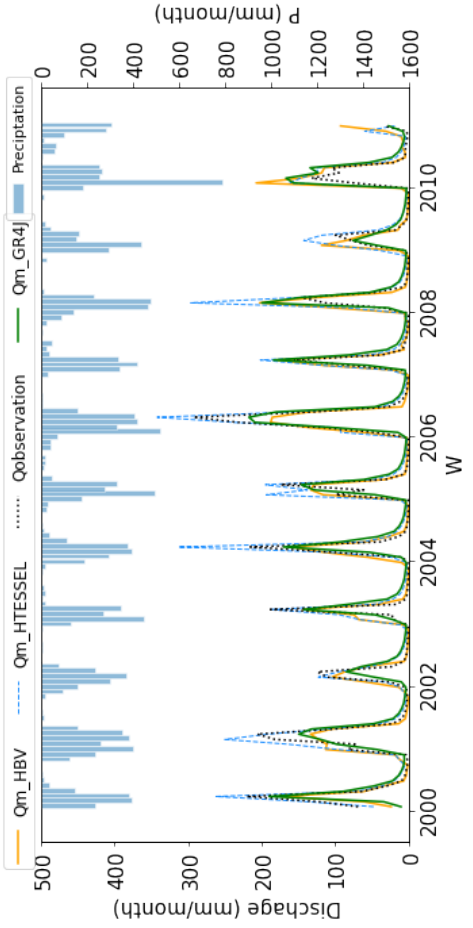
W
Discharge (mm/month)
P (mm/month)
Qm_HBV
Qm_HTESSEL
Qobservation
Qm_GR4J
Preciptation

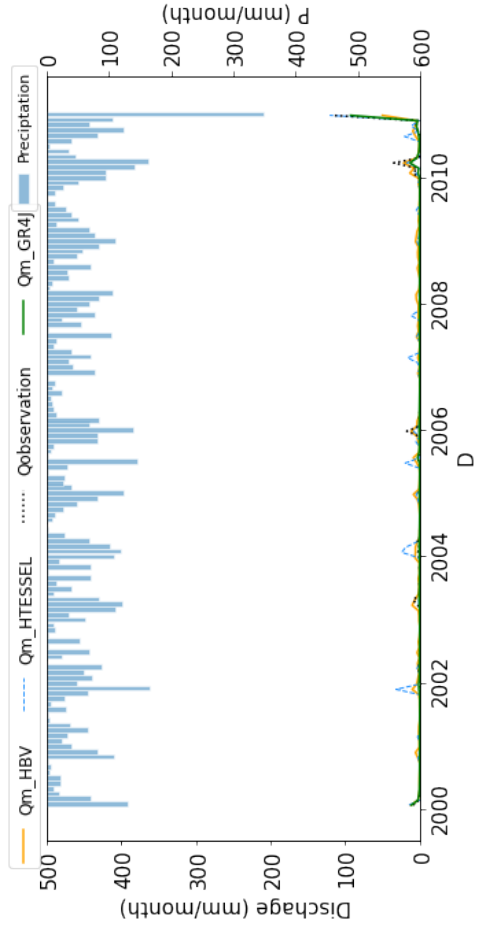
D
Discharge (mm/month)
P (mm/month)
Qm_HBV
Qm_HTESSEL
Qobservation
Qm_GR4J
Preciptation

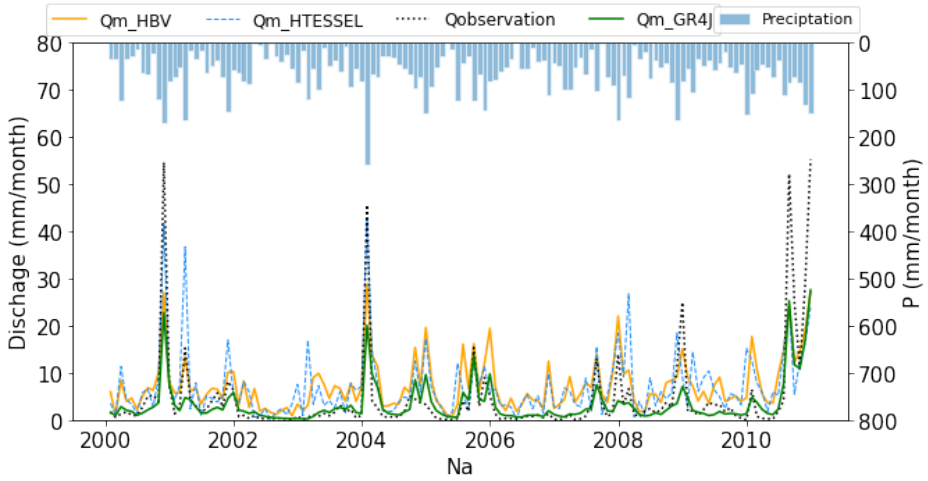
Qm_HBV
Qm_HTESSEL
Qobservation
Qm_GR4J
Preciptation
Dischage (mm/month)
P (mm/month)
Na
2000
2002
2004
2006
2008
2010

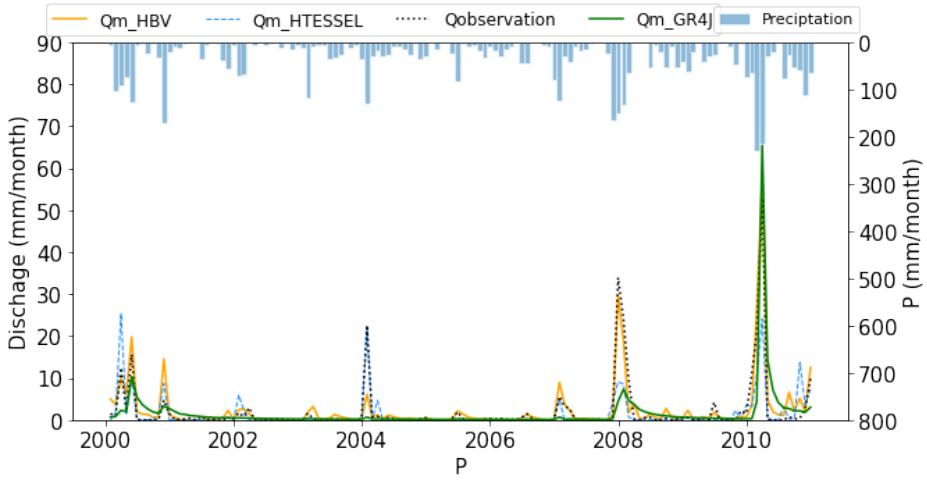
Qm_HBV
Qm_HTESSEL
Qobservation
Qm_GR4J
Preciptation
Dischage (mm/month)
P (mm/month)
P
2000
2002
2004
2006
2008
2010

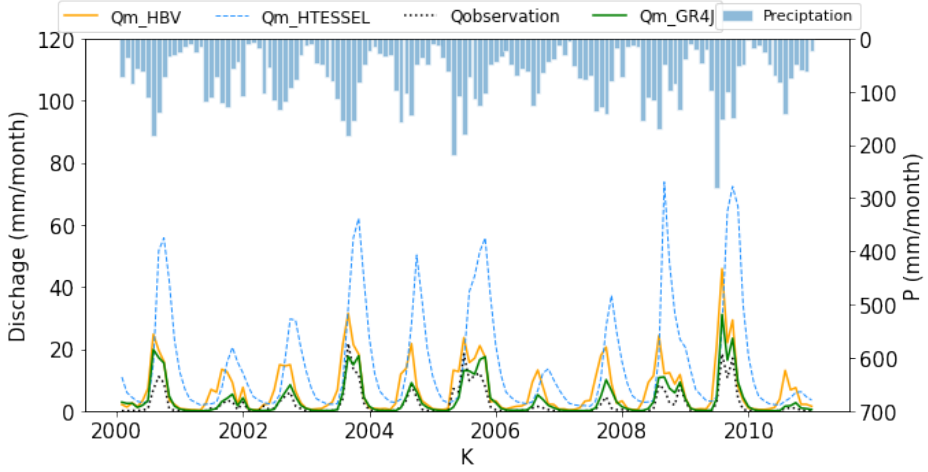
Qm_HBV
Qm_HTESSEL
Qobservation
Qm_GR4J
Preciptation
Dischage (mm/month)
P (mm/month)
K
2000
2002
2004
2006
2008
2010

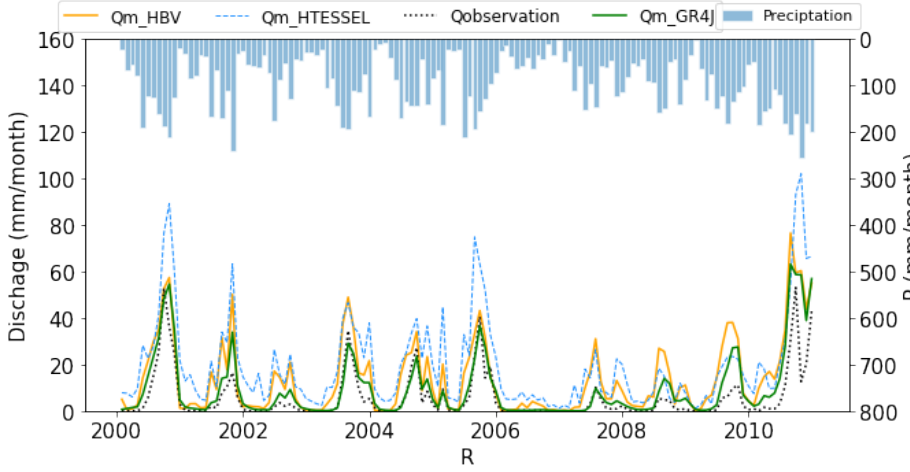
Qm_HBV
Qm_HTESSEL
Qobservation
Qm_GR4J
Preciptation
Dischage (mm/month)
P (mm/month)
R
2000
2002
2004
2006
2008
2010

A.2 THE CALIBRATION RESULTS IN GR4J, HBV AND HT-ESSEL

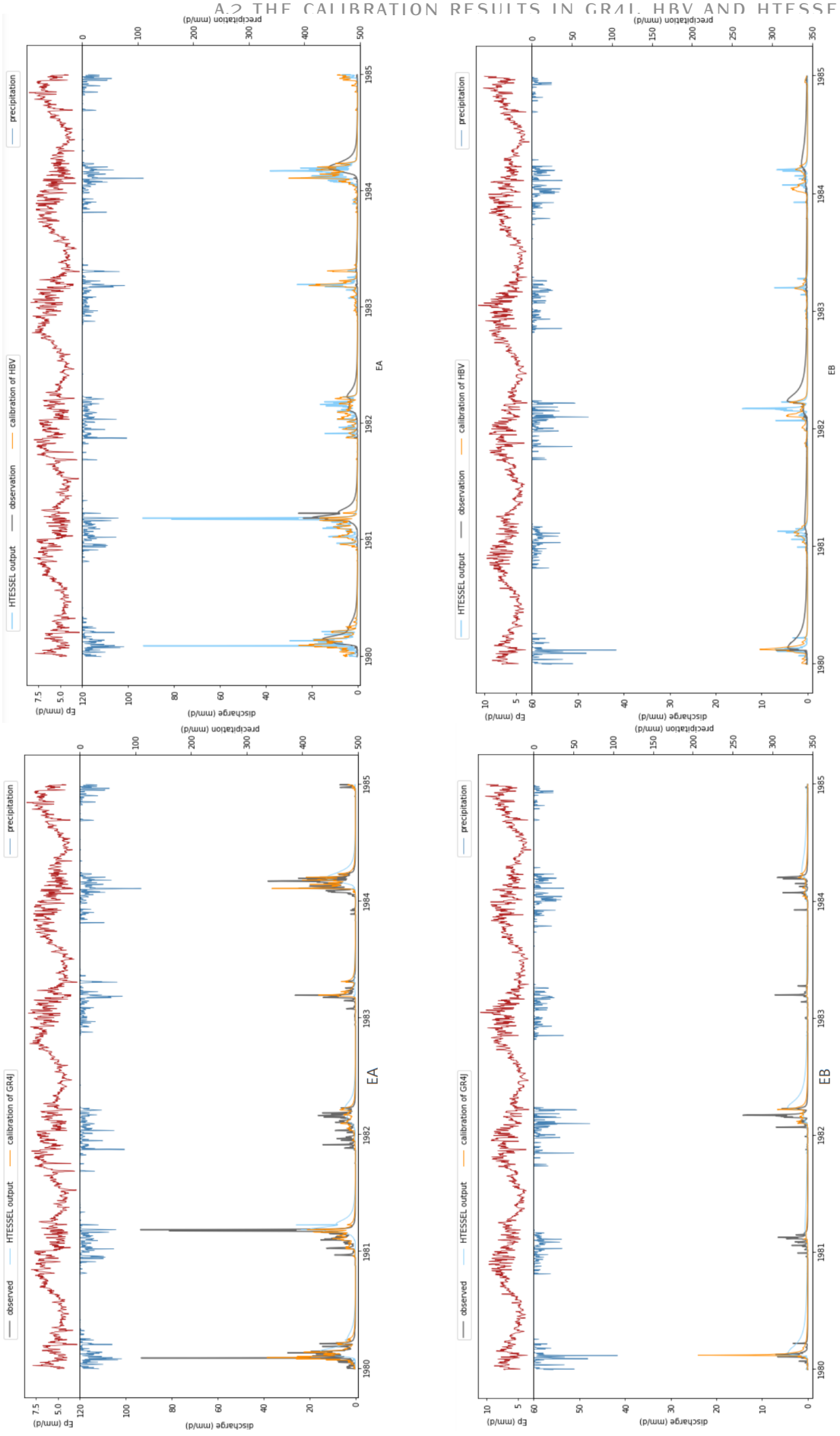
observed
HTESSEL output
calibration of GR4J
precipitation
EA
EB
Ep (mm/d)
discharge (mm/d)
precipitation (mm/d)
HTESSEL output
observation
calibration of HBV
precipitation

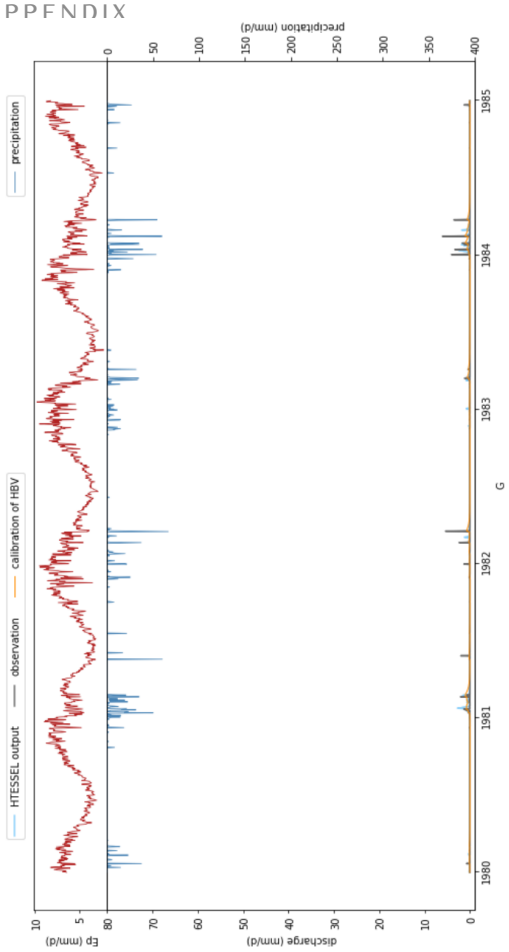
precipitation
HTESSEL output
observation
calibration of HBV
Ep (mm/d)
discharge (mm/d)
precipitation (mm/d)
G

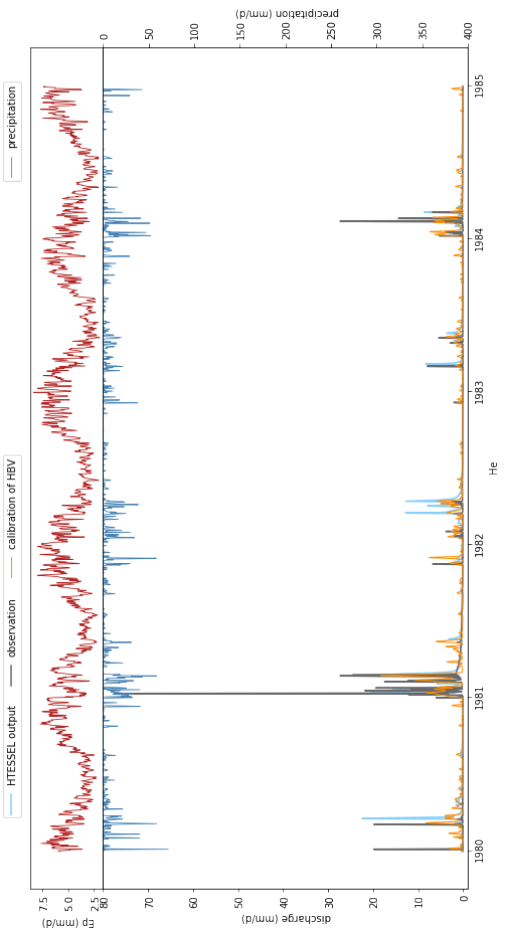
precipitation
HTESSEL output
observation
calibration of HBV
Ep (mm/d)
discharge (mm/d)
precipitation (mm/d)
He

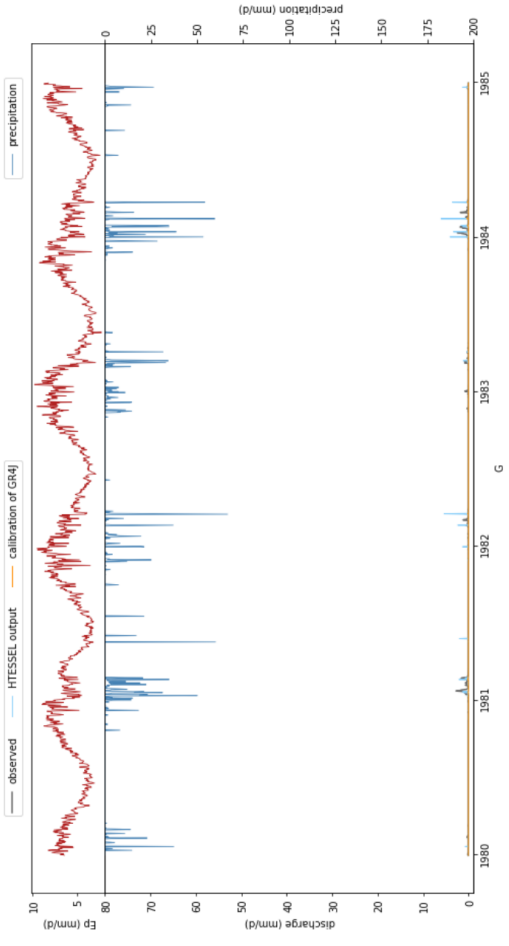
observed
HTESSEL output
calibration of GR4J
precipitation
Ep (mm/d)
discharge (mm/d)
precipitation (mm/d)
G

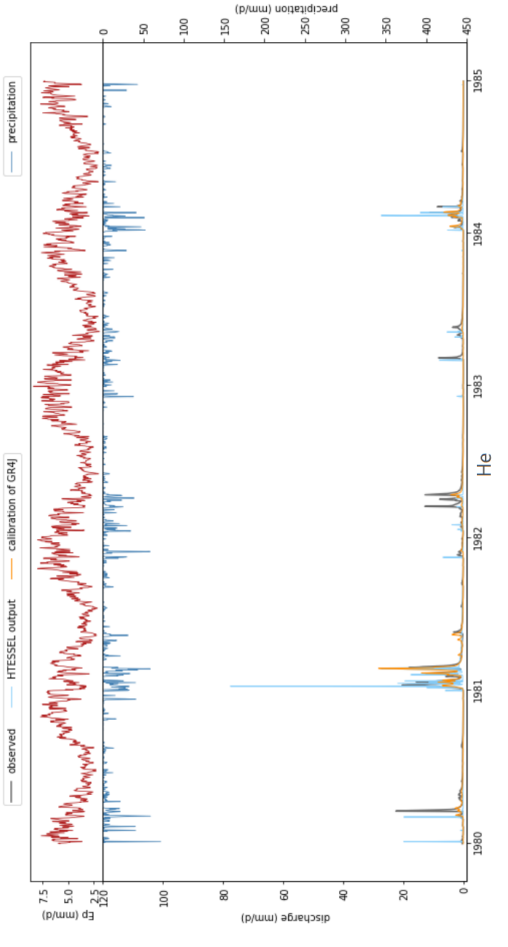
observed
HTESSEL output
calibration of GR4J
precipitation
Ep (mm/d)
discharge (mm/d)
precipitation (mm/d)
He

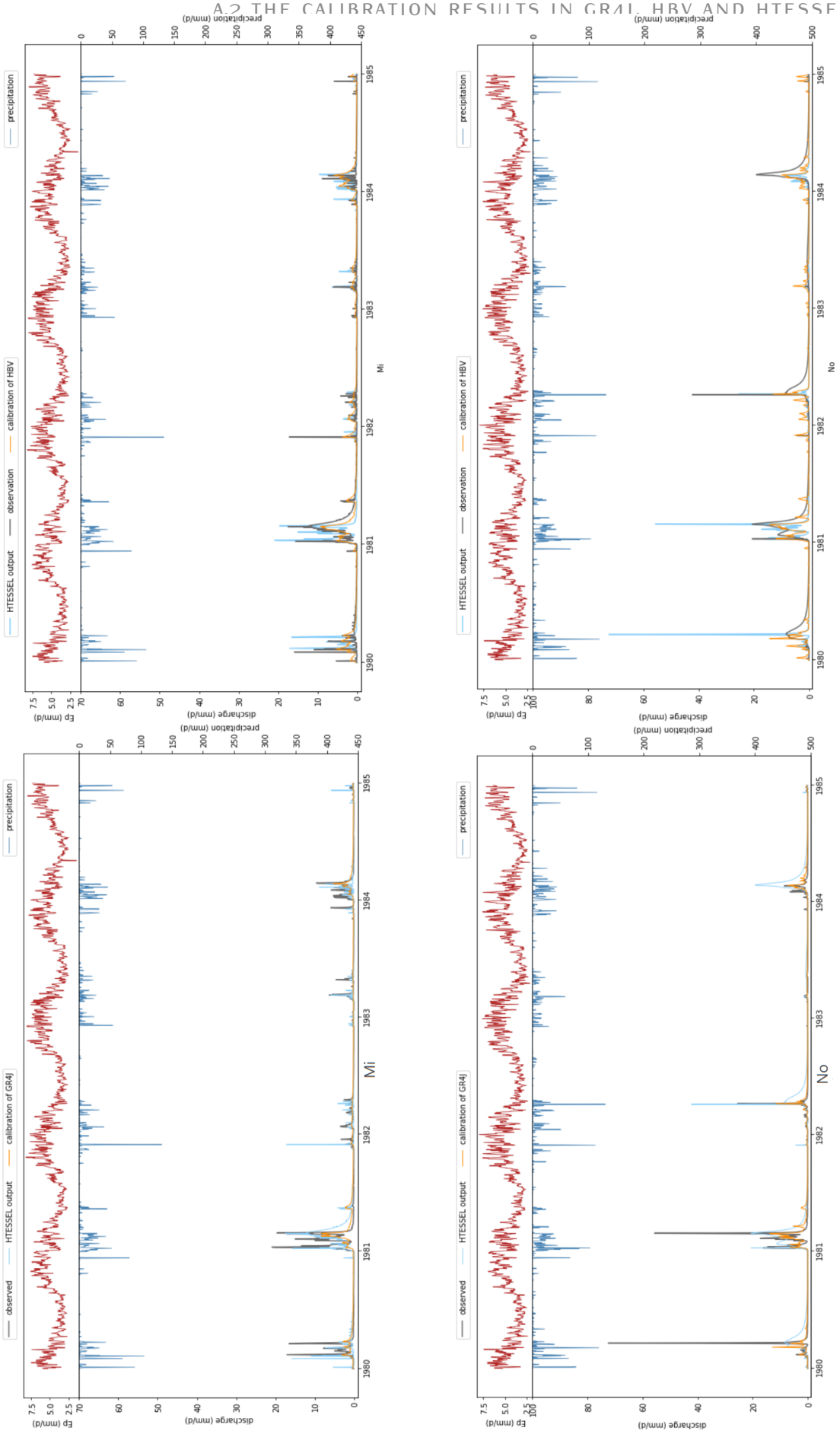
observed
HTESSEL output
calibration of GR4j
calibration of HBV
precipitation
EP (mm/d)
discharge (mm/d)
precipitation (mm/d)
Mi
No

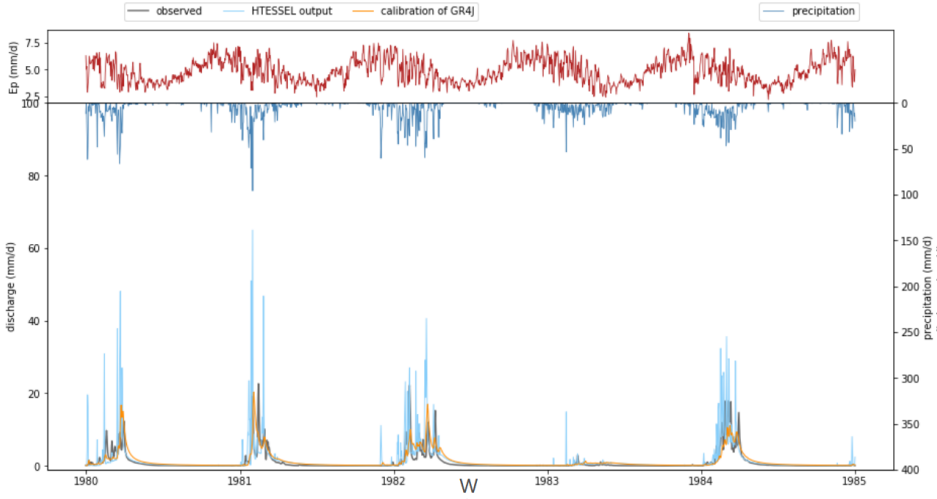
observed
HTESSEL output
calibration of GR4J
precipitation
Ep (mm/d)
discharge (mm/d)
precipitation (mm/d)
W

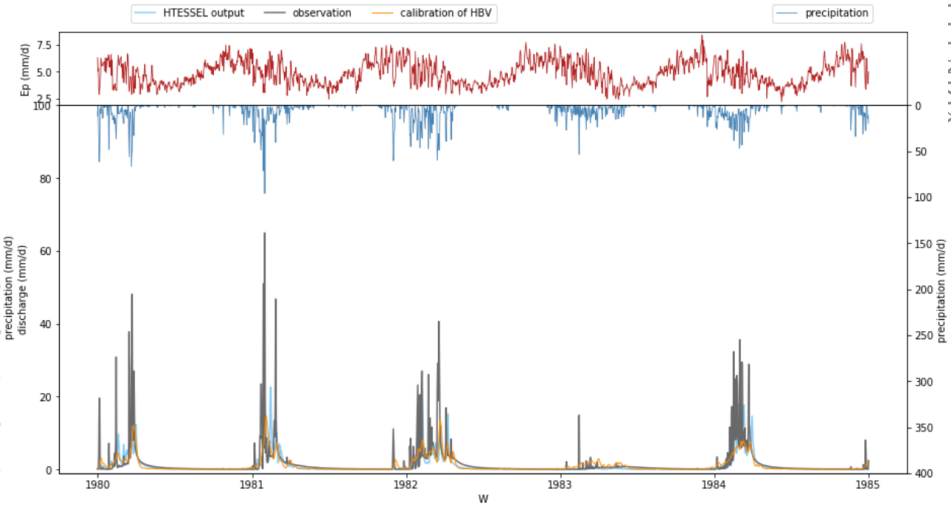
HTESSEL output
observation
calibration of HBV
precipitation
Ep (mm/d)
discharge (mm/d)
precipitation (mm/d)
W

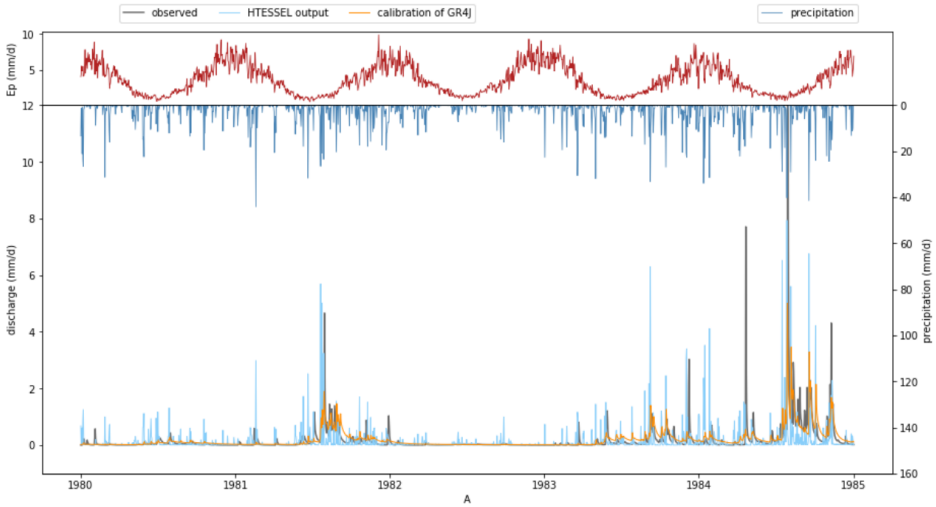
observed
HTESSEL output
calibration of GR4J
precipitation
Ep (mm/d)
discharge (mm/d)
precipitation (mm/d)
A

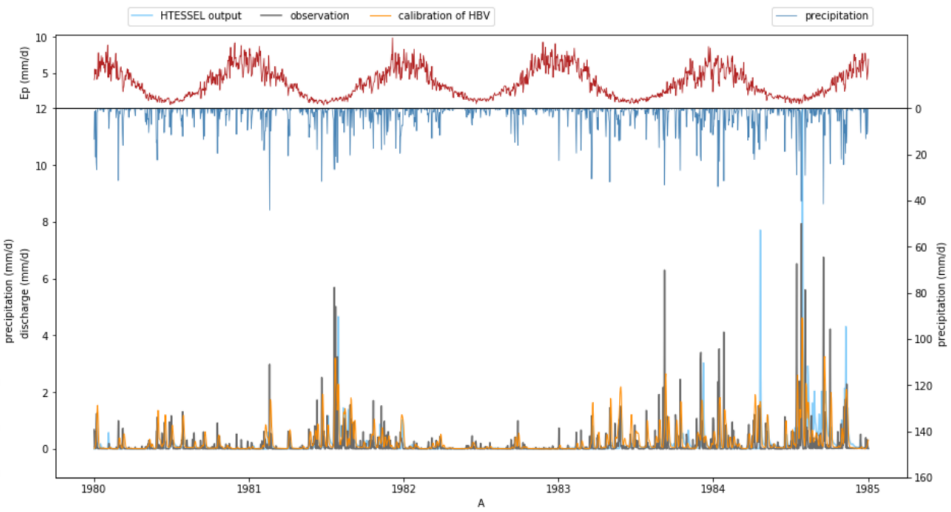
HTESSEL output
observation
calibration of HBV
precipitation
Ep (mm/d)
discharge (mm/d)
precipitation (mm/d)
A

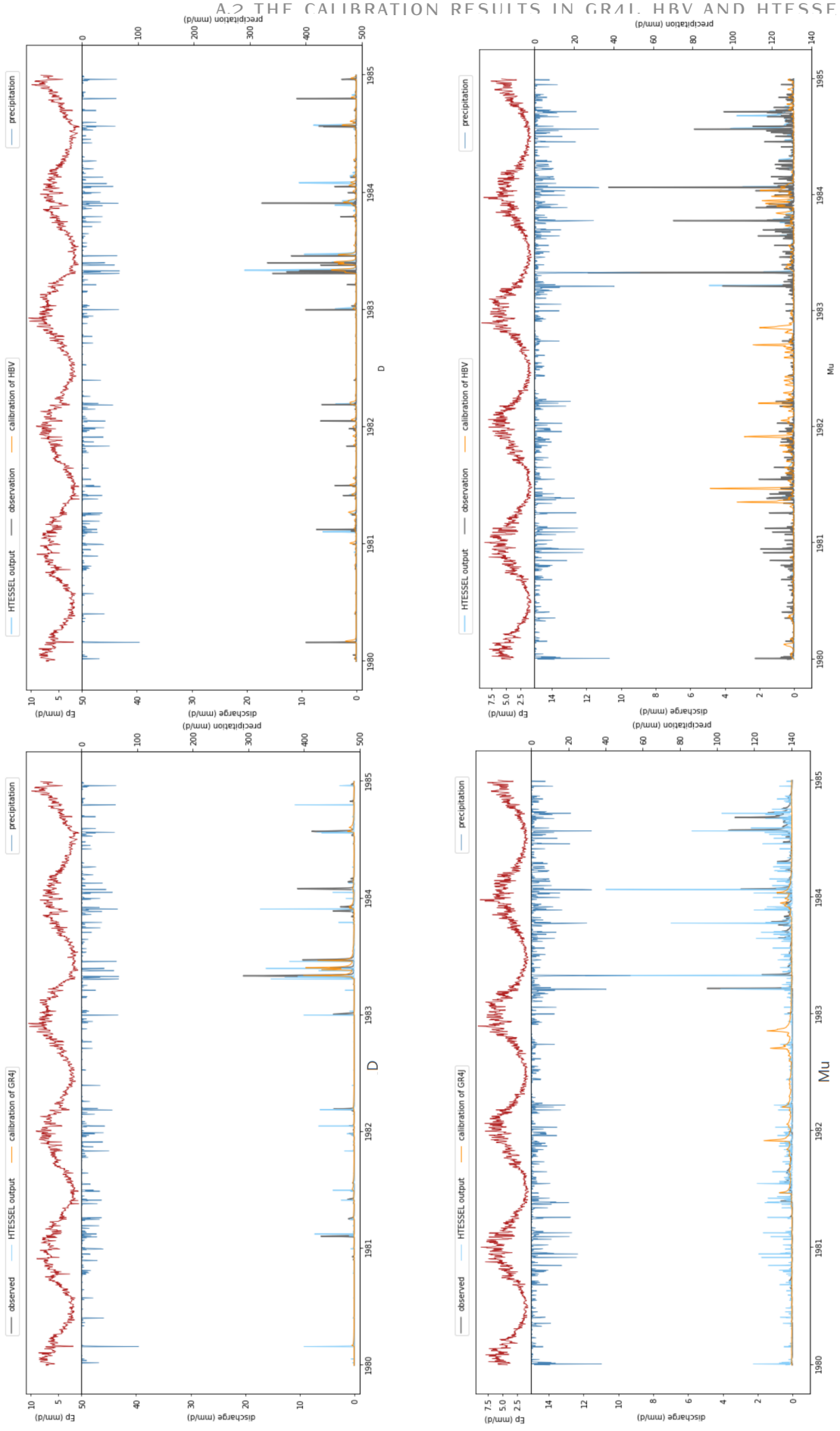
observed
HTESSEL output
calibration of GR4j
precipitation
HTESSEL output
observation
calibration of HBV
precipitation
D
Mu
discharge (mm/d)
precipitation (mm/d)
EP (mm/d)

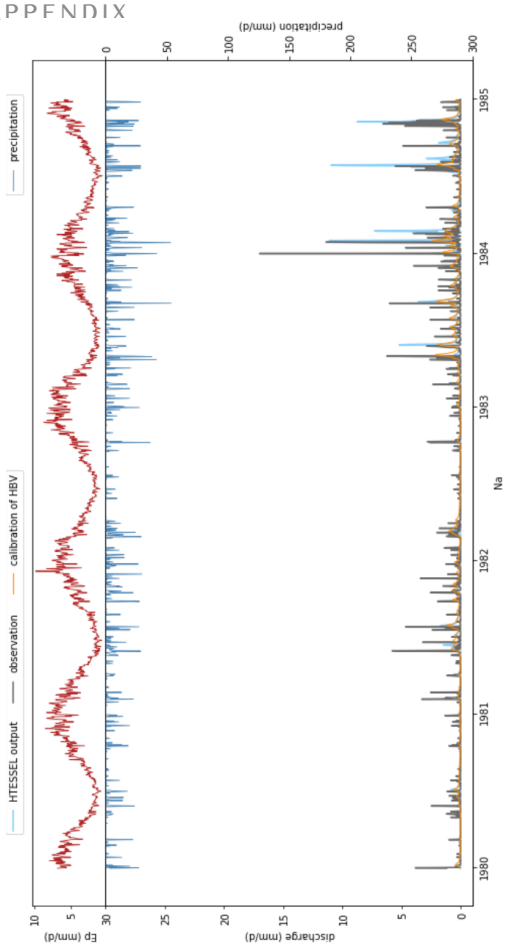
precipitation
HTESSEL output
observation
calibration of HBV
EP (mm/d)
discharge (mm/d)
precipitation (mm/d)
Na

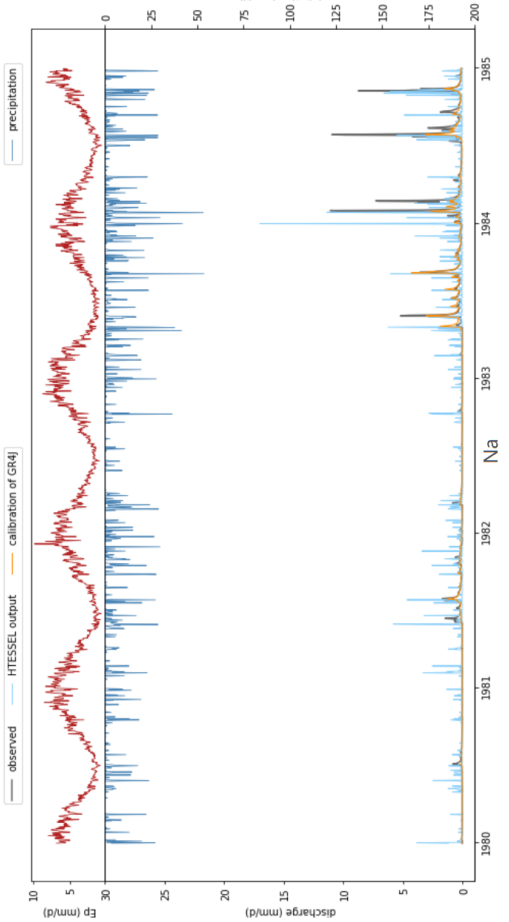
observed
HTESSEL output
calibration of GR4J
precipitation
EP (mm/d)
discharge (mm/d)
precipitation (mm/d)
Na

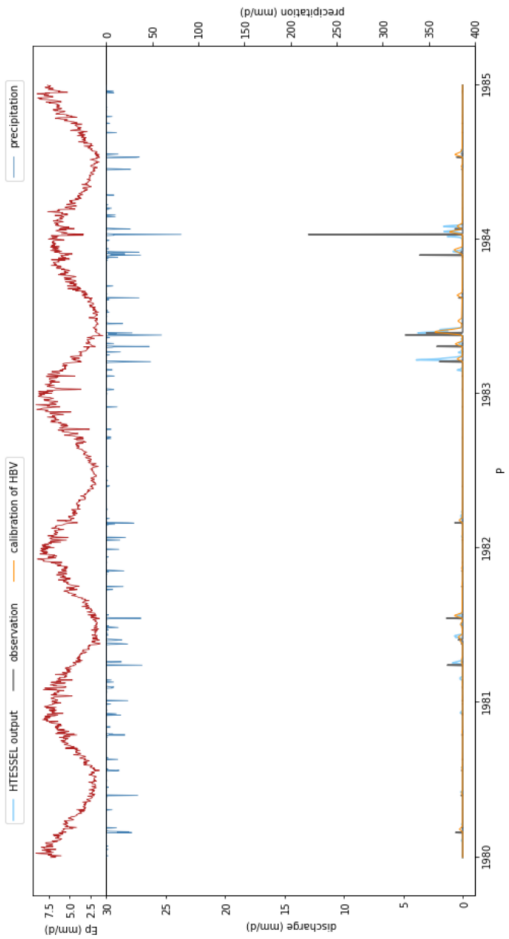
precipitation
HTESSEL output
observation
calibration of HBV
EP (mm/d)
discharge (mm/d)
precipitation (mm/d)
P

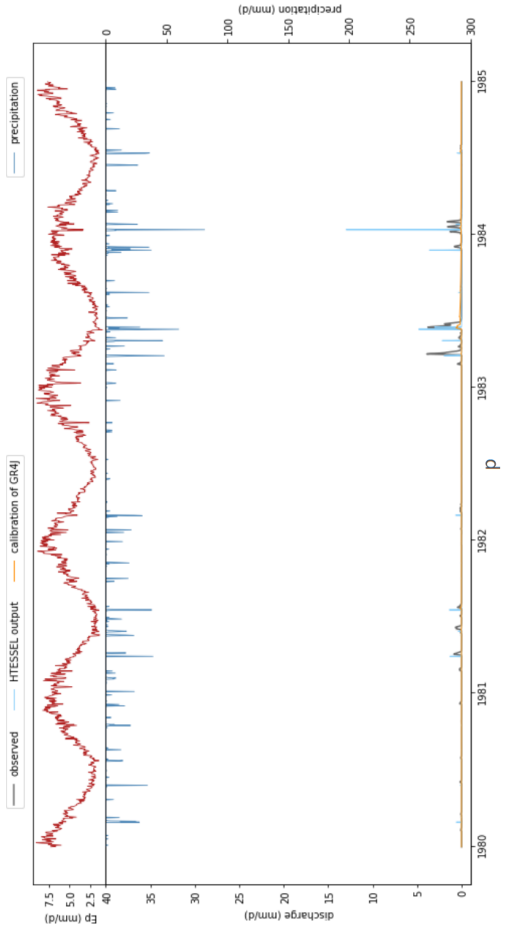
observed
HTESSEL output
calibration of GR4J
precipitation
EP (mm/d)
discharge (mm/d)
precipitation (mm/d)
P

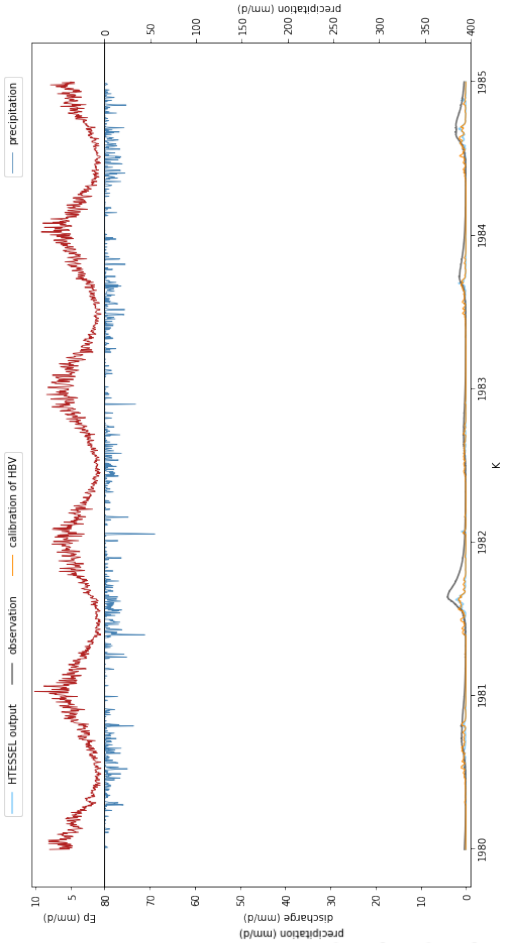
precipitation
HTESSEL output
observation
calibration of HBV
Ep (mm/d)
precipitation (mm/d)
discharge (mm/d)
K

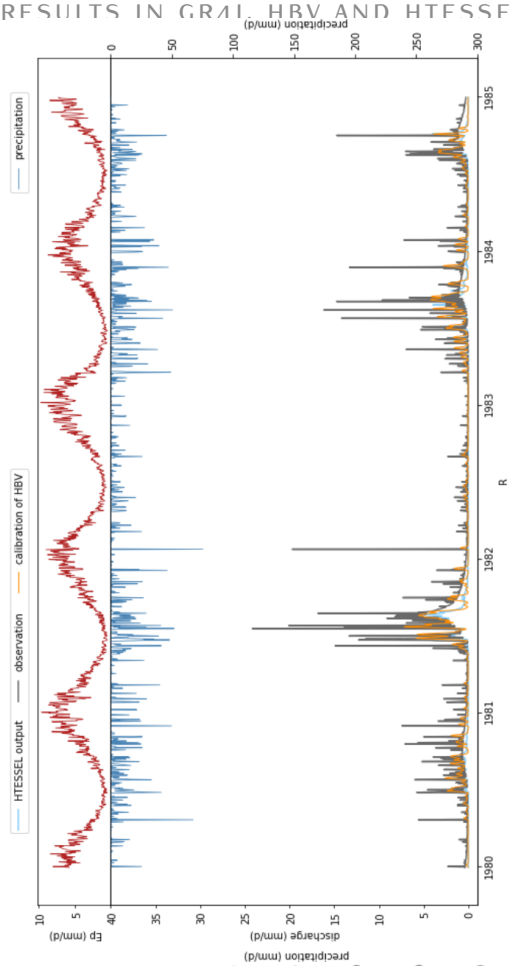
precipitation
HTESSEL output
observation
calibration of HBV
Ep (mm/d)
precipitation (mm/d)
discharge (mm/d)
R

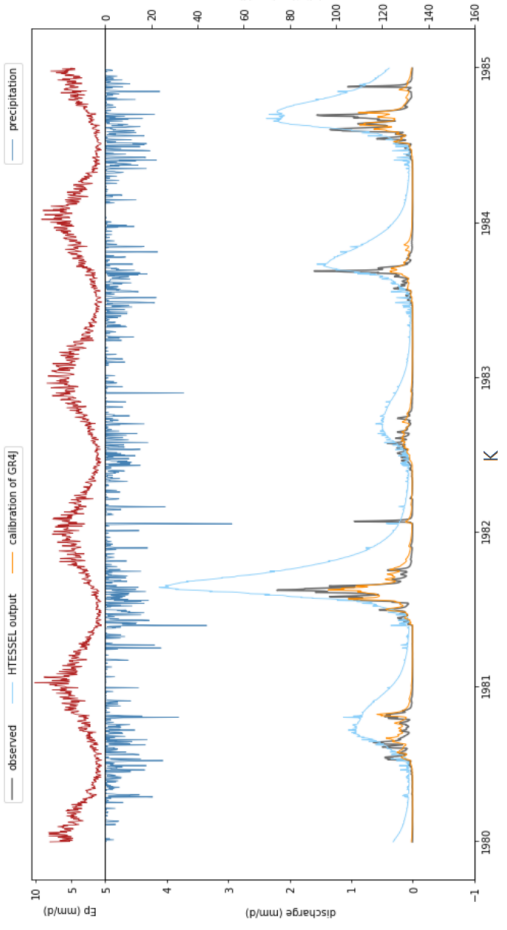
observed
HTESSEL output
calibration of GR4J
precipitation
Ep (mm/d)
discharge (mm/d)
K

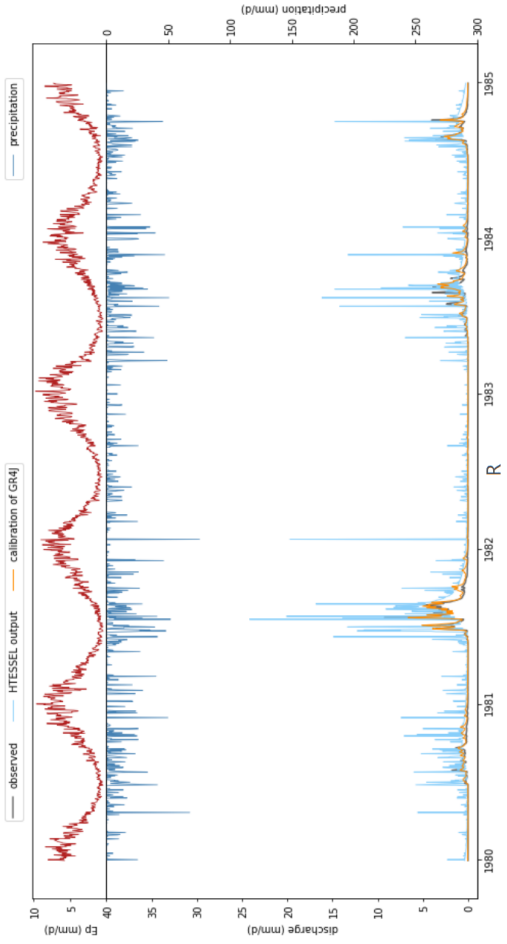
observed
HTESSEL output
calibration of GR4J
precipitation
Ep (mm/d)
discharge (mm/d)
R

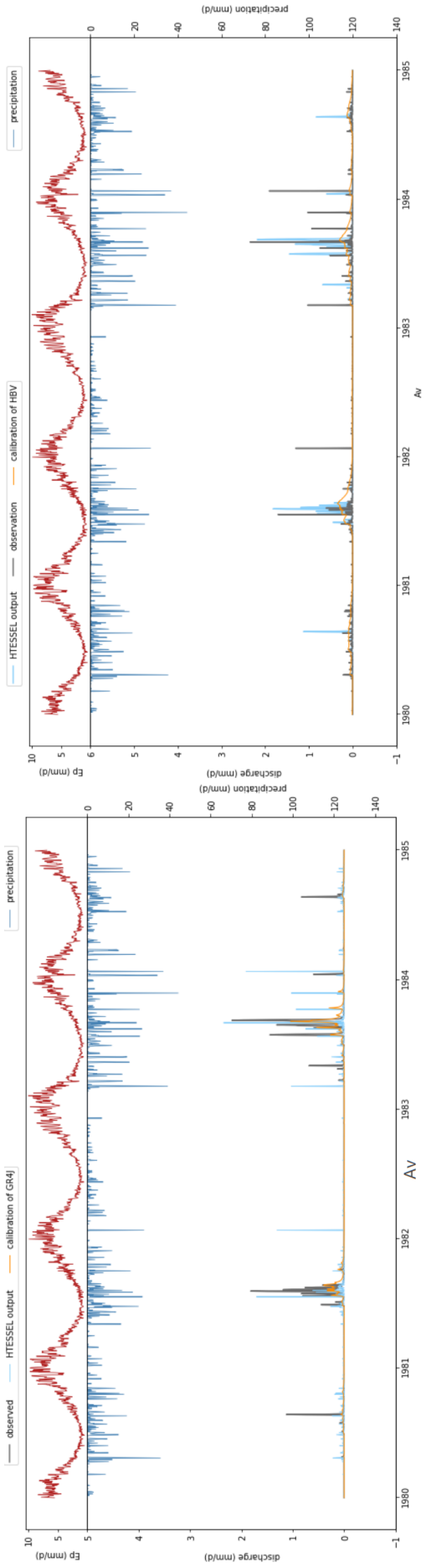
observed
HTESSEL output
calibration of GR4J
precipitation
Ep (mm/d)
discharge (mm/d)
precipitation (mm/d)
Av
HTESSEL output
observation
calibration of HBV
precipitation
Ep (mm/d)
discharge (mm/d)
precipitation (mm/d)
Av

A.3 THE MODEL TEST(VALIDATION) RESULTS IN GR4J, HBV AND HTESSEL

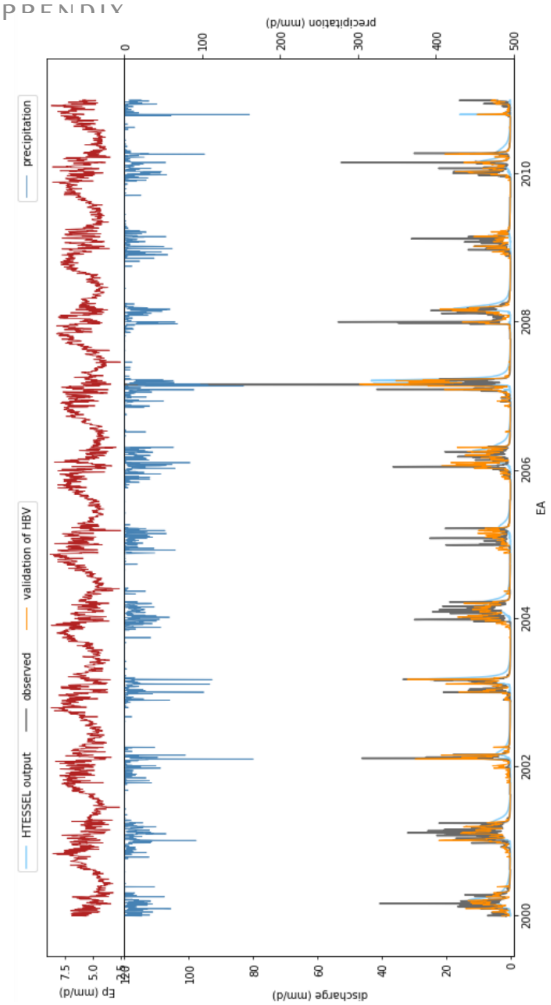
HTESSEL output
observed
validation of HBV
precipitation
EA
discharge (mm/d)
precipitation (mm/d)
EP (mm/d)

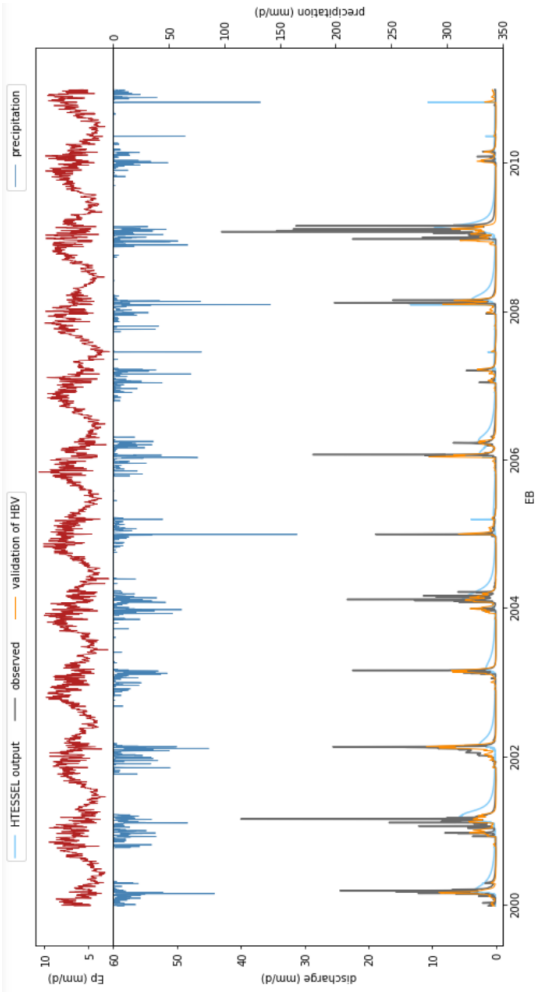
HTESSEL output
observed
validation of HBV
precipitation
EB
discharge (mm/d)
precipitation (mm/d)
EP (mm/d)

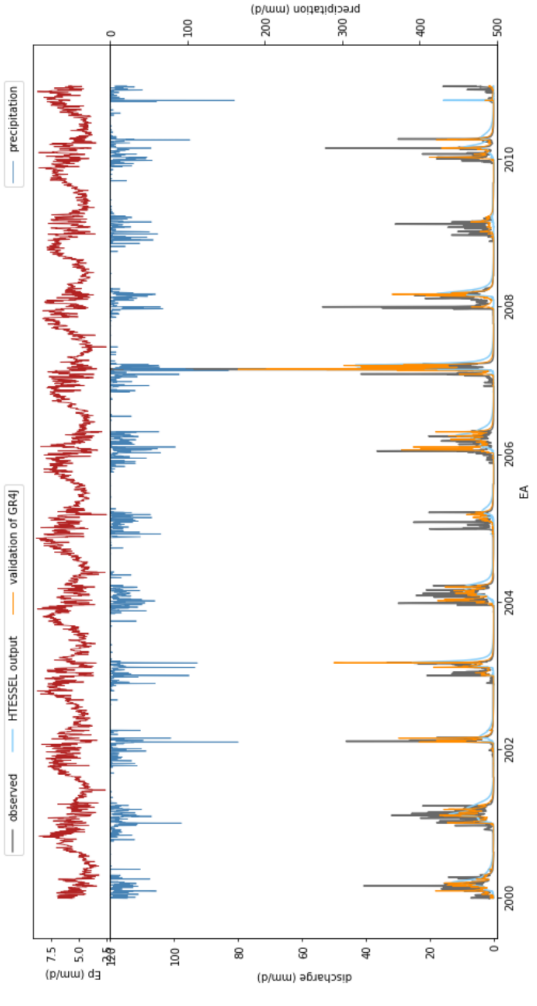
observed
HTESSEL output
validation of GR4J
precipitation
EA
discharge (mm/d)
precipitation (mm/d)
EP (mm/d)

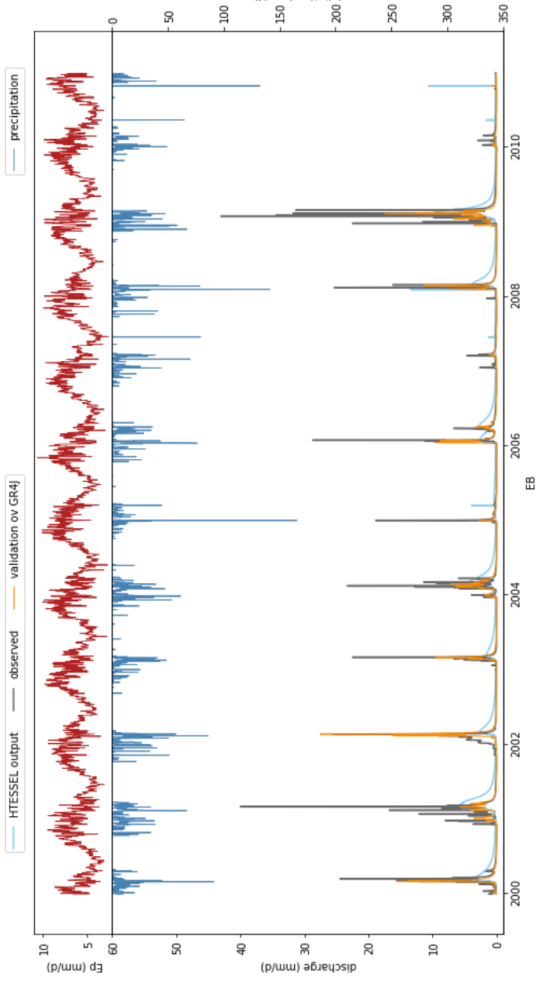
HTESSEL output
observed
validation ov GR4J
precipitation
EB
discharge (mm/d)
precipitation (mm/d)
EP (mm/d)

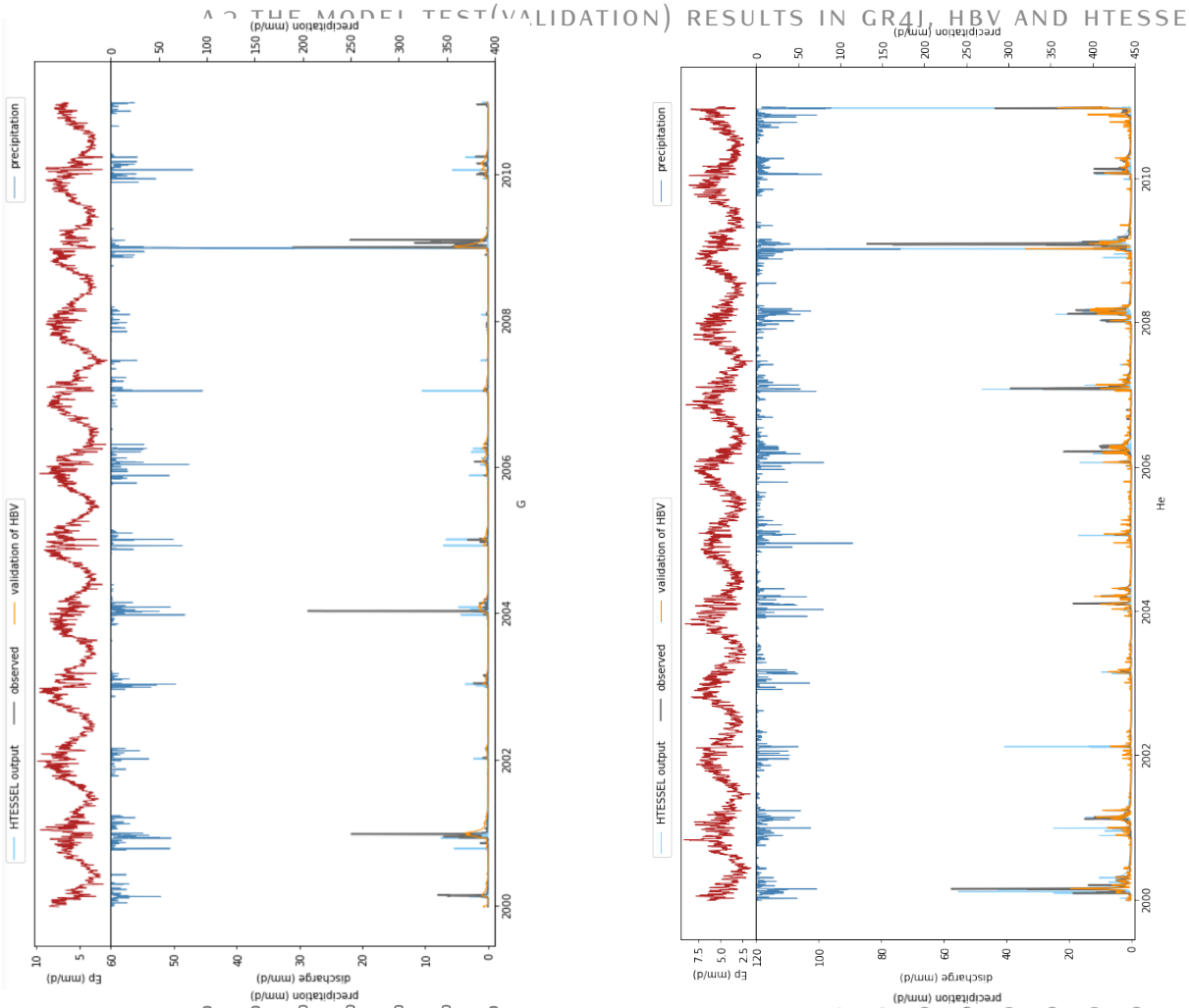
HTESSEL output
observed
validation of HBV
precipitation
Ep (mm/d)
discharge (mm/d)
precipitation (mm/d)
G
He

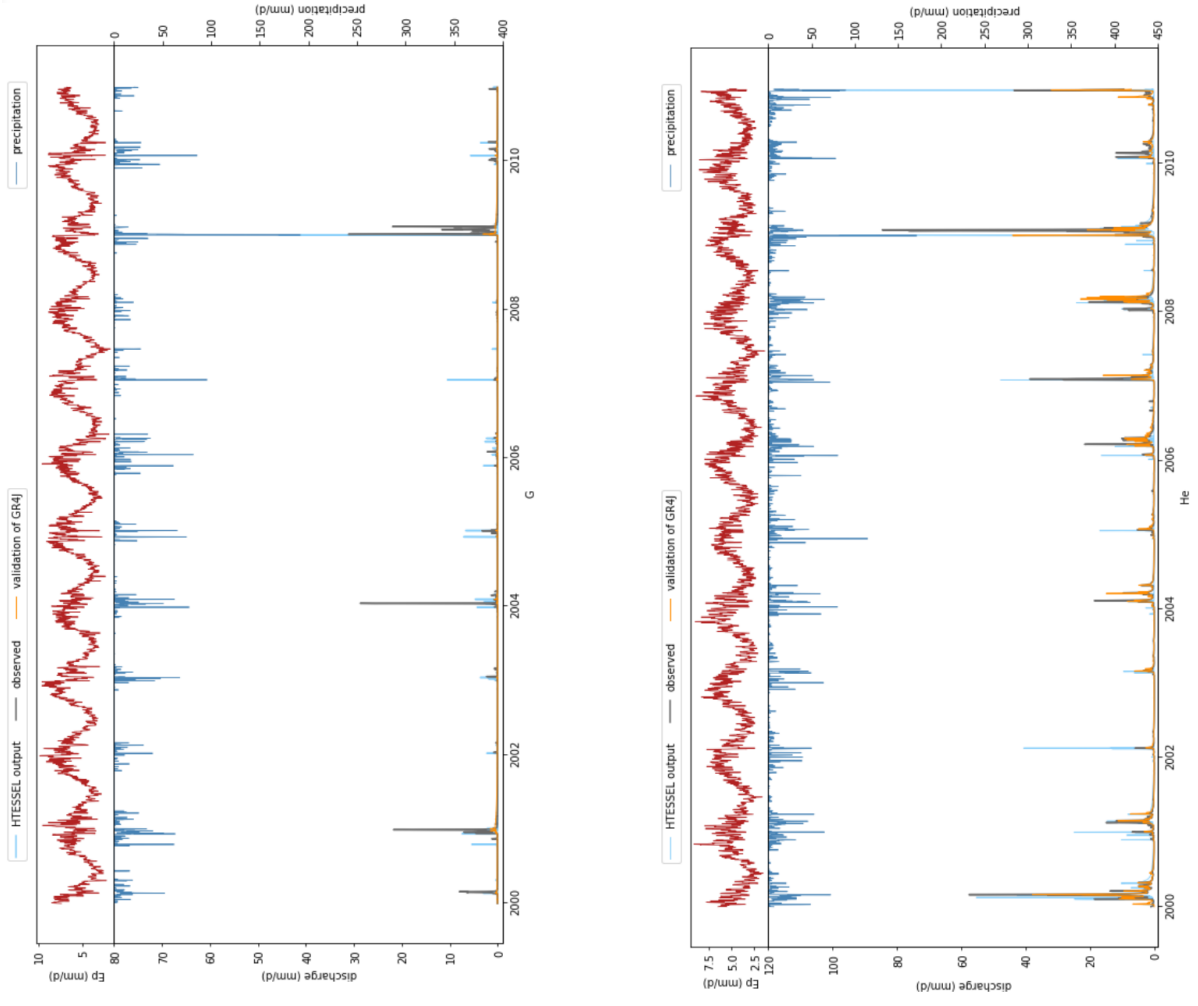
HTESSEL output
observed
validation of GR4J
precipitation
Ep (mm/d)
discharge (mm/d)
precipitation (mm/d)
G
He

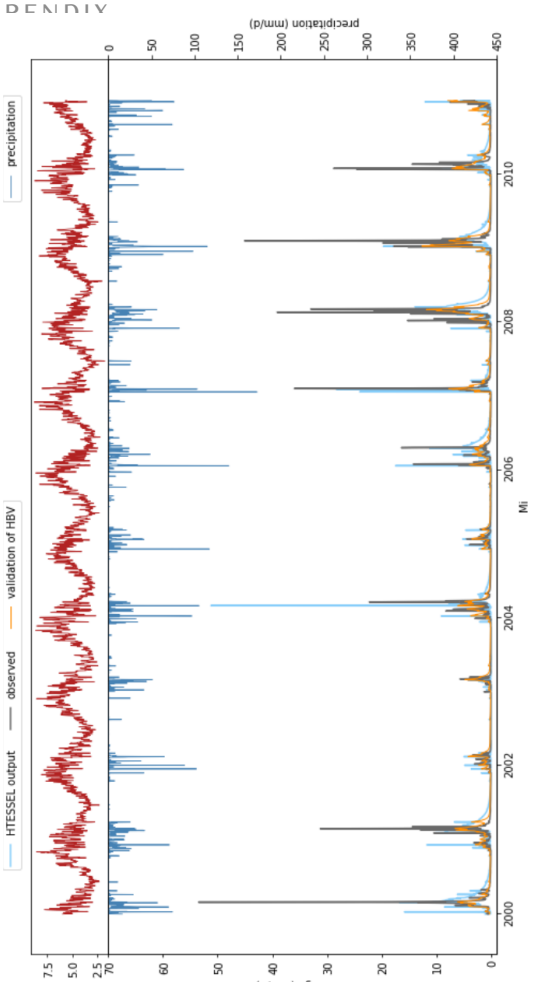
precipitation
HTESSEL output
observed
validation of HBV
precipitation (mm/d)
discharge (mm/d)
EP (mm/d)
Mi

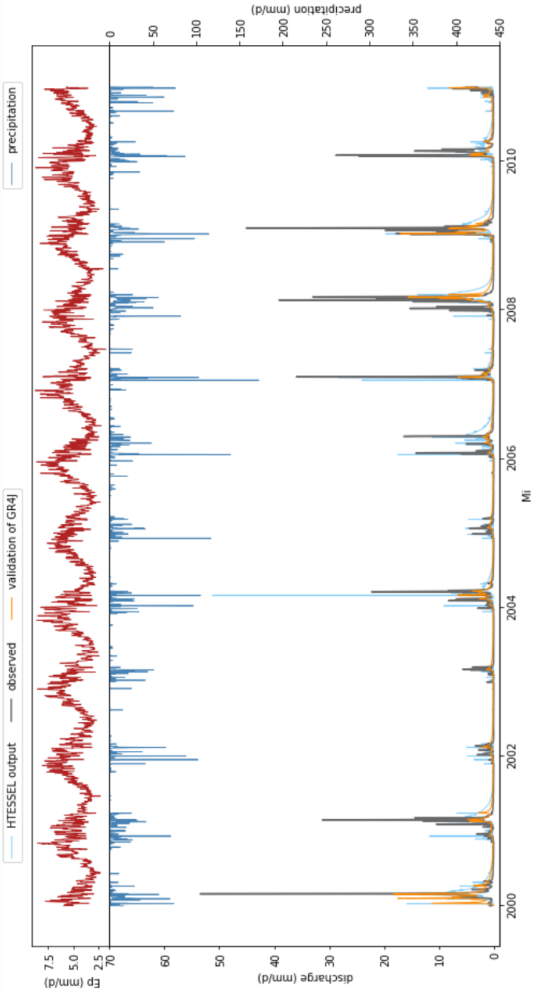
precipitation
HTESSEL output
observed
validation of GR4J
precipitation (mm/d)
discharge (mm/d)
EP (mm/d)
Mi

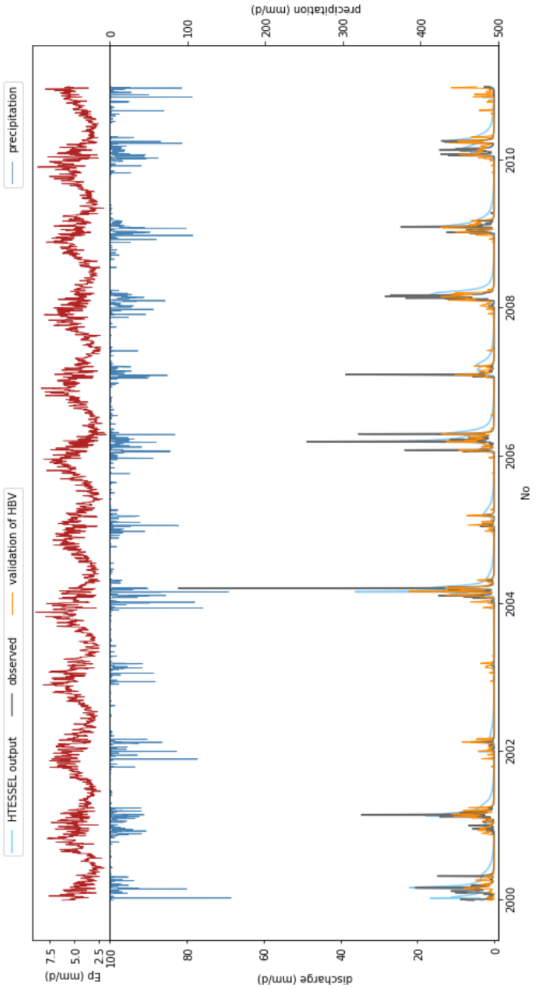
precipitation
HTESSEL output
observed
validation of HBV
precipitation (mm/d)
discharge (mm/d)
EP (mm/d)
No

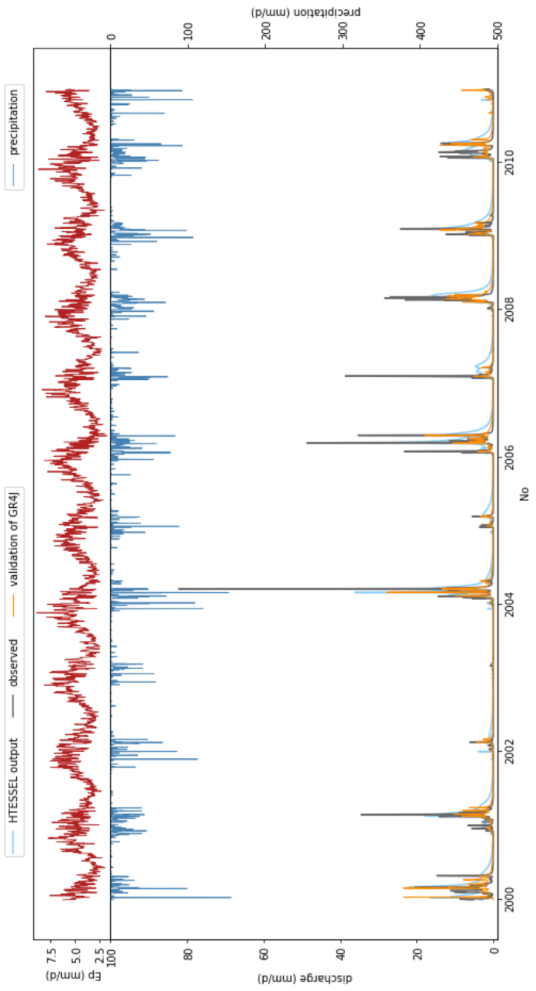
precipitation
HTESSEL output
observed
validation of GR4J
precipitation (mm/d)
discharge (mm/d)
EP (mm/d)
No

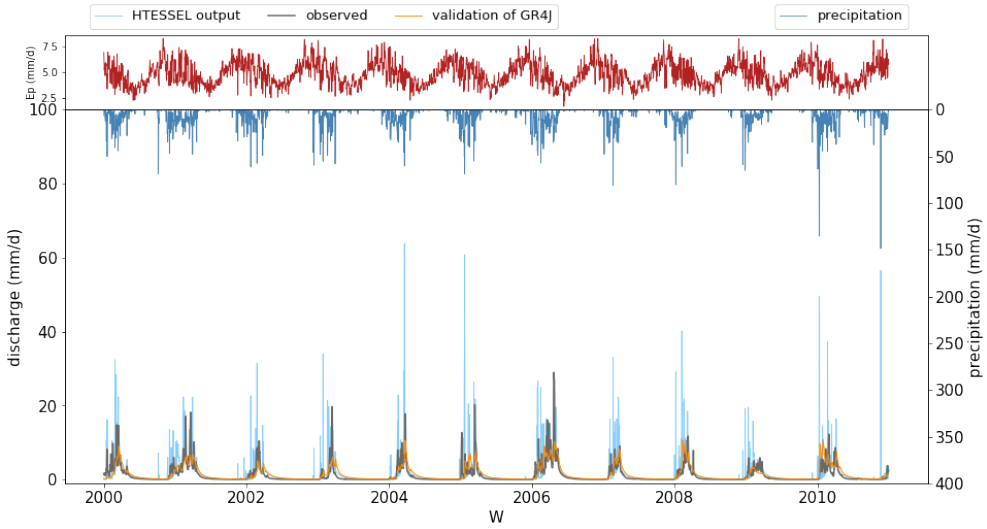
HTESSEL output
observed
validation of GR4J
precipitation
Ep (mm/d)
discharge (mm/d)
precipitation (mm/d)
W

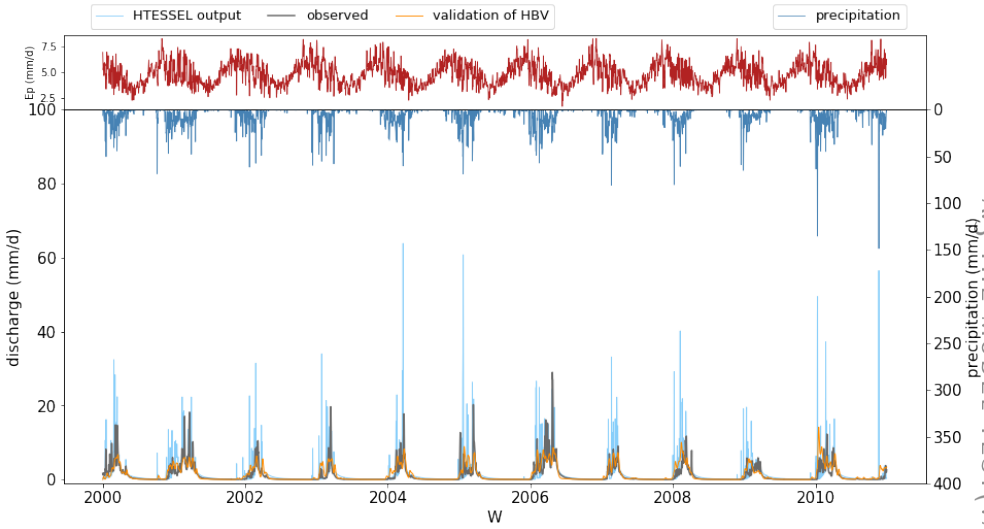
HTESSEL output
observed
validation of HBV
precipitation
Ep (mm/d)
discharge (mm/d)
precipitation (mm/d)
W

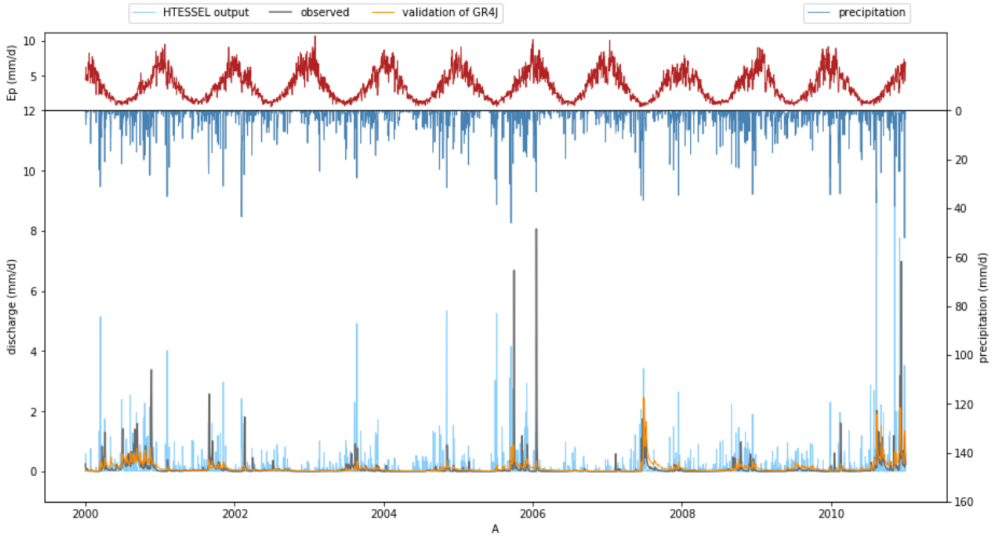
HTESSEL output
observed
validation of GR4J
precipitation
Ep (mm/d)
discharge (mm/d)
precipitation (mm/d)
A

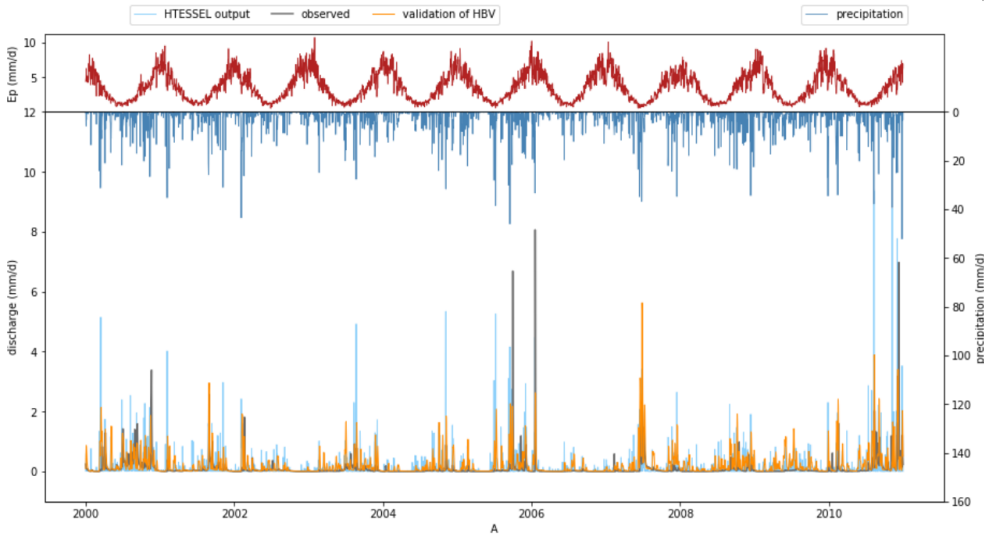
HTESSEL output
observed
validation of HBV
precipitation
Ep (mm/d)
discharge (mm/d)
precipitation (mm/d)
A

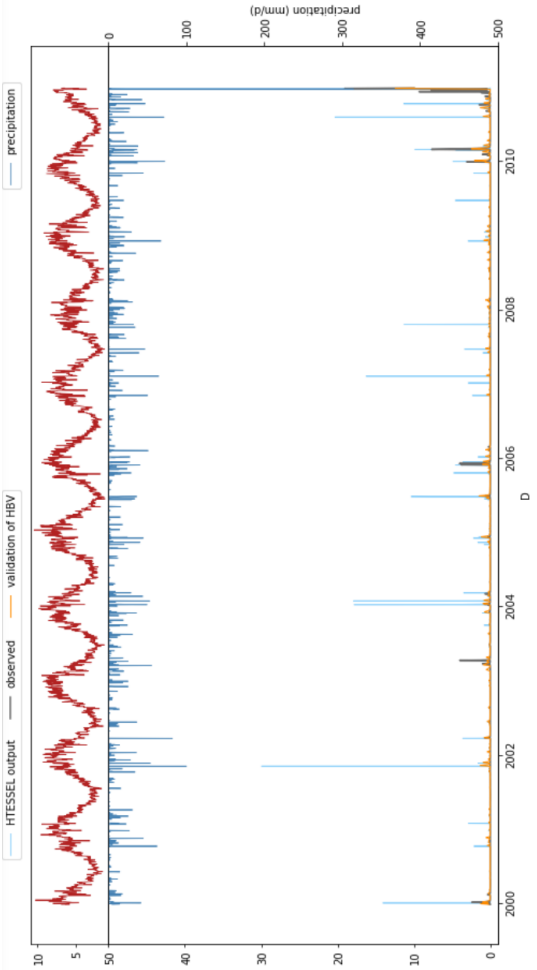
precipitation
HTESSEL output
observed
validation of HBV
precipitation (mm/d)
discharge (mm/d)
Ep (mm/d)
D

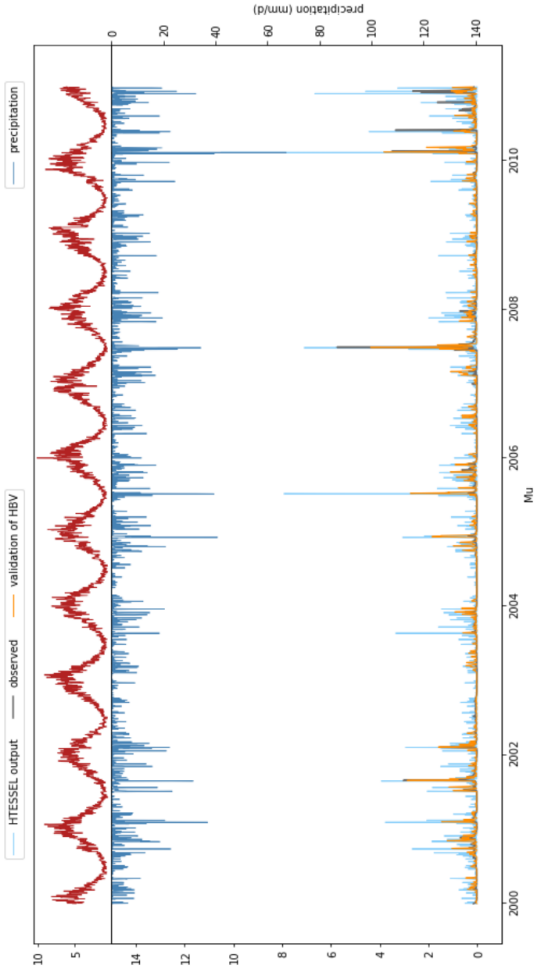
precipitation
HTESSEL output
observed
validation of HBV
precipitation (mm/d)
discharge (mm/d)
Ep (mm/d)
Mu

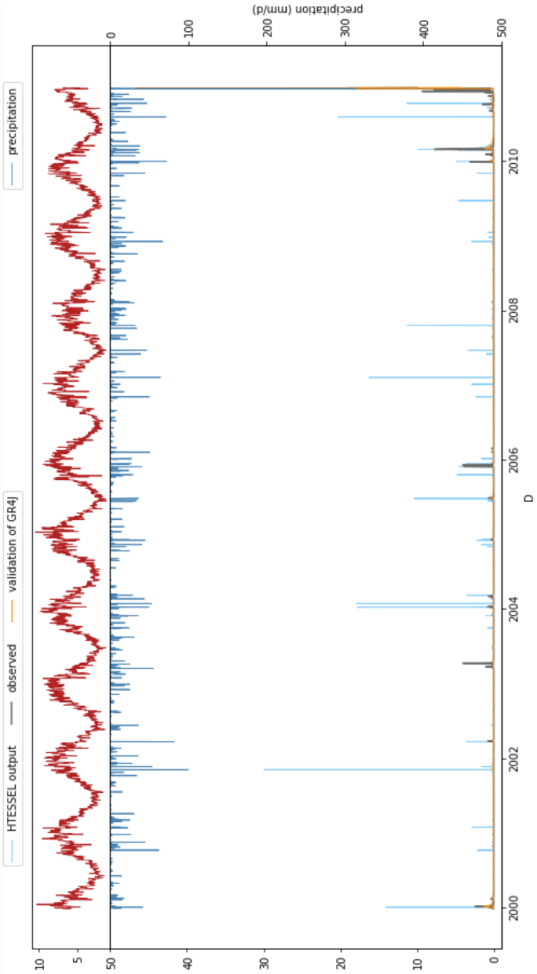
precipitation
HTESSEL output
observed
validation of GR4J
precipitation (mm/d)
discharge (mm/d)
Ep (mm/d)
D

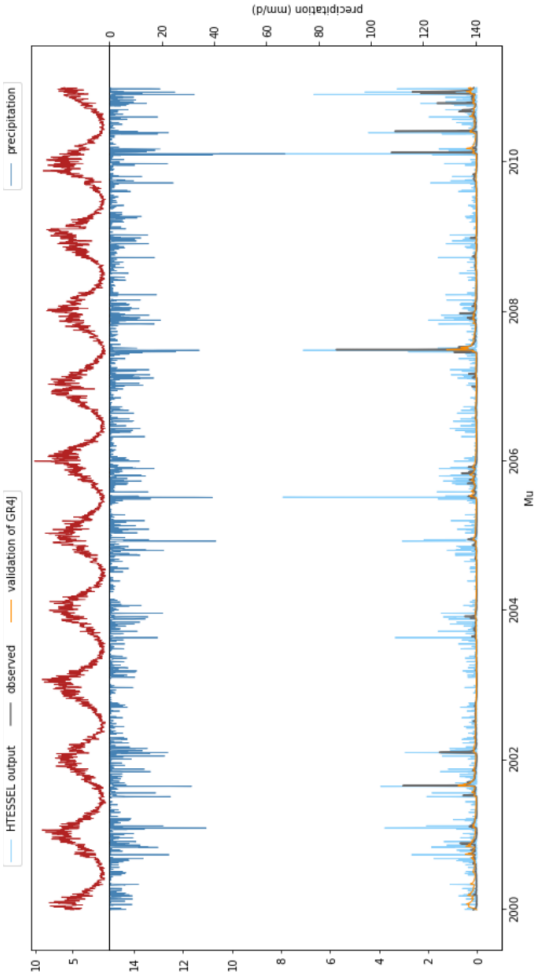
precipitation
HTESSEL output
observed
validation of GR4J
precipitation (mm/d)
discharge (mm/d)
Ep (mm/d)
Mu

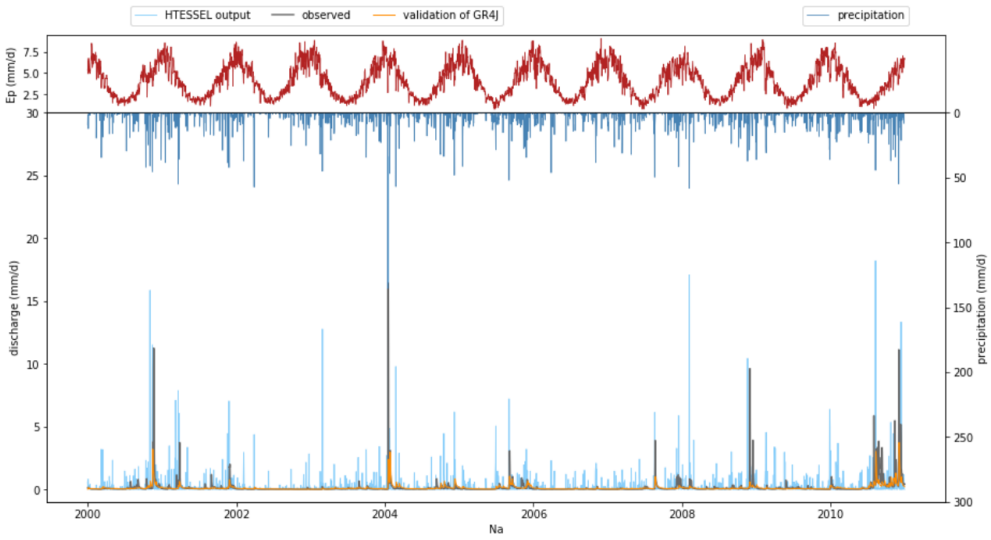
HTESSEL output
observed
validation of GR4J
precipitation
Ep (mm/d)
discharge (mm/d)
precipitation (mm/d)
Na

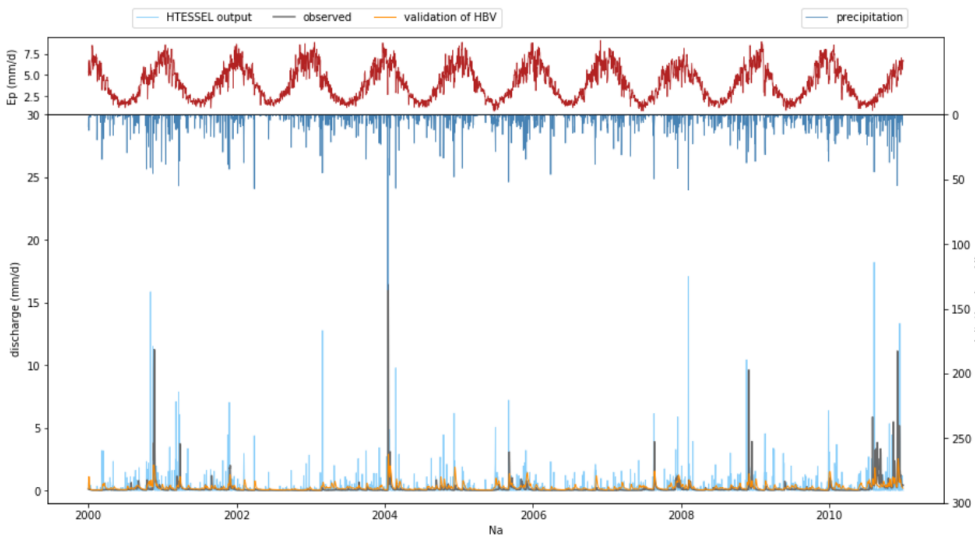
HTESSEL output
observed
validation of HBV
precipitation
Ep (mm/d)
discharge (mm/d)
precipitation (mm/d)
Na

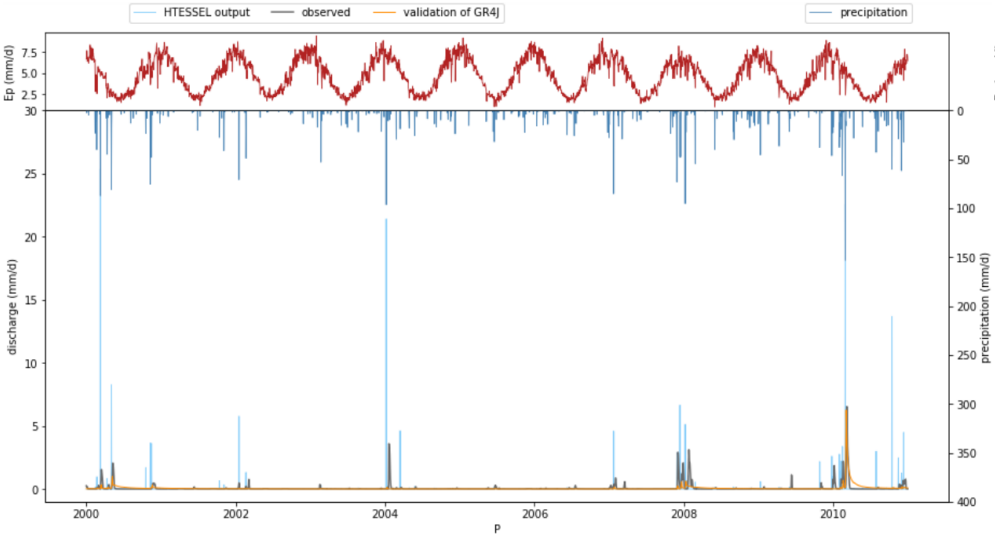
HTESSEL output
observed
validation of GR4J
precipitation
Ep (mm/d)
discharge (mm/d)
precipitation (mm/d)
P

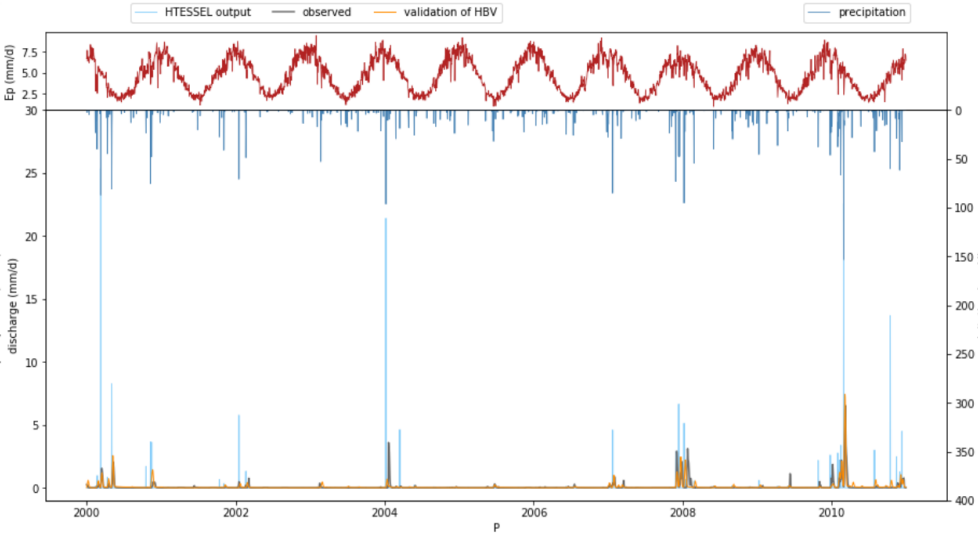
HTESSEL output
observed
validation of HBV
precipitation
Ep (mm/d)
discharge (mm/d)
precipitation (mm/d)
P

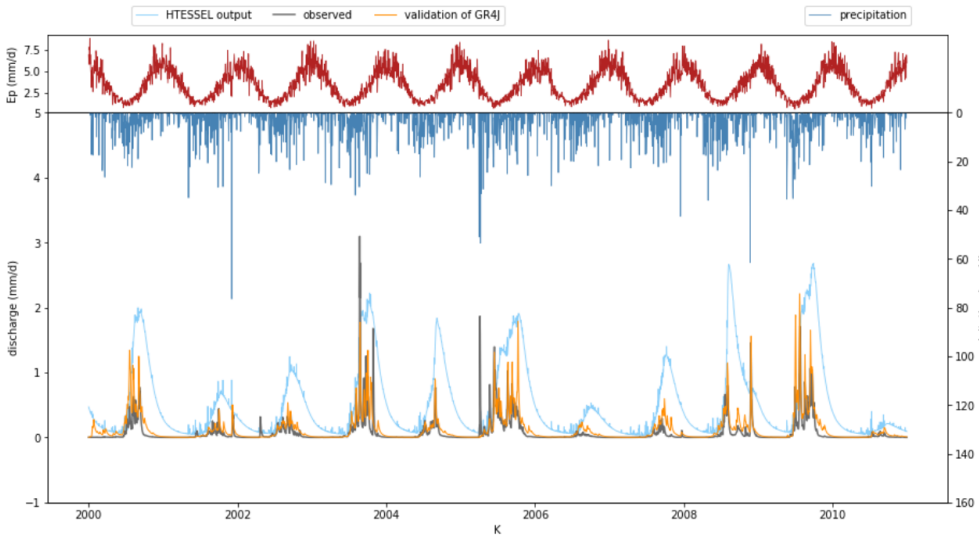
HTESSEL output
observed
validation of GR4J
precipitation
Ep (mm/d)
discharge (mm/d)
precipitation (mm/d)
K

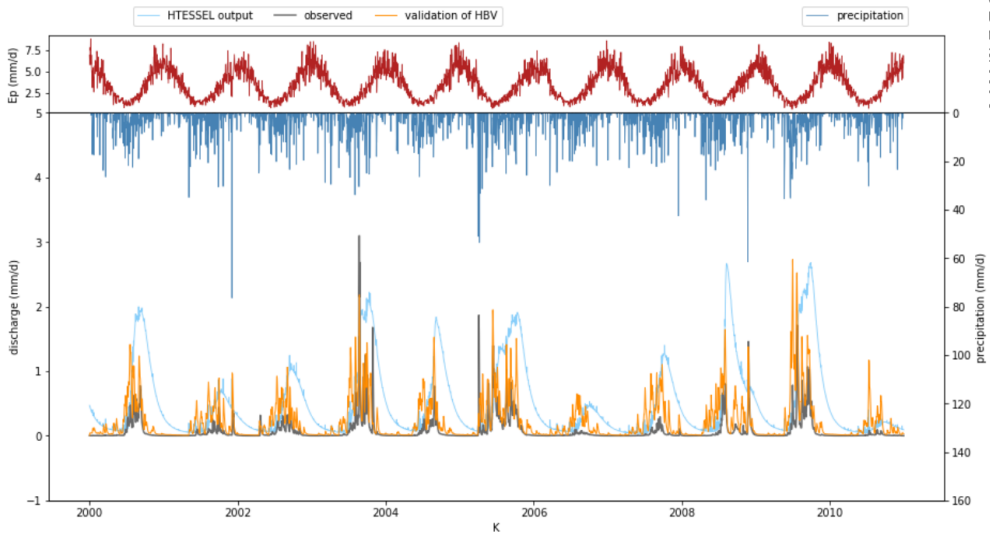
HTESSEL output
observed
validation of HBV
precipitation
Ep (mm/d)
discharge (mm/d)
precipitation (mm/d)
K

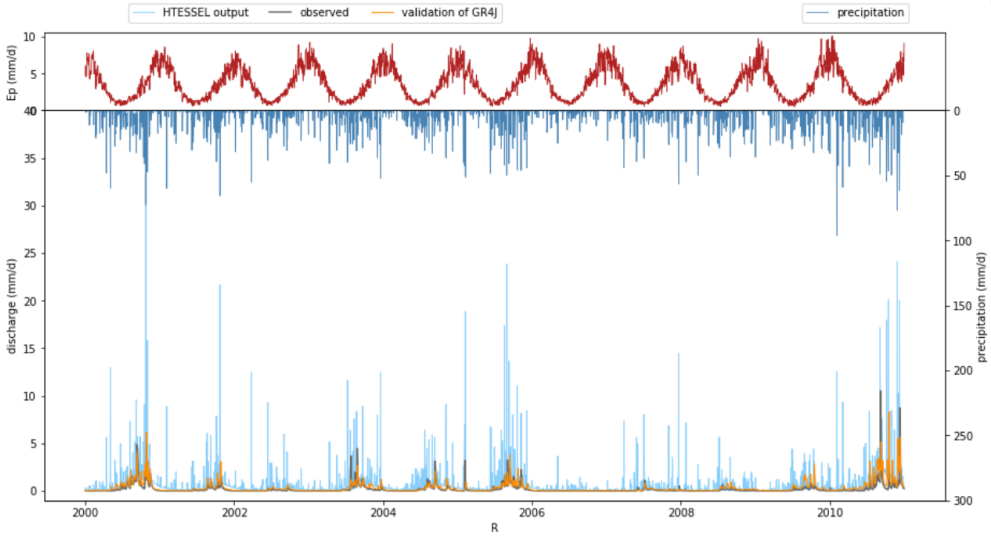
HTESSEL output
observed
validation of GR4J
precipitation
Ep (mm/d)
discharge (mm/d)
precipitation (mm/d)
R

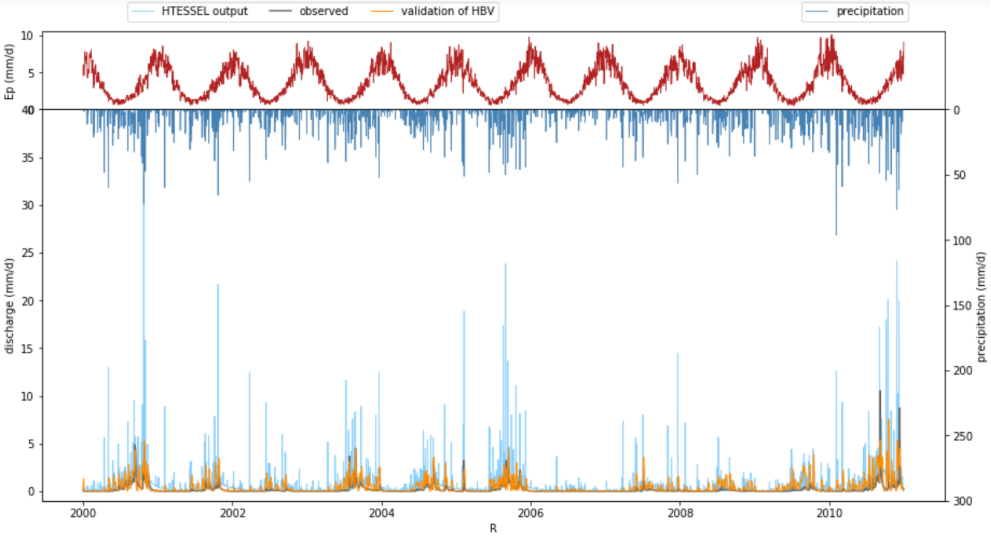
HTESSEL output
observed
validation of HBV
precipitation
Ep (mm/d)
discharge (mm/d)
precipitation (mm/d)
R

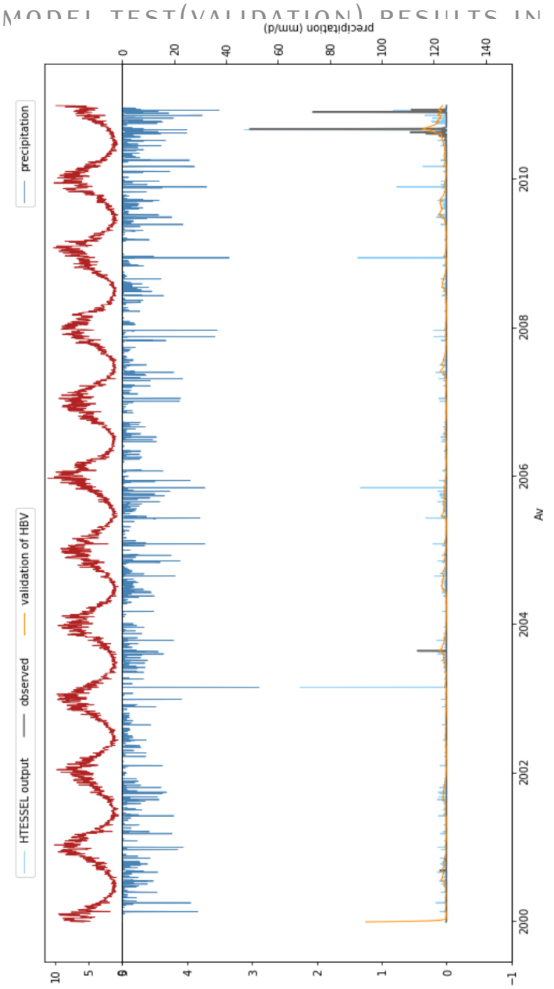
precipitation (mm/d)
0
20
40
60
80
100
120
140
precipitation
HTESSEL output
observed
validation of HBV
discharge (mm/d)
−1
0
1
2
3
4
EP (mm/d)
0
5
10
2000
2002
2004
2006
2008
2010
Av

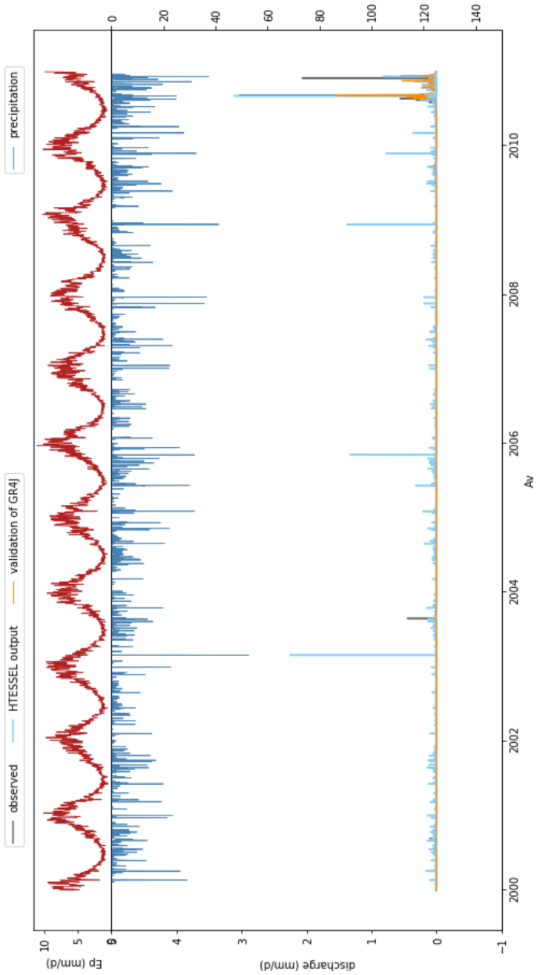
precipitation
observed
HTESSEL output
validation of GR4J
discharge (mm/d)
−1
0
1
2
3
4
EP (mm/d)
0
5
10
2000
2002
2004
2006
2008
2010
Av

A.4 THE RANGE OF 8 PARAMETERS IN HBV BEFORE AND AFTER CHANGES

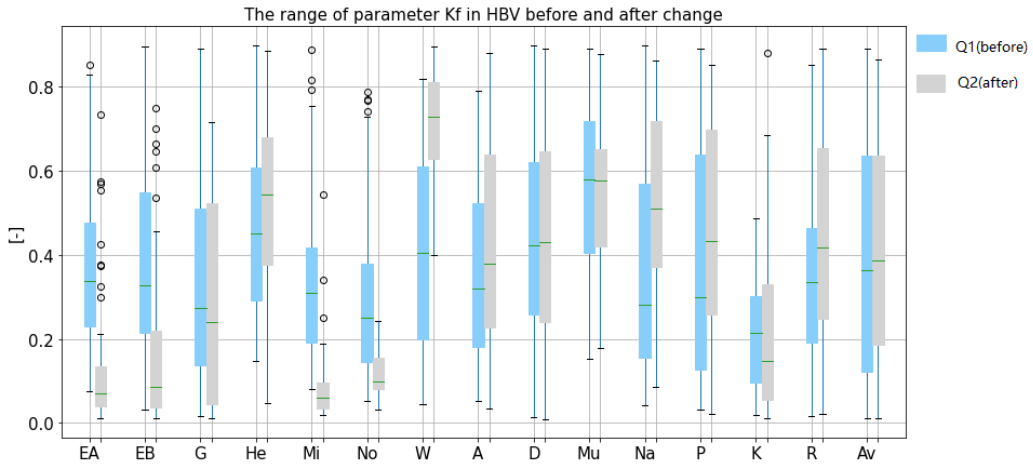

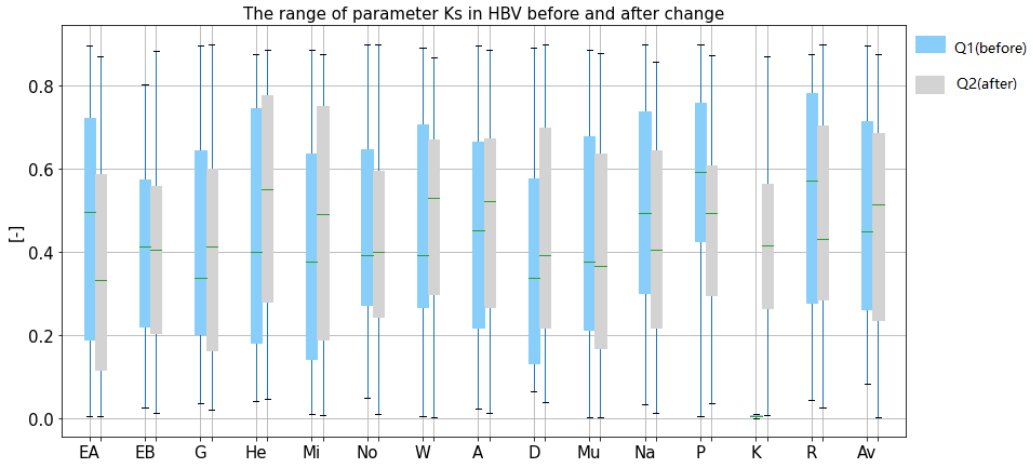

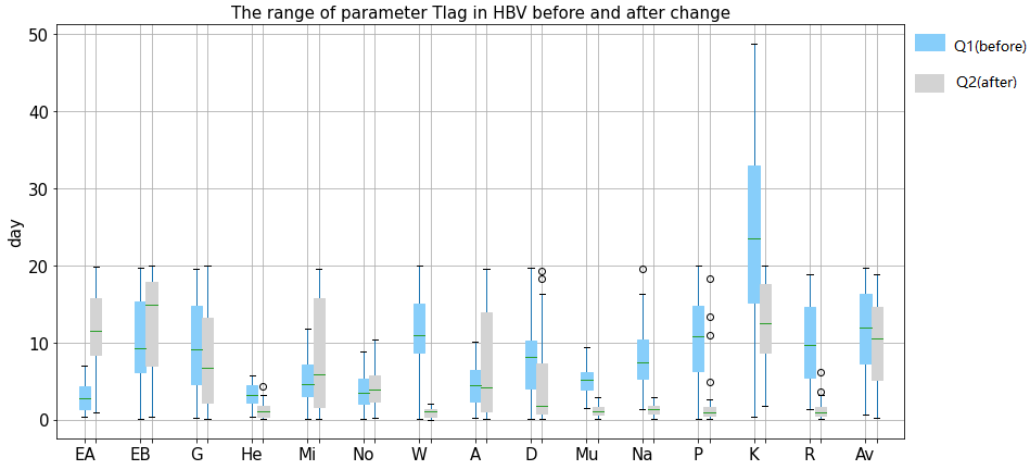

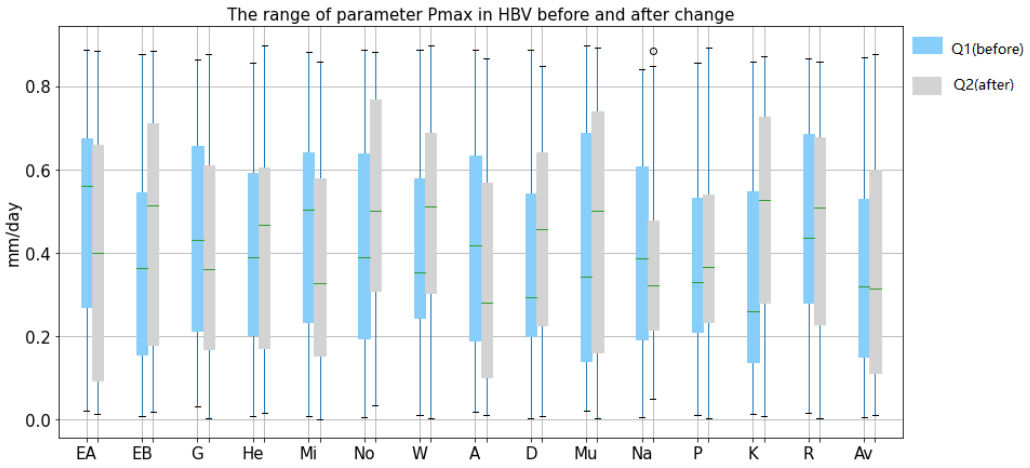
The range of parameter Pmax in HBV before and after change
mm/day
0.0
0.2
0.4
0.6
0.8
EA EB G He Mi No W A D Mu Na P K R Av
Q1(before)
Q2(after)

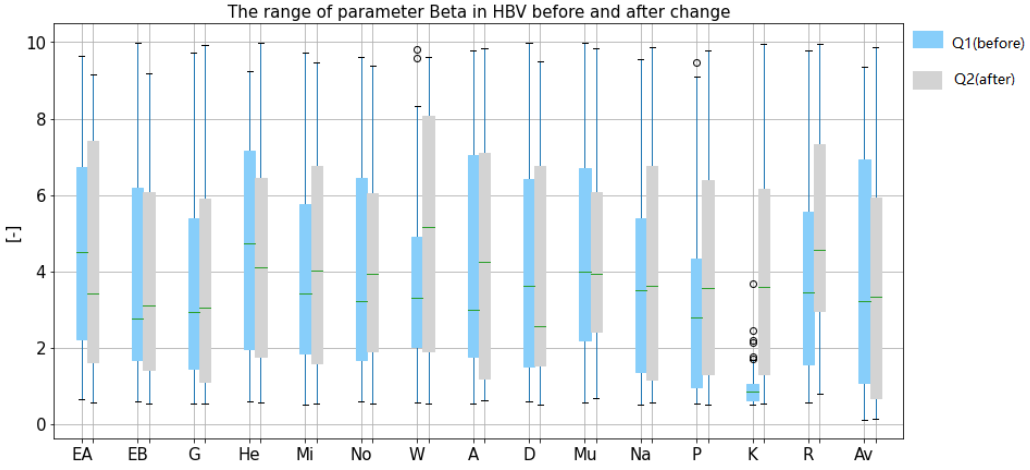
The range of parameter Beta in HBV before and after change
[-]
0
2
4
6
8
10
EA EB G He Mi No W A D Mu Na P K R Av
Q1(before)
Q2(after)

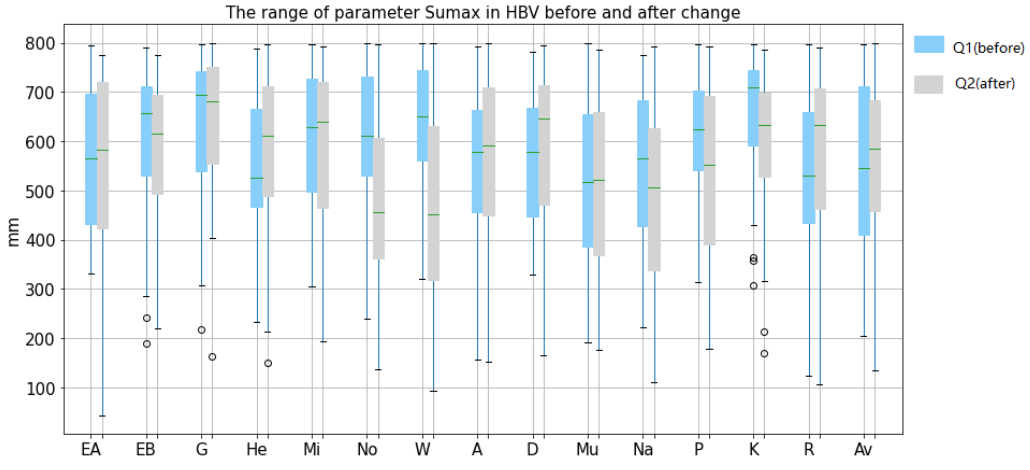
The range of parameter Sumax in HBV before and after change
mm
100
200
300
400
500
600
700
800
EA EB G He Mi No W A D Mu Na P K R Av
Q1(before)
Q2(after)

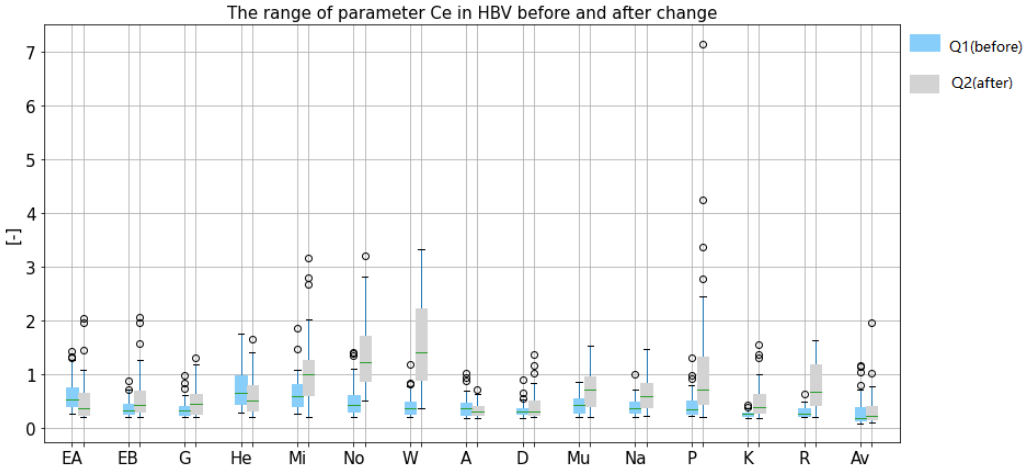
The range of parameter Ce in HBV before and after change
[-]
0
1
2
3
4
5
6
7
EA
EB
G
He
Mi
No
W
A
D
Mu
Na
P
K
R
Av
Q1(before)
Q2(after)

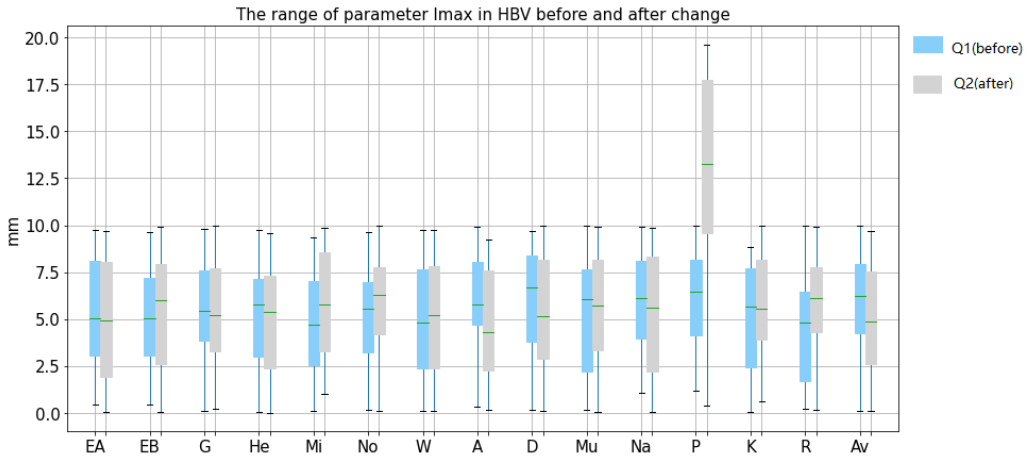
The range of parameter Imax in HBV before and after change
mm
0.0
2.5
5.0
7.5
10.0
12.5
15.0
17.5
20.0
EA
EB
G
He
Mi
No
W
A
D
Mu
Na
P
K
R
Av
Q1(before)
Q2(after)

A.5 THE INTERNAL COMPONENTS OF GR4J AND HTESSEL BEFORE AND AFTER CHANGE

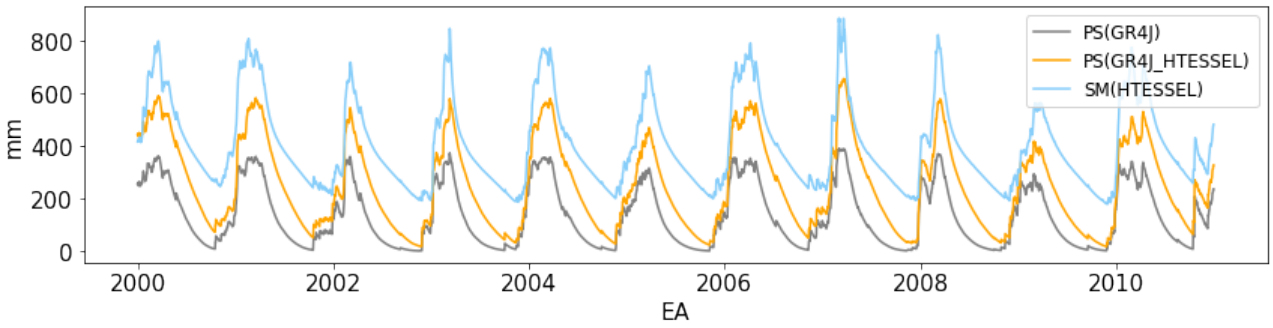

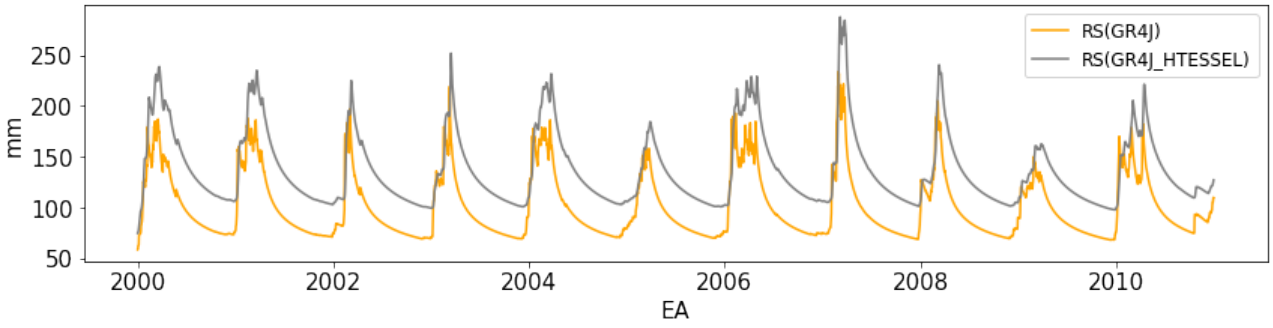

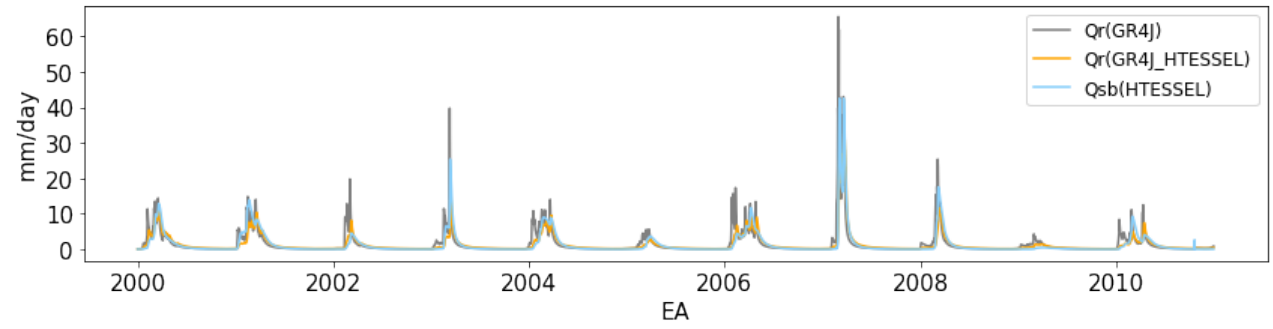

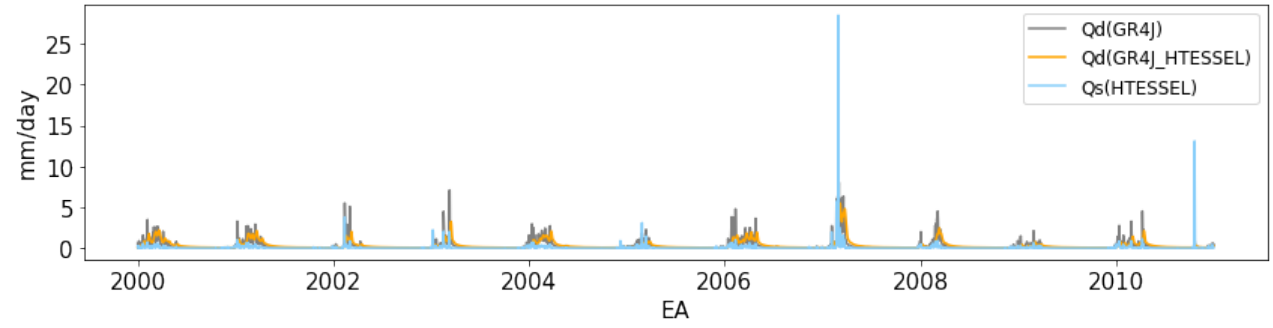

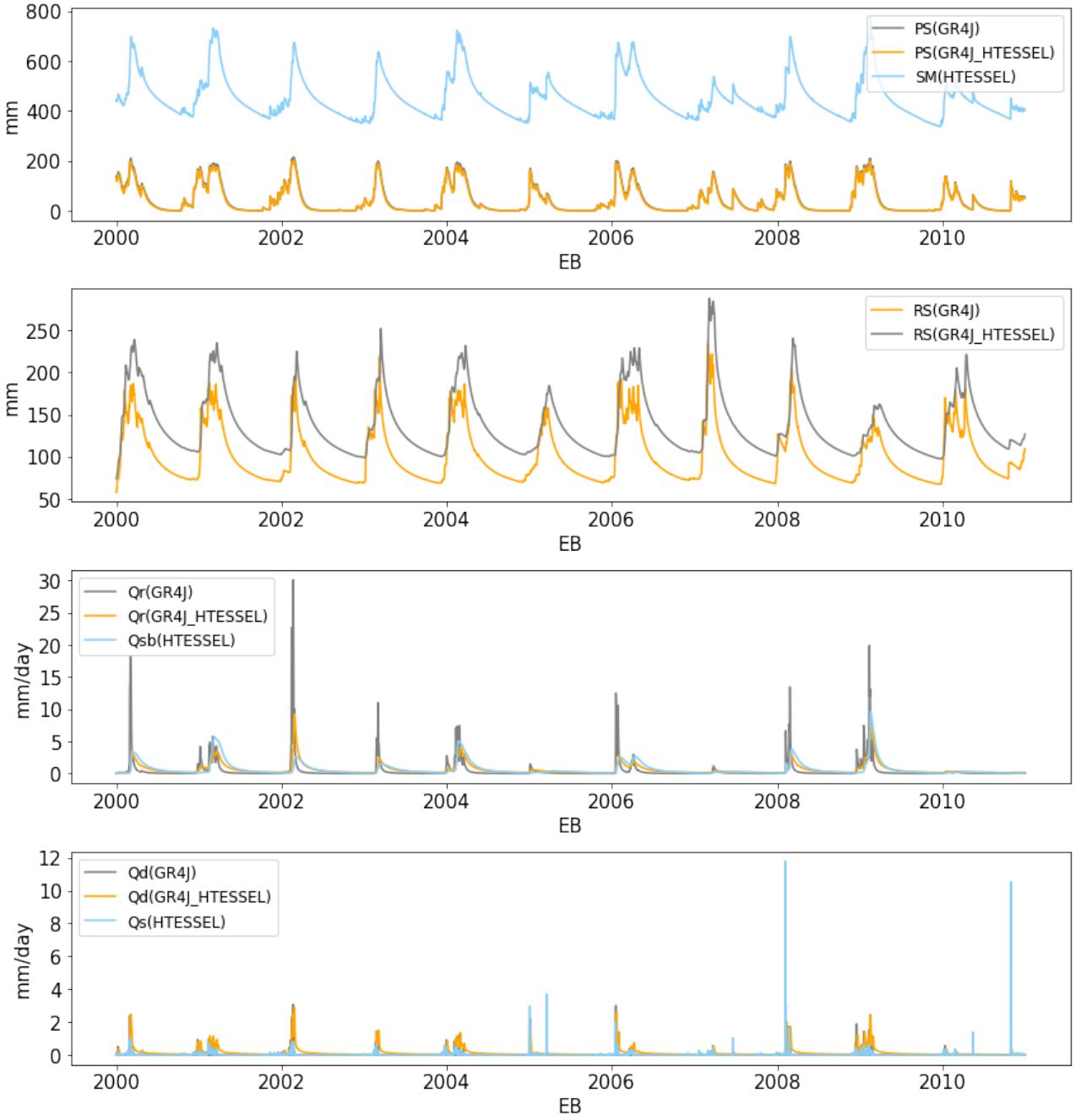
PS(GR4J)
PS(GR4J_HTESSEL)
SM(HTESSEL)
mm
EB
RS(GR4J)
RS(GR4J_HTESSEL)
mm
EB
Qr(GR4J)
Qr(GR4J_HTESSEL)
Qsb(HTESSEL)
mm/day
EB
Qd(GR4J)
Qd(GR4J_HTESSEL)
Qs(HTESSEL)
mm/day
EB

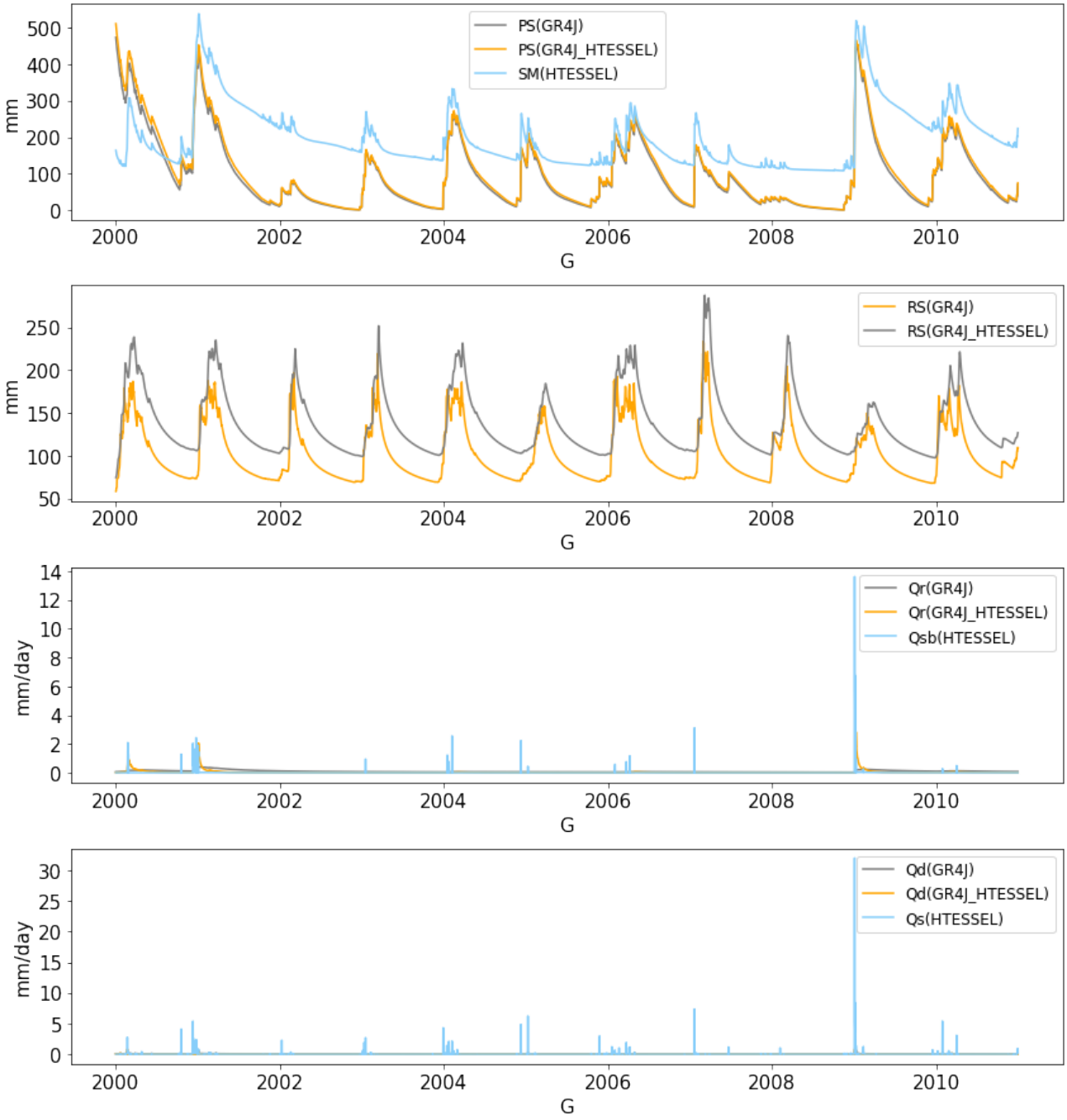
PS(GR4J)
PS(GR4J_HTESSEL)
SM(HTESSEL)
mm
G
RS(GR4J)
RS(GR4J_HTESSEL)
mm
G
Qr(GR4J)
Qr(GR4J_HTESSEL)
Qsb(HTESSEL)
mm/day
G
Qd(GR4J)
Qd(GR4J_HTESSEL)
Qs(HTESSEL)
mm/day
G

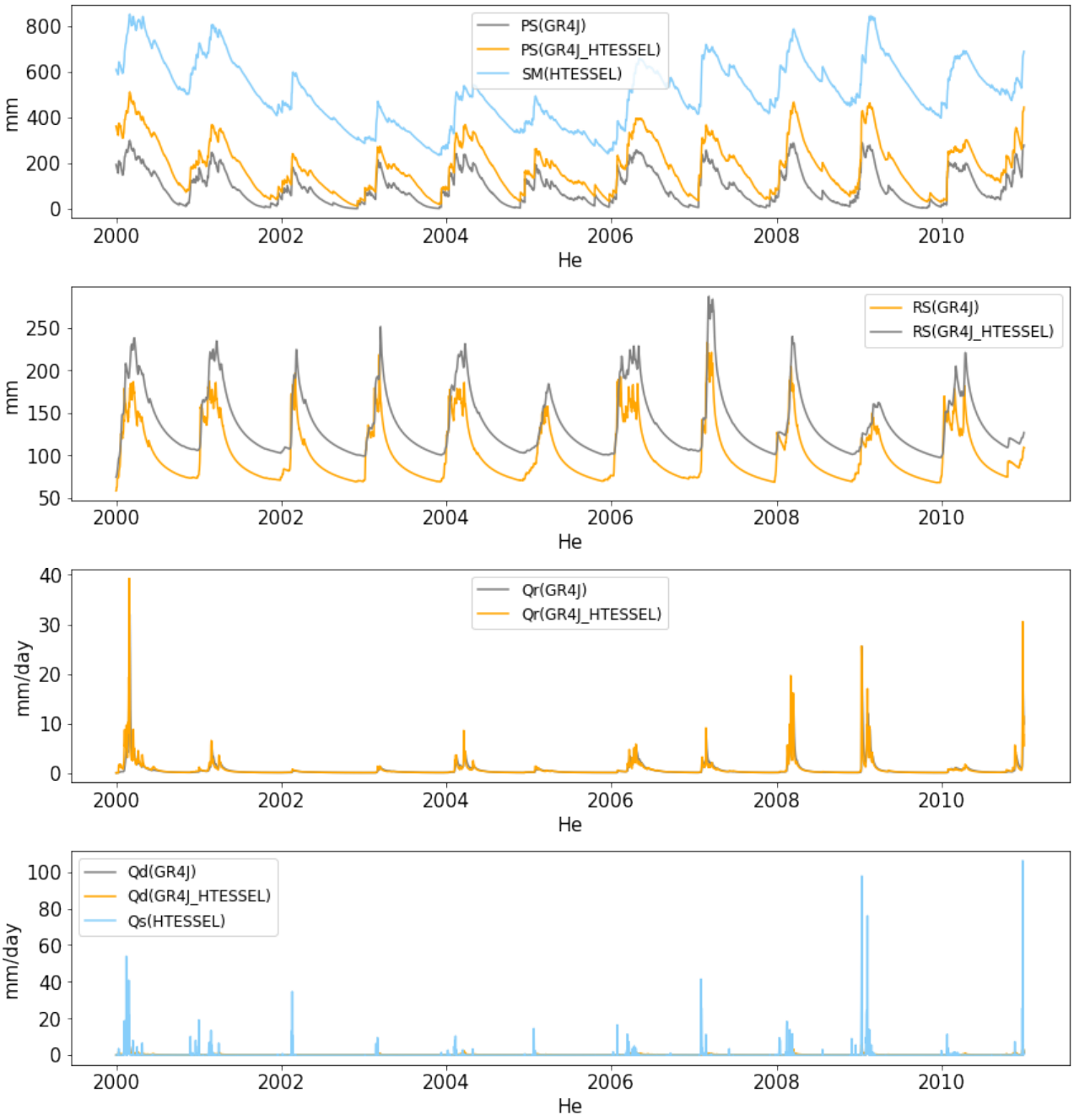
PS(GR4J)
PS(GR4J_HTESSEL)
SM(HTESSEL)
mm
He
RS(GR4J)
RS(GR4J_HTESSEL)
mm
He
Qr(GR4J)
Qr(GR4J_HTESSEL)
mm/day
He
Qd(GR4J)
Qd(GR4J_HTESSEL)
Qs(HTESSEL)
mm/day
He

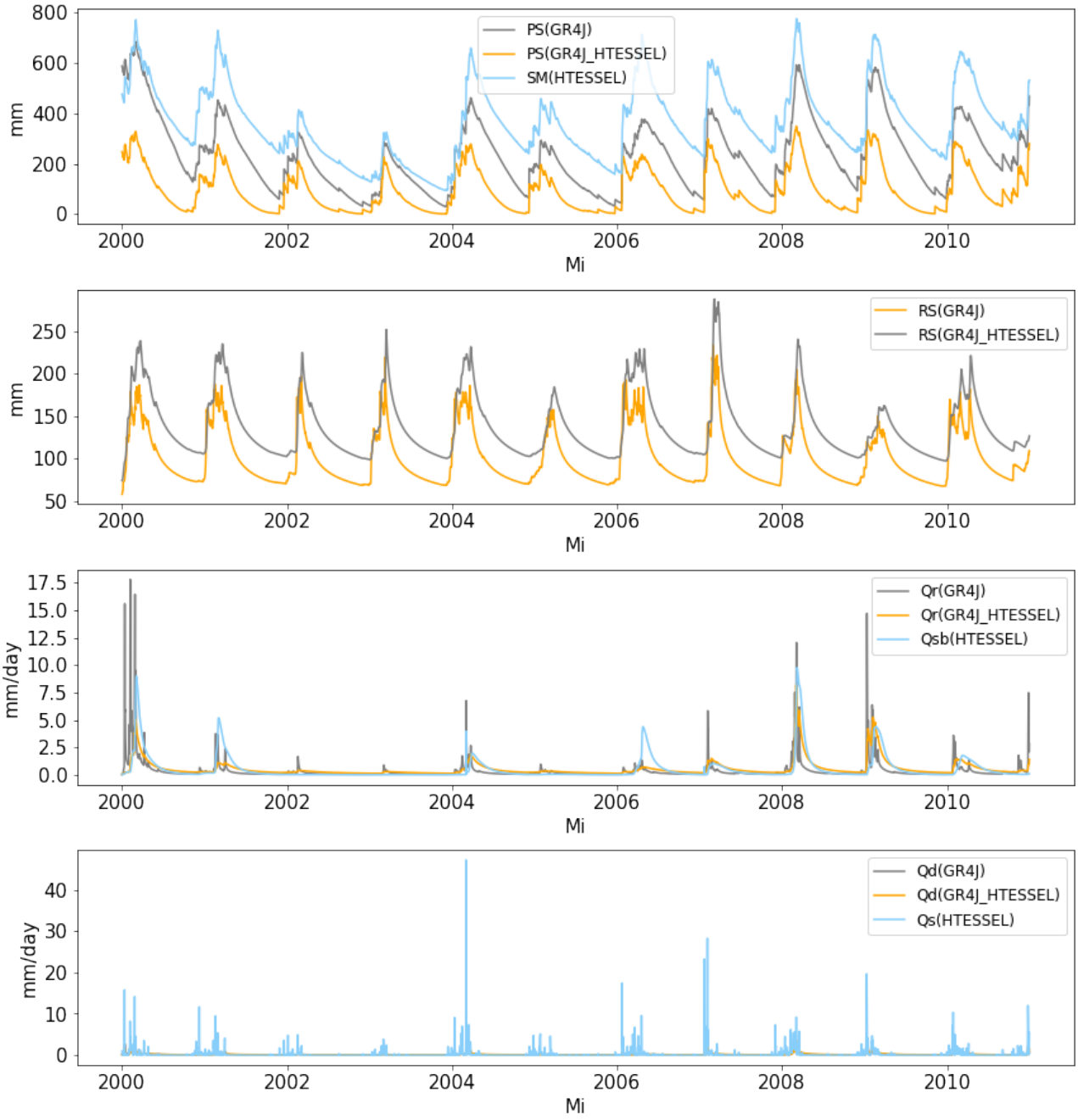
PS(GR4J)
PS(GR4J_HTESSEL)
SM(HTESSEL)
mm
Mi
RS(GR4J)
RS(GR4J_HTESSEL)
mm
Mi
Qr(GR4J)
Qr(GR4J_HTESSEL)
Qsb(HTESSEL)
mm/day
Mi
Qd(GR4J)
Qd(GR4J_HTESSEL)
Qs(HTESSEL)
mm/day
Mi

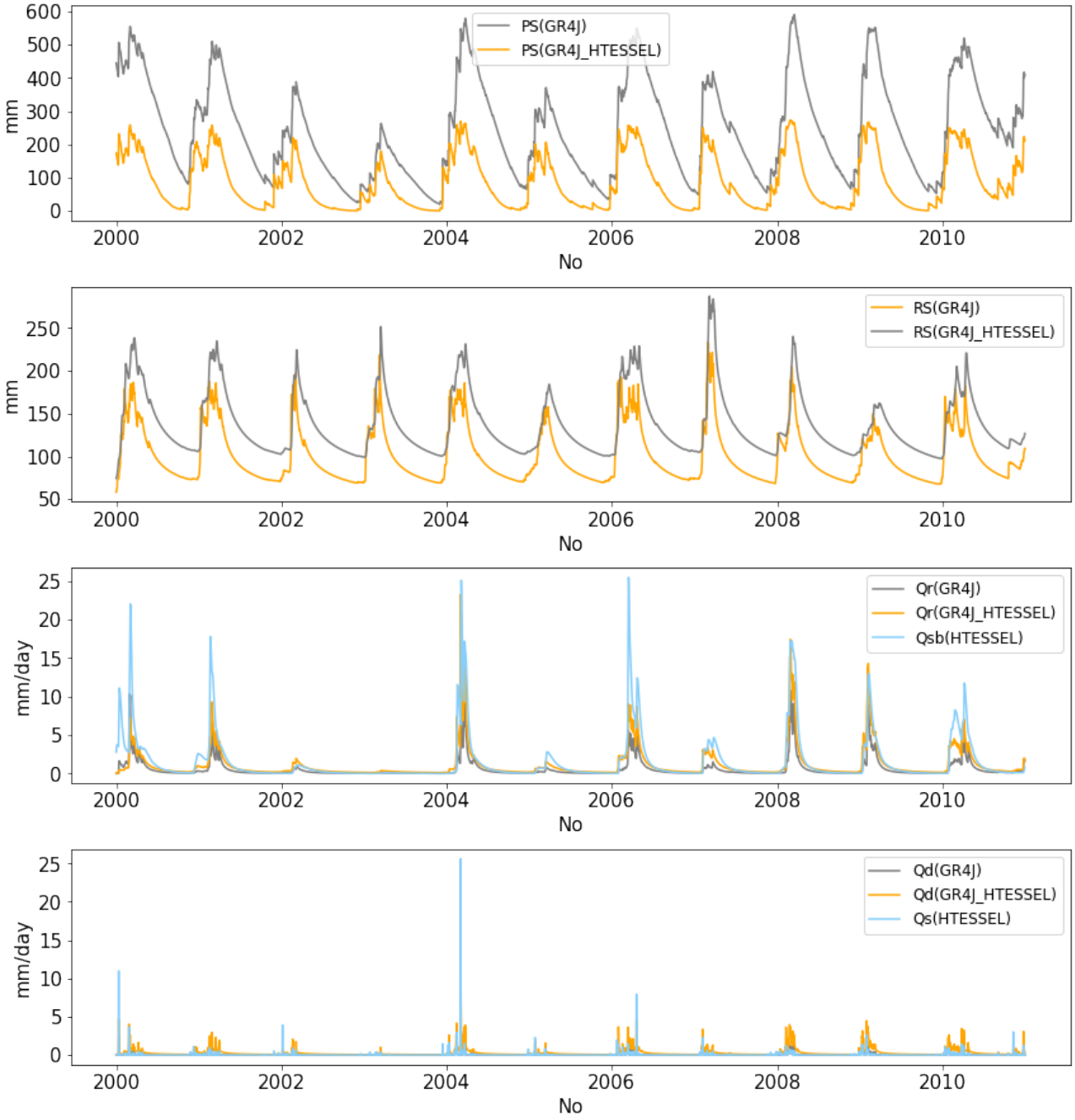
PS(GR4J)
PS(GR4J_HTESSEL)
mm
No
RS(GR4J)
RS(GR4J_HTESSEL)
mm
No
Qr(GR4J)
Qr(GR4J_HTESSEL)
Qsb(HTESSEL)
mm/day
No
Qd(GR4J)
Qd(GR4J_HTESSEL)
Qs(HTESSEL)
mm/day
No

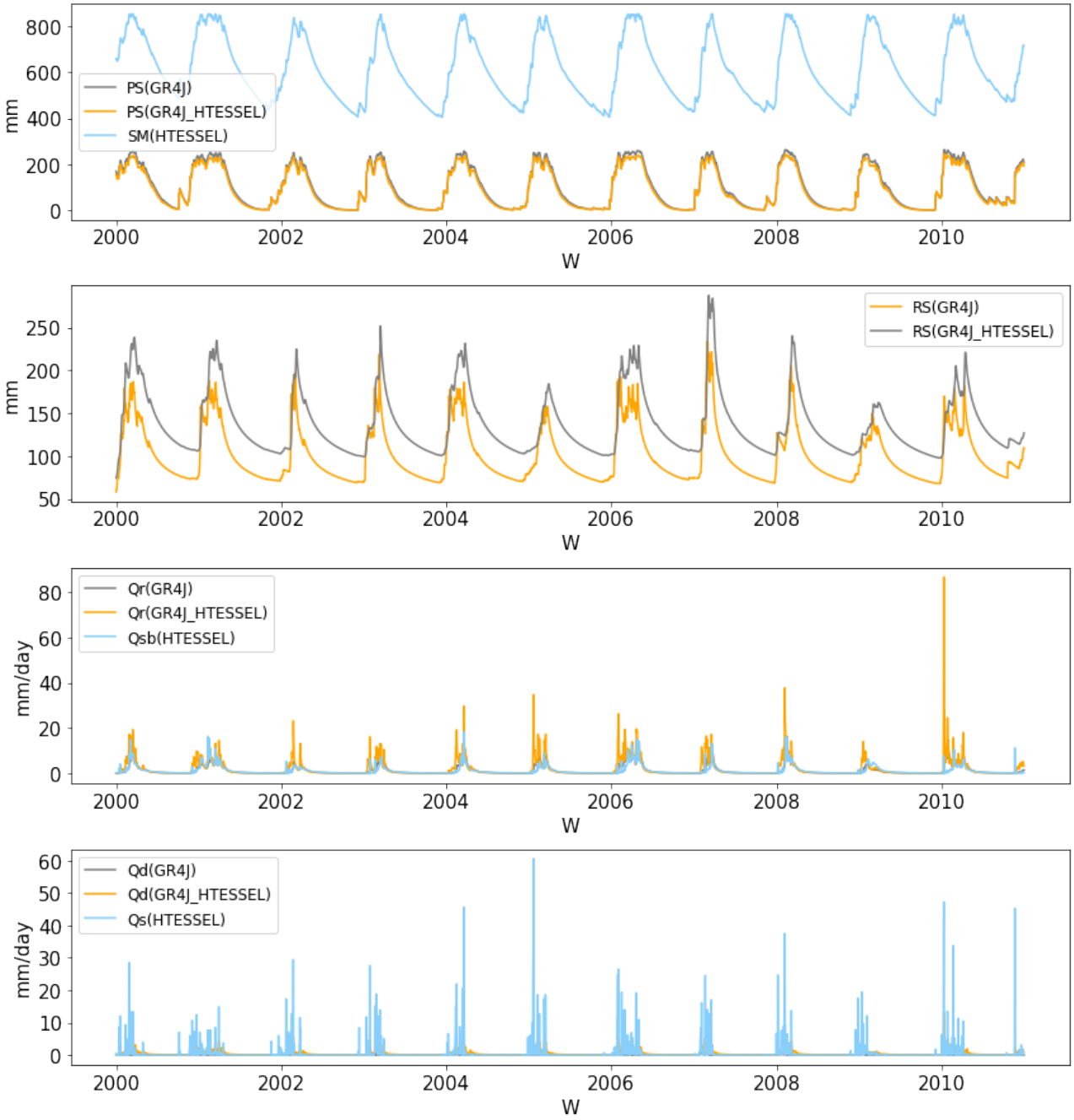
PS(GR4J)
PS(GR4J_HTESSEL)
SM(HTESSEL)
mm
W
RS(GR4J)
RS(GR4J_HTESSEL)
mm
W
Qr(GR4J)
Qr(GR4J_HTESSEL)
Qsb(HTESSEL)
mm/day
W
Qd(GR4J)
Qd(GR4J_HTESSEL)
Qs(HTESSEL)
mm/day
W

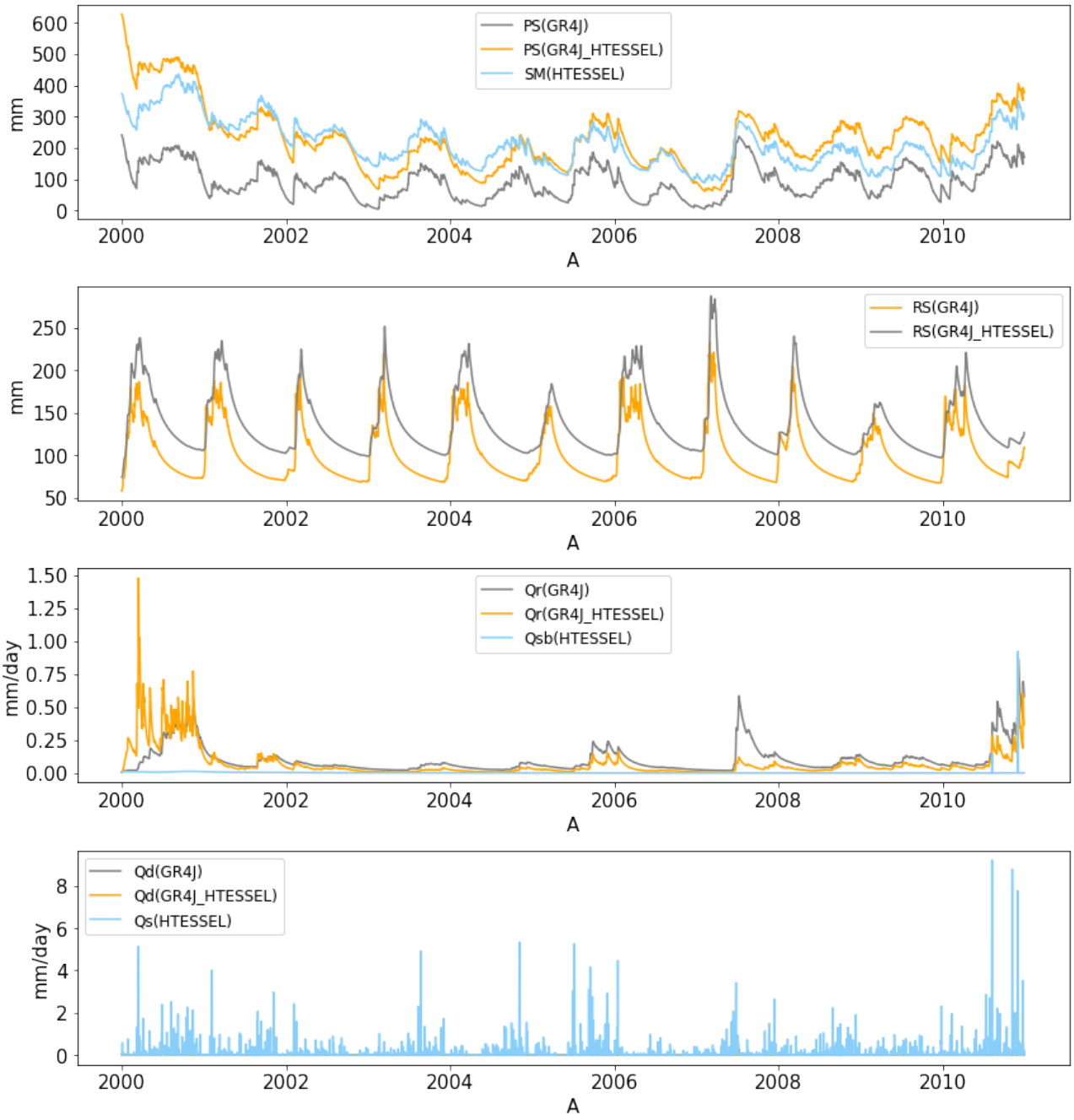
PS(GR4J)
PS(GR4J_HTESSEL)
SM(HTESSEL)
mm
A
RS(GR4J)
RS(GR4J_HTESSEL)
mm
A
Qr(GR4J)
Qr(GR4J_HTESSEL)
Qsb(HTESSEL)
mm/day
A
Qd(GR4J)
Qd(GR4J_HTESSEL)
Qs(HTESSEL)
mm/day
A

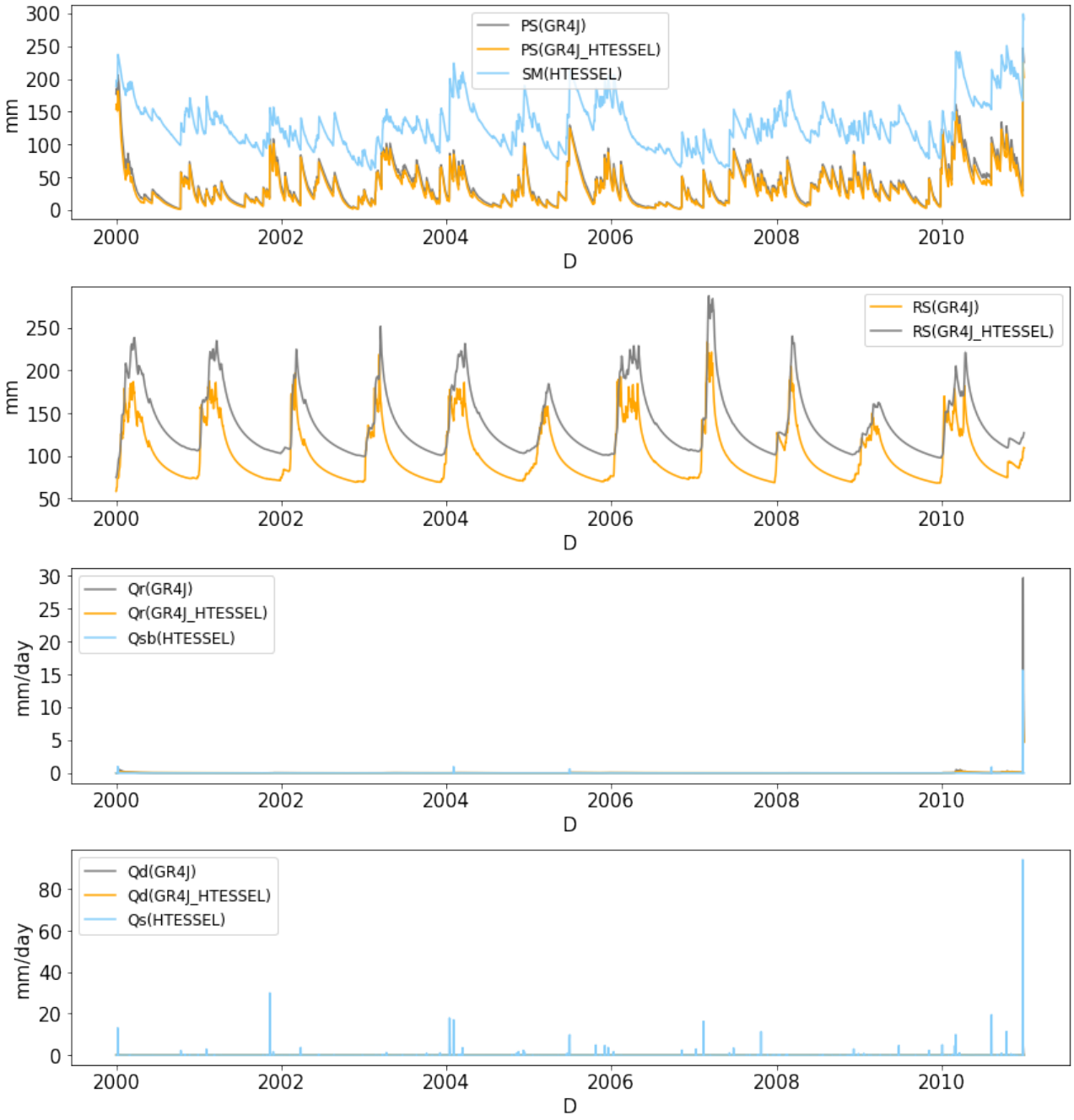
PS(GR4J)
PS(GR4J_HTESSEL)
SM(HTESSEL)
mm
D
RS(GR4J)
RS(GR4J_HTESSEL)
mm
D
Qr(GR4J)
Qr(GR4J_HTESSEL)
Qsb(HTESSEL)
mm/day
D
Qd(GR4J)
Qd(GR4J_HTESSEL)
Qs(HTESSEL)
mm/day
D

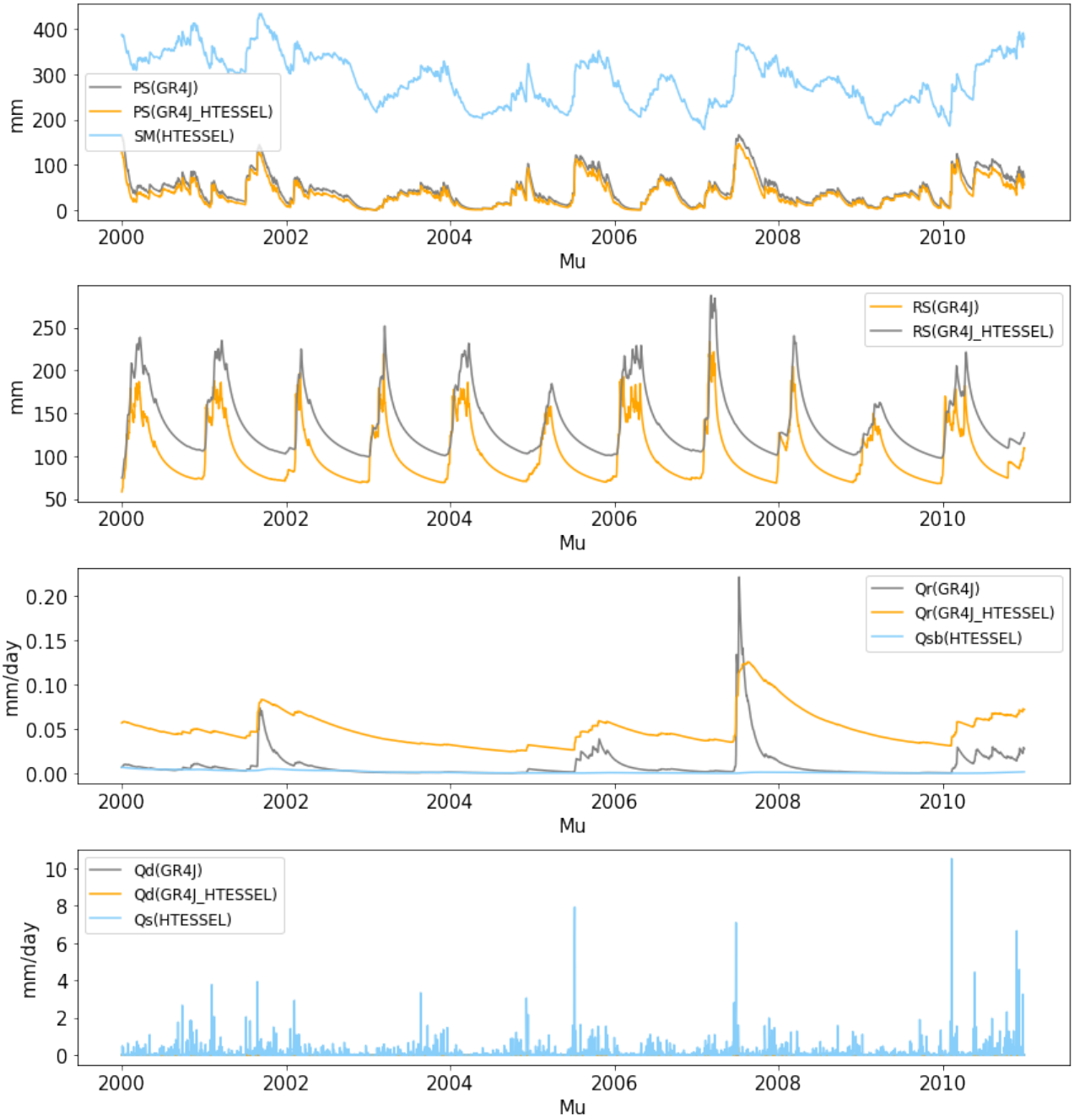
PS(GR4J)
PS(GR4J_HTESSEL)
SM(HTESSEL)
mm
Mu
RS(GR4J)
RS(GR4J_HTESSEL)
mm
Mu
Qr(GR4J)
Qr(GR4J_HTESSEL)
Qsb(HTESSEL)
mm/day
Mu
Qd(GR4J)
Qd(GR4J_HTESSEL)
Qs(HTESSEL)
mm/day
Mu

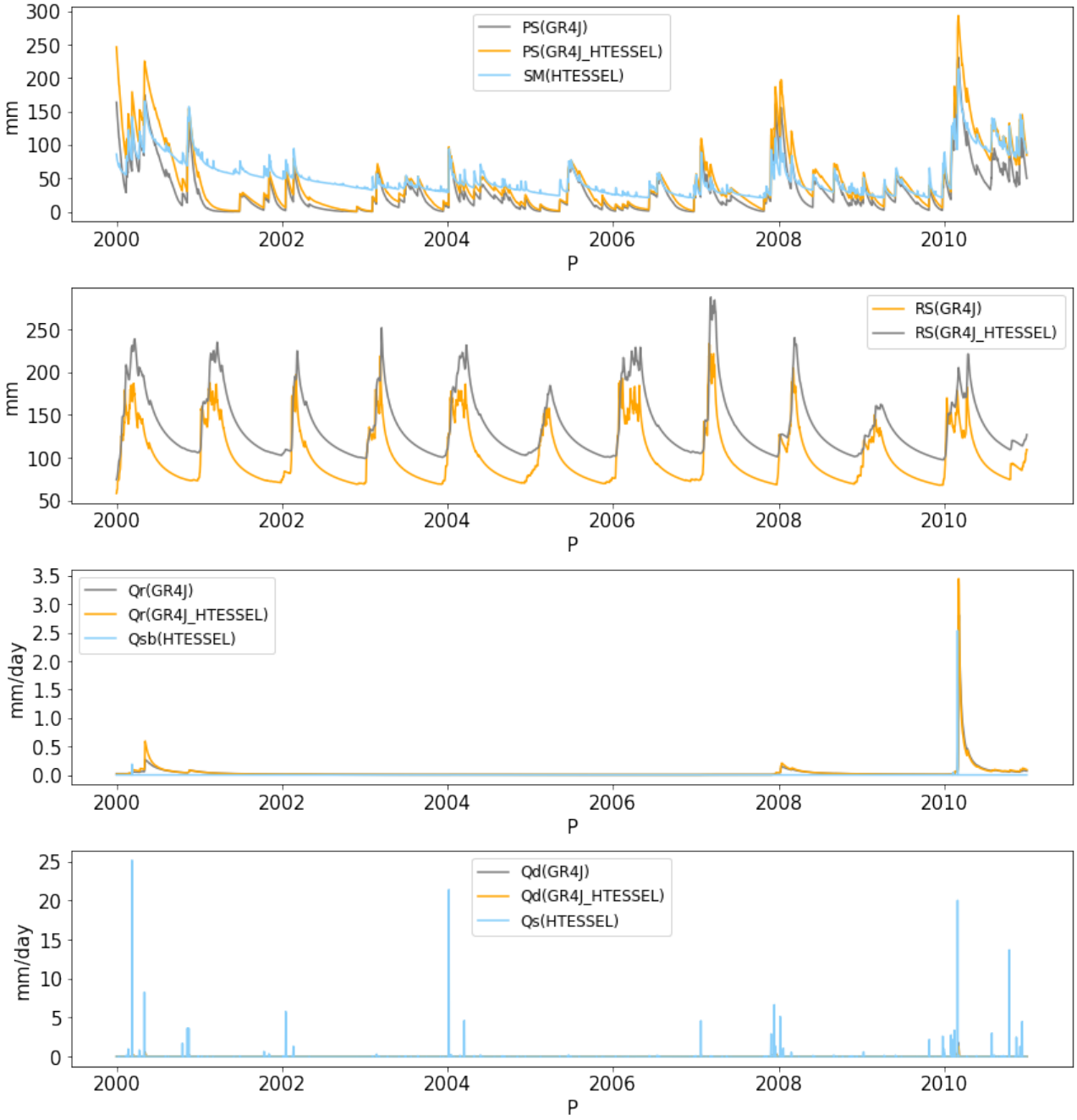
PS(GR4J)
PS(GR4J_HTESSEL)
SM(HTESSEL)
mm
P
RS(GR4J)
RS(GR4J_HTESSEL)
mm
P
Qr(GR4J)
Qr(GR4J_HTESSEL)
Qsb(HTESSEL)
mm/day
P
Qd(GR4J)
Qd(GR4J_HTESSEL)
Qs(HTESSEL)
mm/day
P

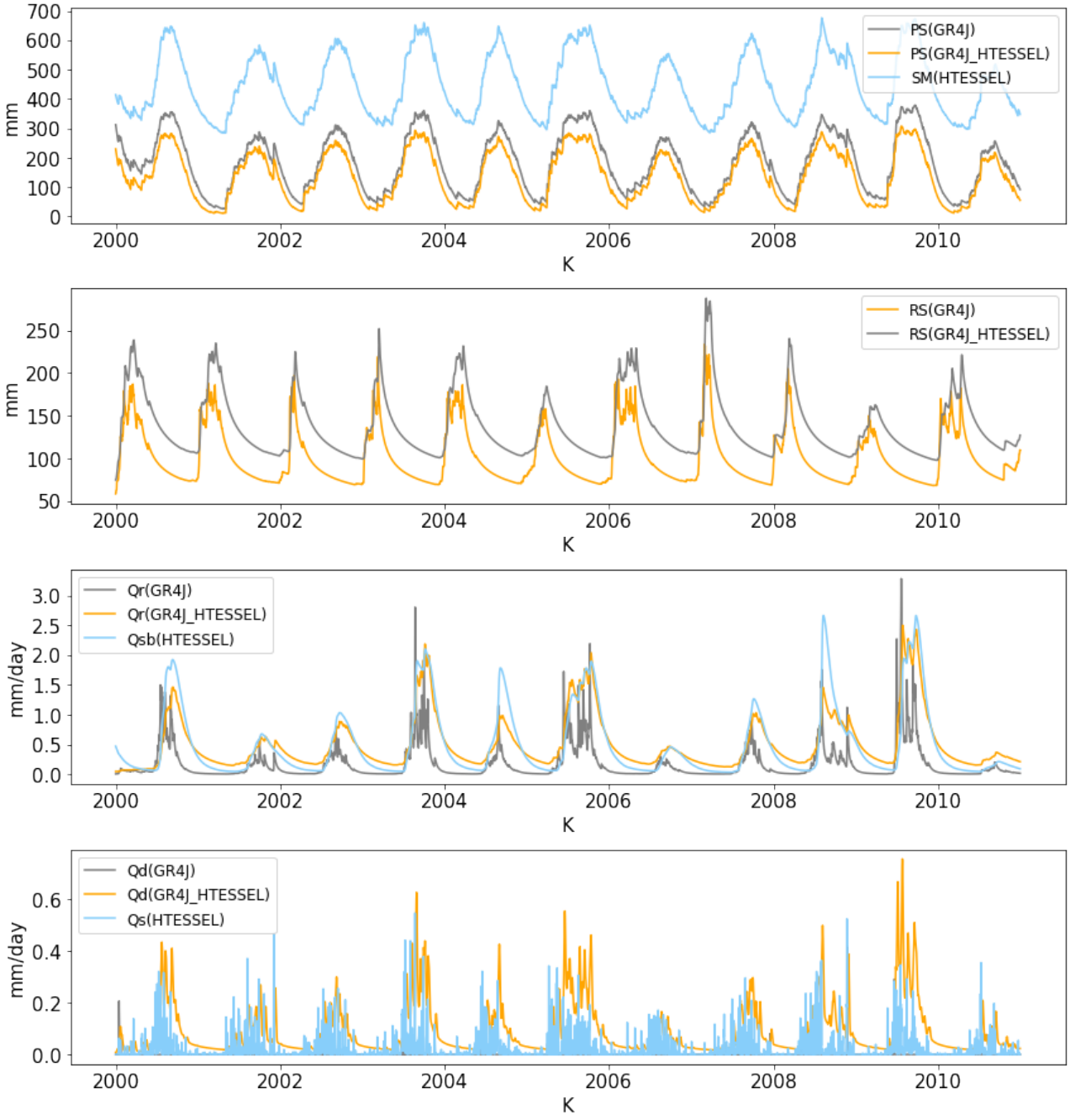
PS(GR4J)
PS(GR4J_HTESSEL)
SM(HTESSEL)
mm
K
RS(GR4J)
RS(GR4J_HTESSEL)
mm
K
Qr(GR4J)
Qr(GR4J_HTESSEL)
Qsb(HTESSEL)
mm/day
K
Qd(GR4J)
Qd(GR4J_HTESSEL)
Qs(HTESSEL)
mm/day
K

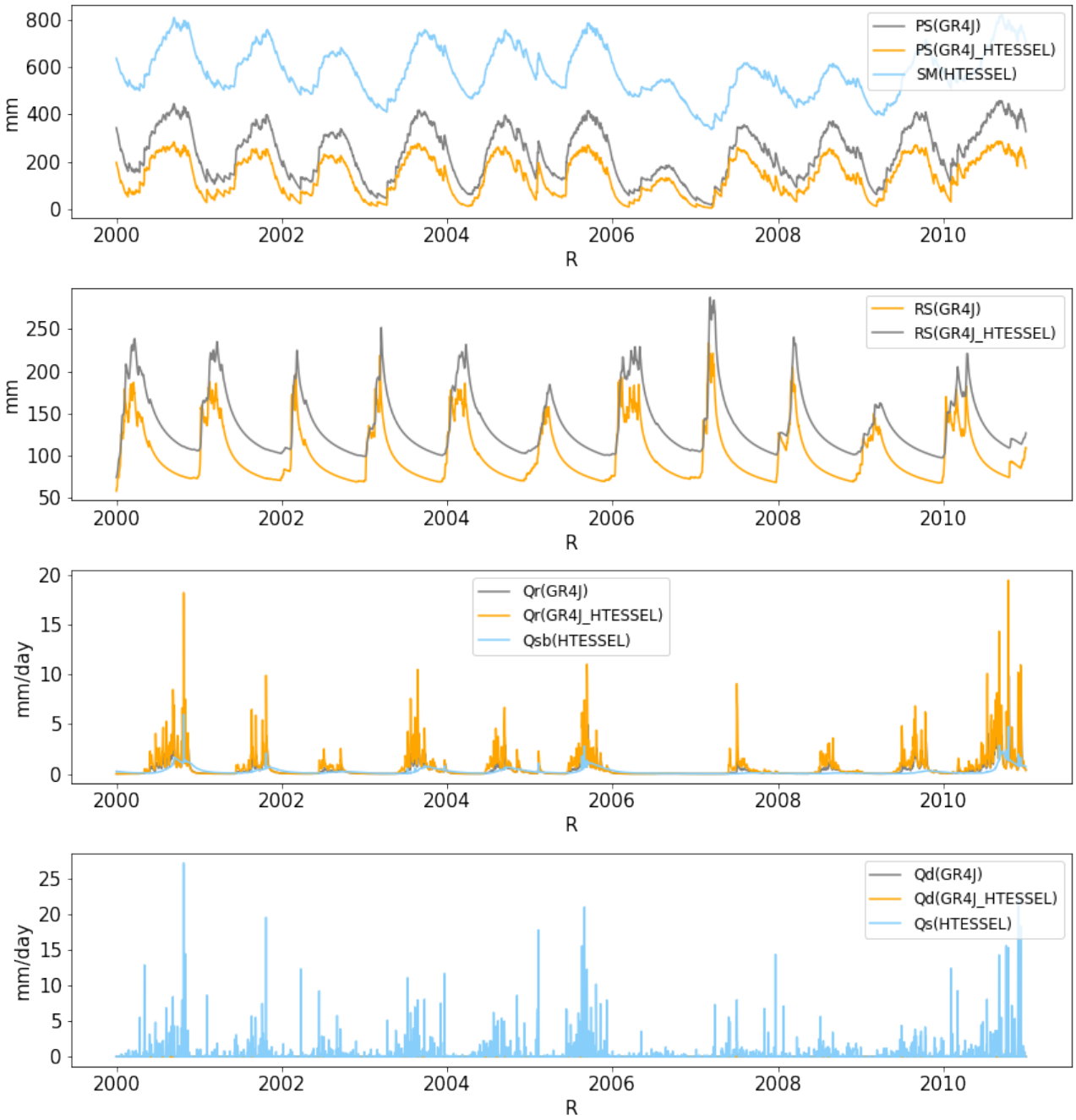
PS(GR4J)
PS(GR4J_HTESSEL)
SM(HTESSEL)
mm
R
RS(GR4J)
RS(GR4J_HTESSEL)
mm
R
Qr(GR4J)
Qr(GR4J_HTESSEL)
Qsb(HTESSEL)
mm/day
R
Qd(GR4J)
Qd(GR4J_HTESSEL)
Qs(HTESSEL)
mm/day
R

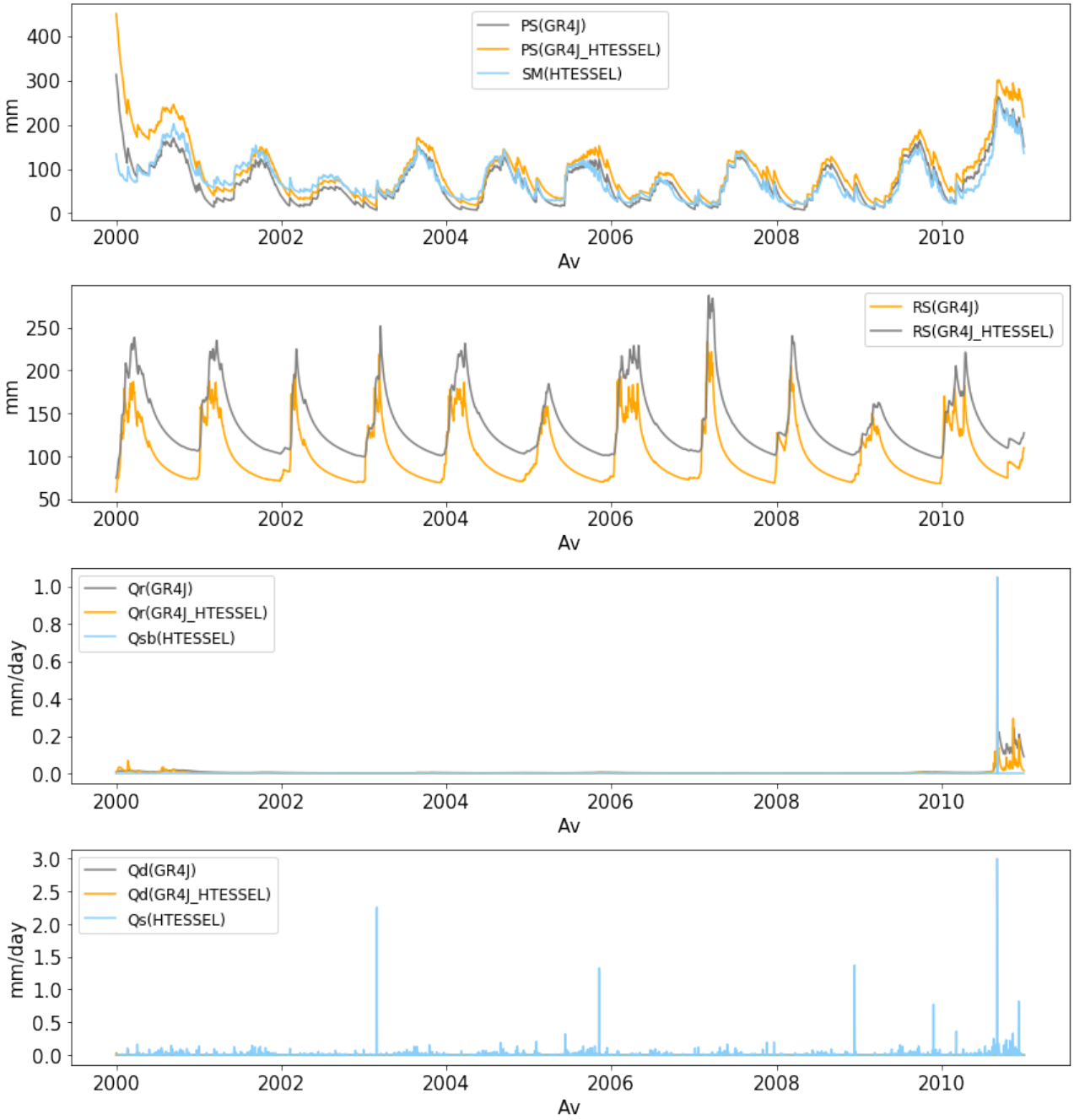
PS(GR4J)
PS(GR4J_HTESSEL)
SM(HTESSEL)
mm
Av
RS(GR4J)
RS(GR4J_HTESSEL)
mm
Av
Qr(GR4J)
Qr(GR4J_HTESSEL)
Qsb(HTESSEL)
mm/day
Av
Qd(GR4J)
Qd(GR4J_HTESSEL)
Qs(HTESSEL)
mm/day
Av

A.6 THE INTERNAL COMPONENTS OF HBV AND HTESSEL BEFORE AND AFTER CHANGE

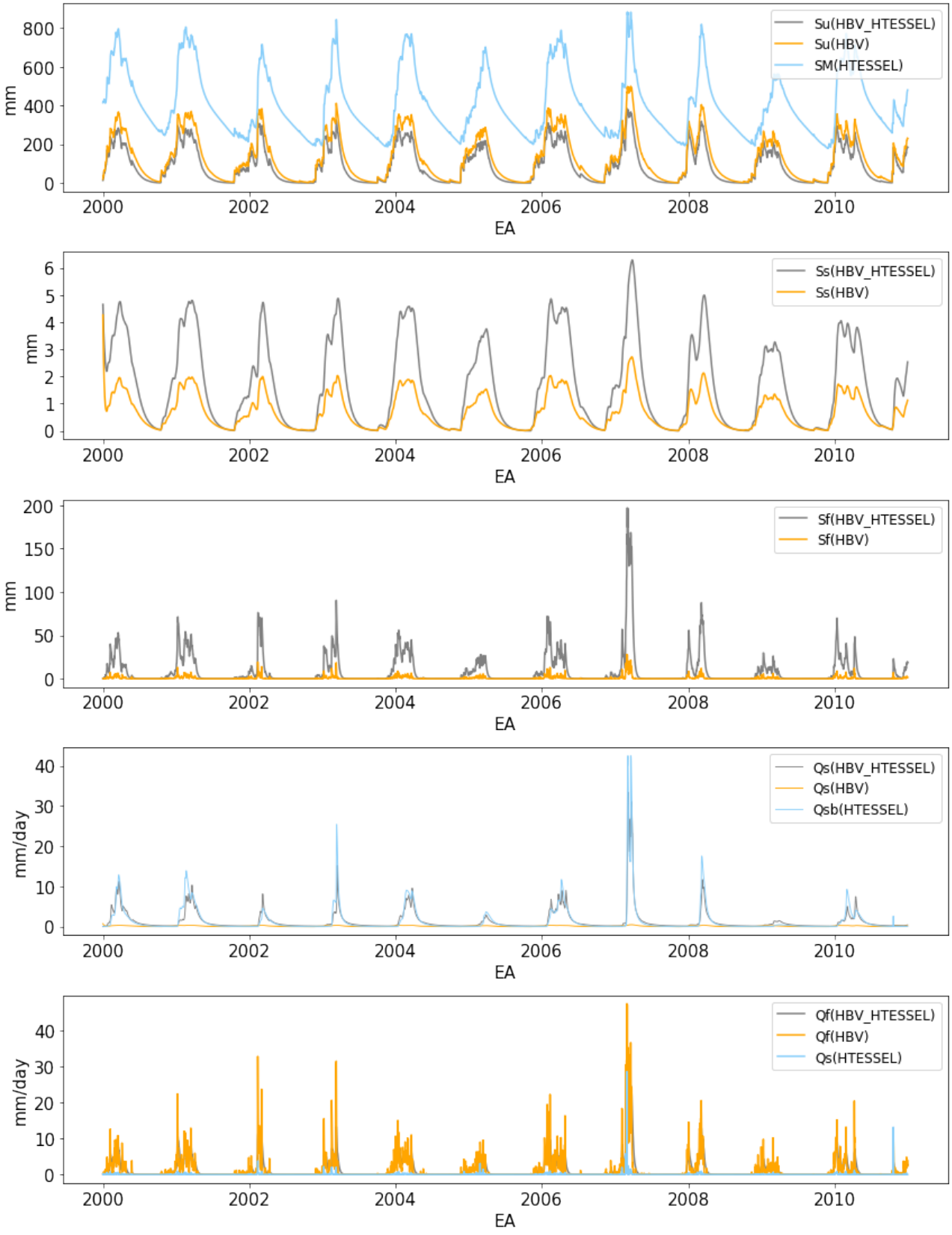

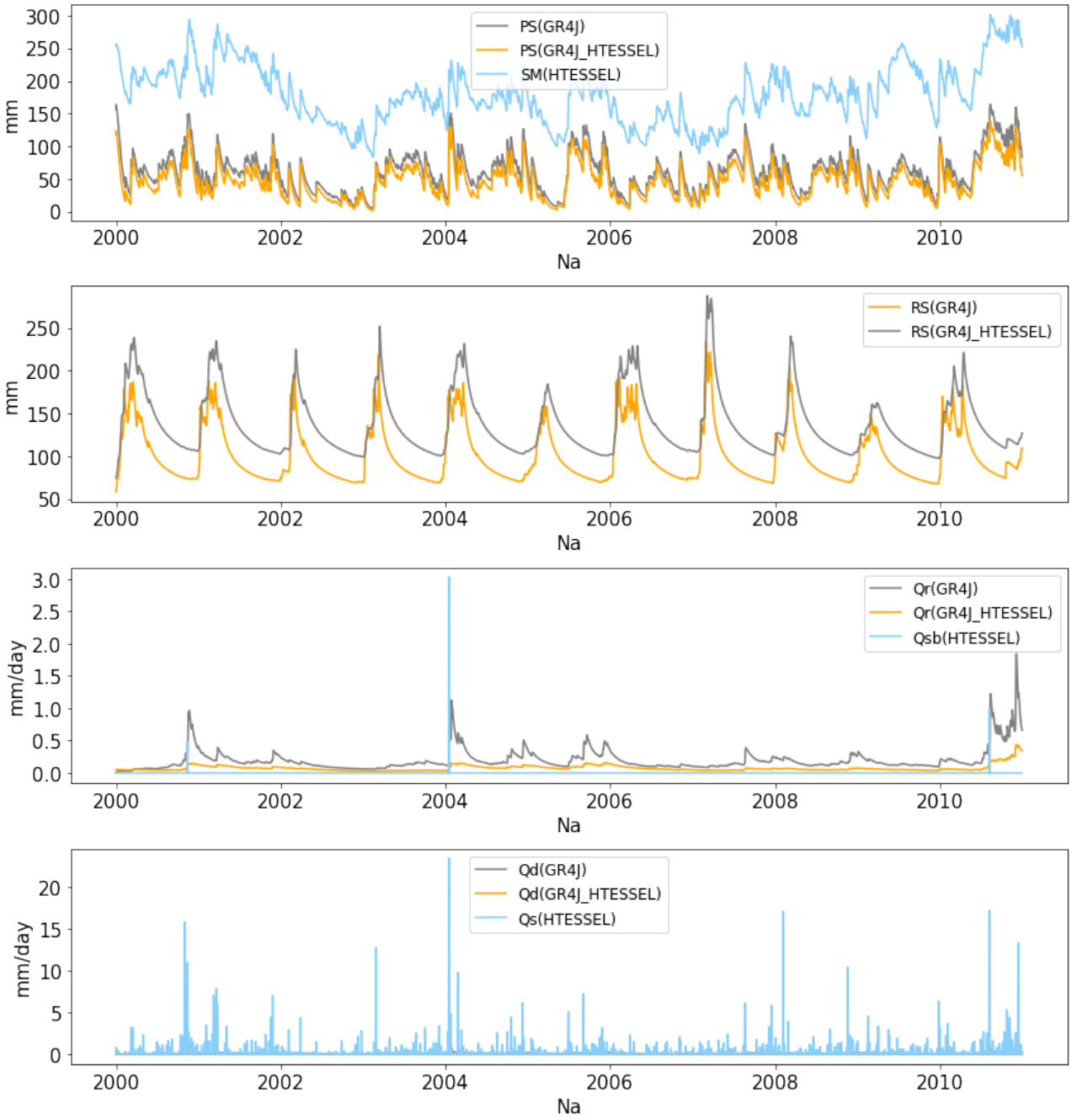
PS(GR4J)
PS(GR4J_HTESSEL)
SM(HTESSEL)
mm
Na
RS(GR4J)
RS(GR4J_HTESSEL)
mm
Na
Qr(GR4J)
Qr(GR4J_HTESSEL)
Qsb(HTESSEL)
mm/day
Na
Qd(GR4J)
Qd(GR4J_HTESSEL)
Qs(HTESSEL)
mm/day
Na

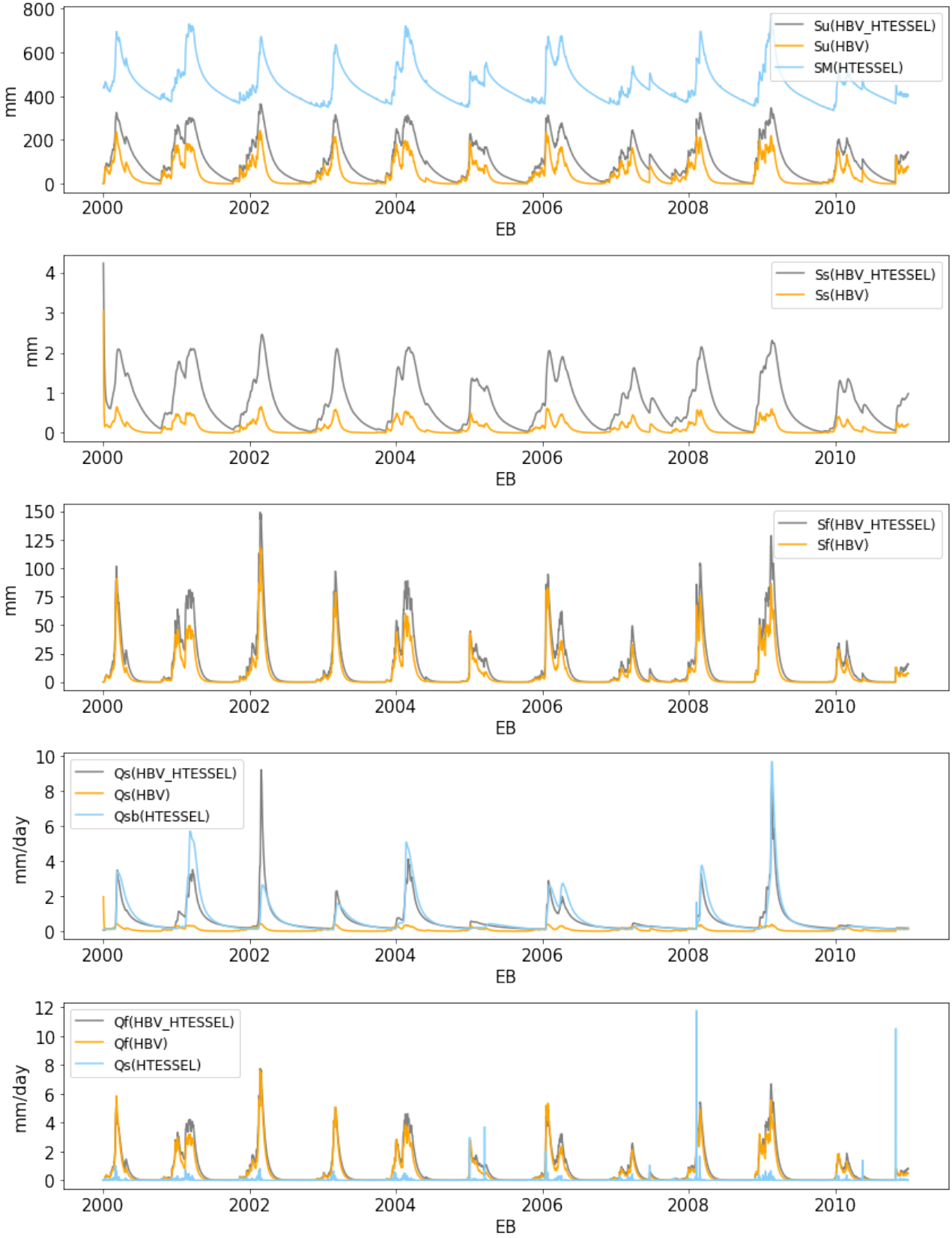
Su(HBV_HTESSEL)
Su(HBV)
SM(HTESSEL)
mm
EB
Ss(HBV_HTESSEL)
Ss(HBV)
mm
EB
Sf(HBV_HTESSEL)
Sf(HBV)
mm
EB
Qs(HBV_HTESSEL)
Qs(HBV)
Qsb(HTESSEL)
mm/day
EB
Qf(HBV_HTESSEL)
Qf(HBV)
Qs(HTESSEL)
mm/day
EB

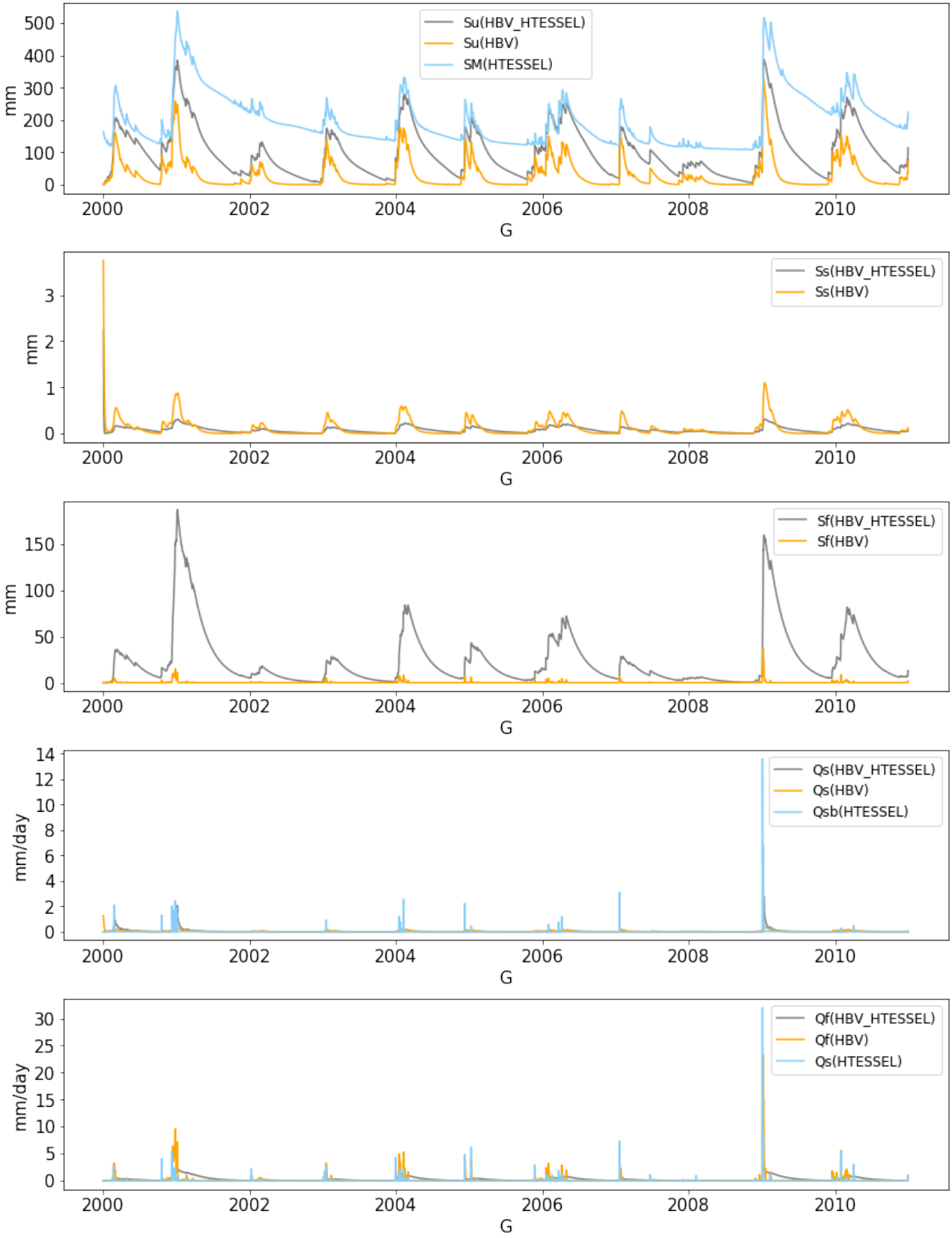
Su(HBV_HTESSEL)
Su(HBV)
SM(HTESSEL)
mm
G
Ss(HBV_HTESSEL)
Ss(HBV)
mm
G
Sf(HBV_HTESSEL)
Sf(HBV)
mm
G
Qs(HBV_HTESSEL)
Qs(HBV)
Qsb(HTESSEL)
mm/day
G
Qf(HBV_HTESSEL)
Qf(HBV)
Qs(HTESSEL)
mm/day
G

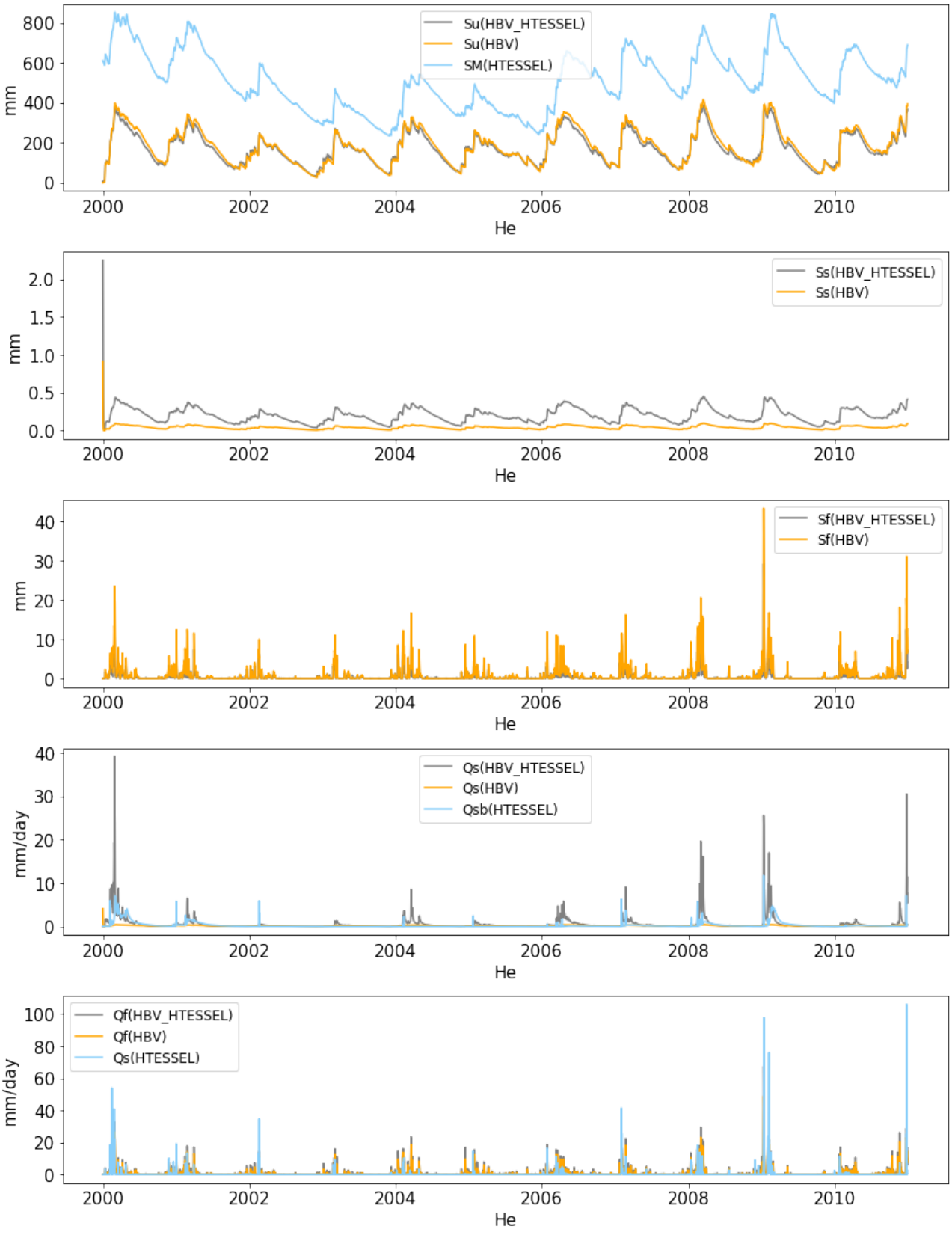
Su(HBV_HTESSEL)
Su(HBV)
SM(HTESSEL)
mm
He
Ss(HBV_HTESSEL)
Ss(HBV)
Sf(HBV_HTESSEL)
Sf(HBV)
Qs(HBV_HTESSEL)
Qs(HBV)
Qsb(HTESSEL)
mm/day
Qf(HBV_HTESSEL)
Qf(HBV)
Qs(HTESSEL)

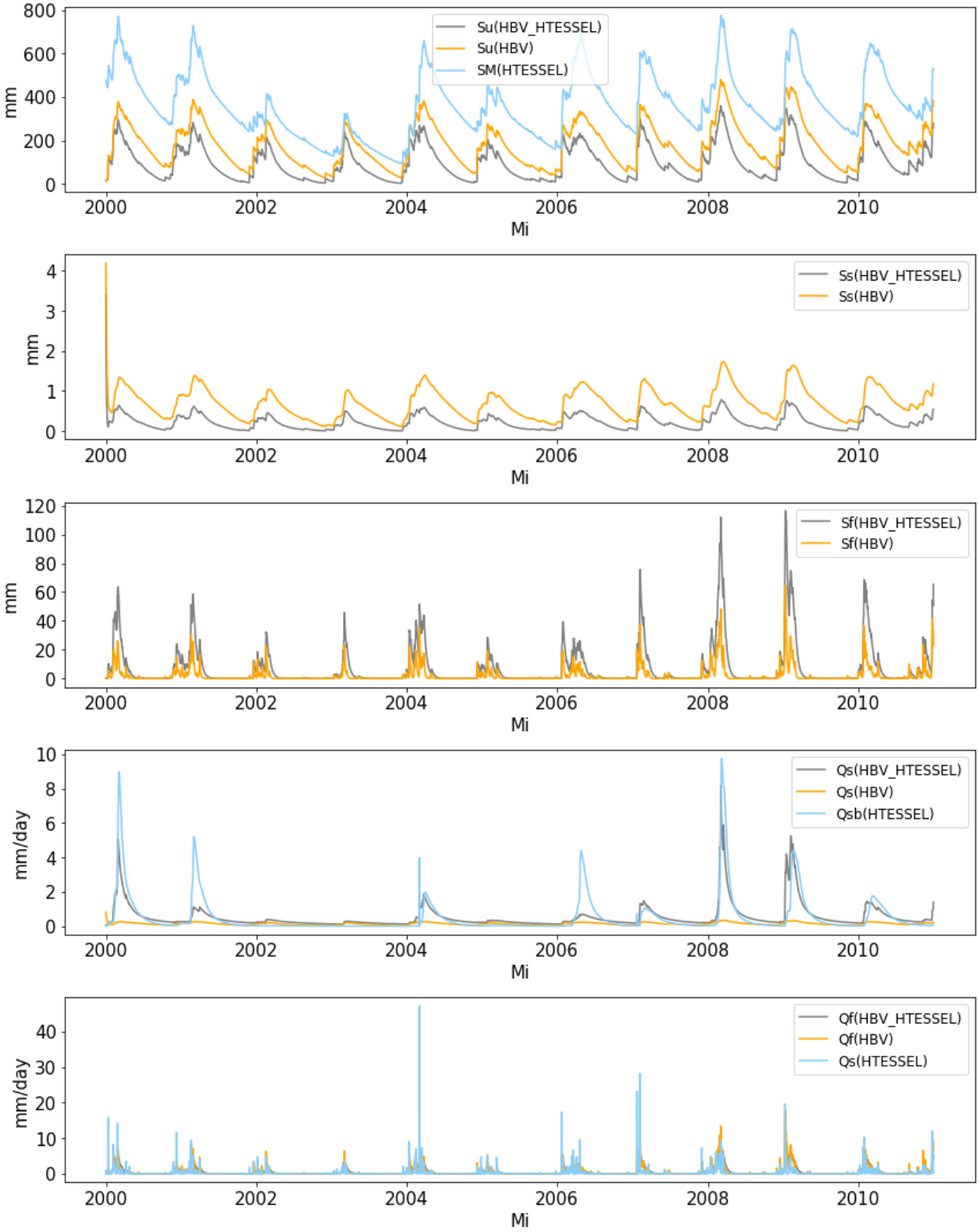
Su(HBV_HTESSEL)
Su(HBV)
SM(HTESSEL)
mm
Mi
Ss(HBV_HTESSEL)
Ss(HBV)
mm
Mi
Sf(HBV_HTESSEL)
Sf(HBV)
mm
Mi
Qs(HBV_HTESSEL)
Qs(HBV)
Qsb(HTESSEL)
mm/day
Mi
Qf(HBV_HTESSEL)
Qf(HBV)
Qs(HTESSEL)
mm/day
Mi

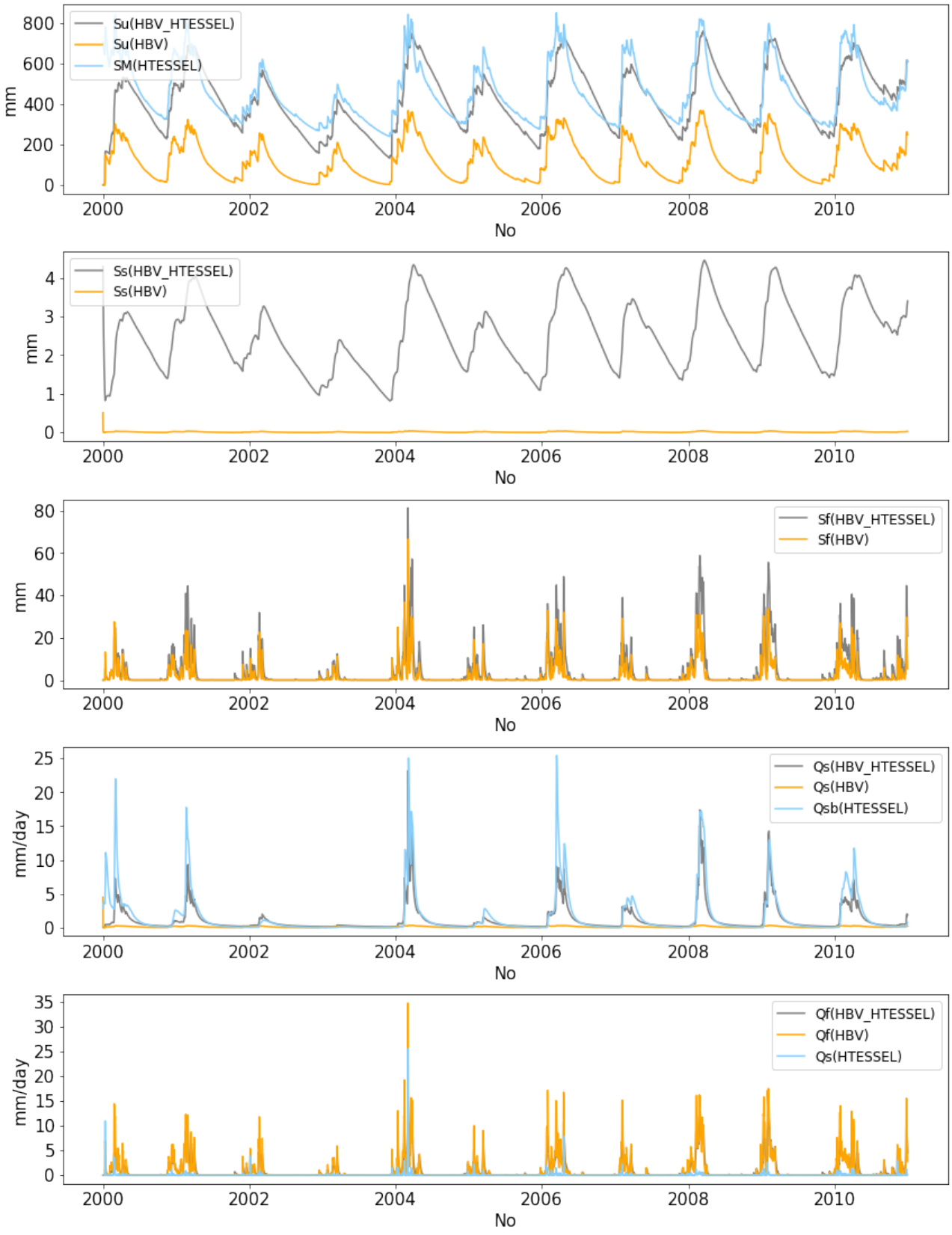
Su(HBV_HTESSEL)
Su(HBV)
SM(HTESSEL)
mm
No
Ss(HBV_HTESSEL)
Ss(HBV)
mm
No
Sf(HBV_HTESSEL)
Sf(HBV)
mm
No
Qs(HBV_HTESSEL)
Qs(HBV)
Qsb(HTESSEL)
mm/day
No
Qf(HBV_HTESSEL)
Qf(HBV)
Qs(HTESSEL)
mm/day
No

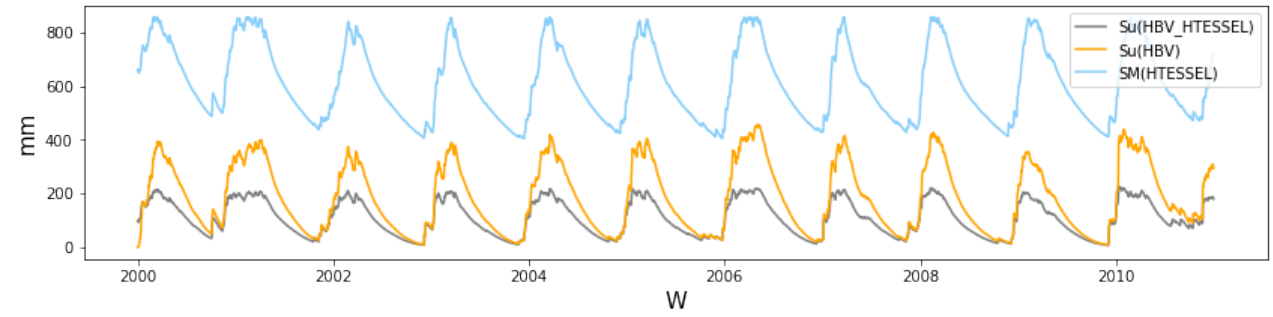
Su(HBV_HTESSEL)
Su(HBV)
SM(HTESSEL)
mm
W

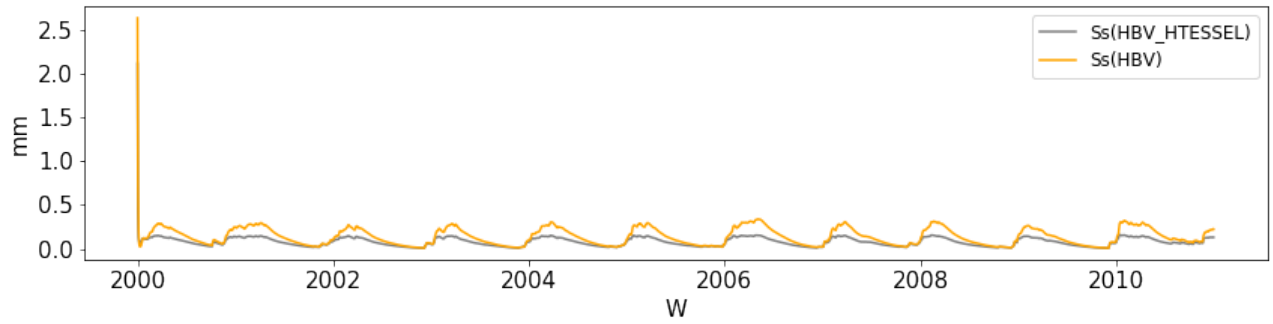
Ss(HBV_HTESSEL)
Ss(HBV)
mm
W

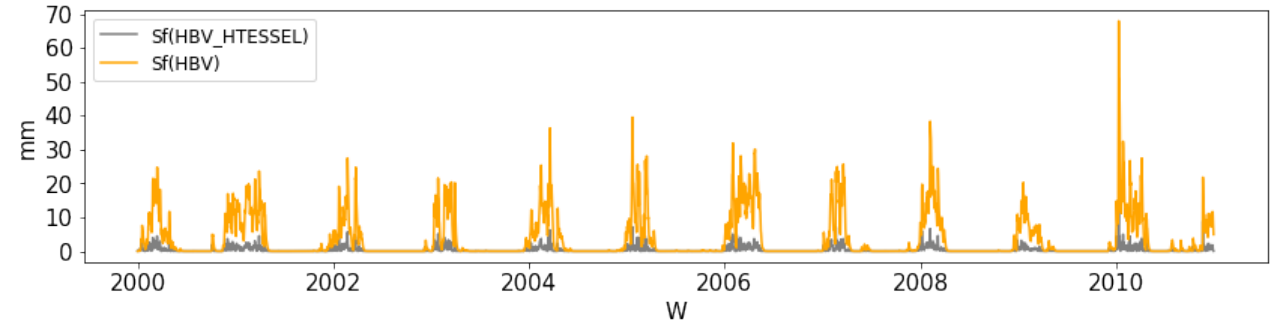
Sf(HBV_HTESSEL)
Sf(HBV)
mm
W

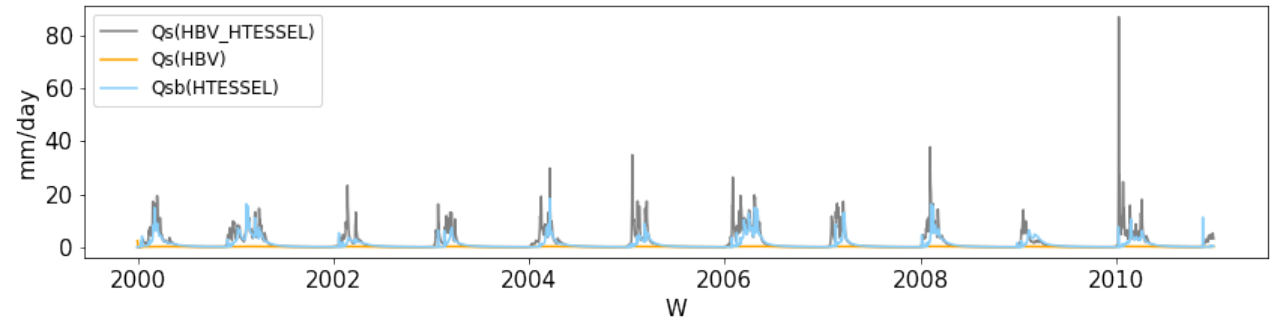
Qs(HBV_HTESSEL)
Qs(HBV)
Qsb(HTESSEL)
mm/day
W

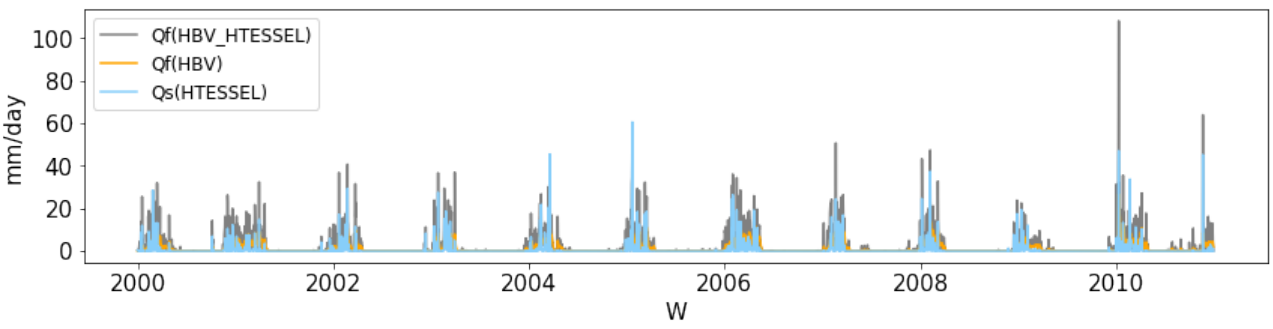
Qf(HBV_HTESSEL)
Qf(HBV)
Qs(HTESSEL)
mm/day
W


Su(HBV_HTESSEL)
Su(HBV)
SM(HTESSEL)
mm
A
Ss(HBV_HTESSEL)
Ss(HBV)
mm
A
Sf(HBV_HTESSEL)
Sf(HBV)
mm
A
Qs(HBV_HTESSEL)
Qs(HBV)
Qsb(HTESSEL)
mm/day
A
Qf(HBV_HTESSEL)
Qf(HBV)
Qs(HTESSEL)
mm/day
A

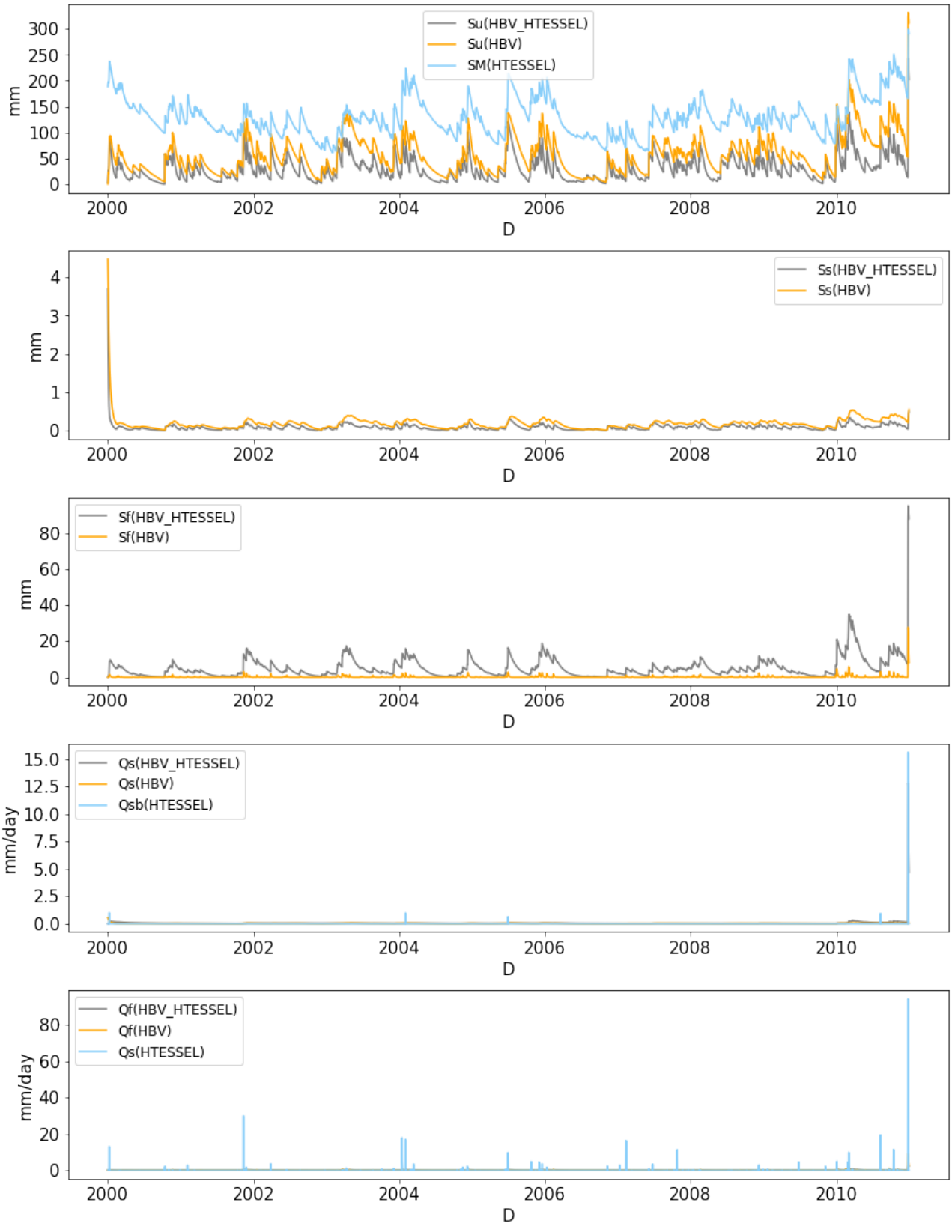
Su(HBV_HTESSEL)
Su(HBV)
SM(HTESSEL)
mm
D
Ss(HBV_HTESSEL)
Ss(HBV)
mm
D
Sf(HBV_HTESSEL)
Sf(HBV)
mm
D
Qs(HBV_HTESSEL)
Qs(HBV)
Qsb(HTESSEL)
mm/day
D
Qf(HBV_HTESSEL)
Qf(HBV)
Qs(HTESSEL)
mm/day
D

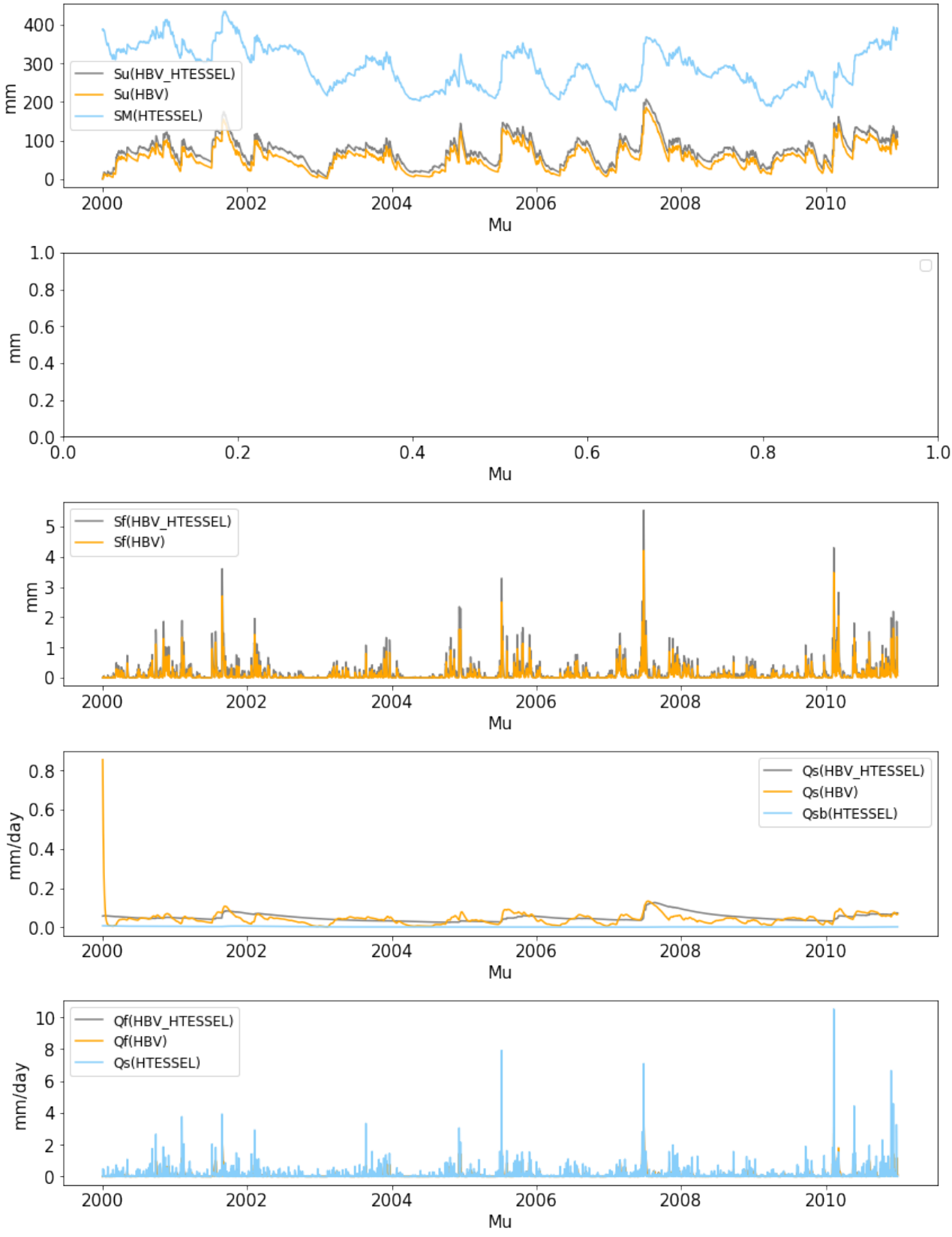
Su(HBV_HTESSEL)
Su(HBV)
SM(HTESSEL)
mm
Mu
Sf(HBV_HTESSEL)
Sf(HBV)
Qs(HBV_HTESSEL)
Qs(HBV)
Qsb(HTESSEL)
mm/day
Qf(HBV_HTESSEL)
Qf(HBV)
Qs(HTESSEL)

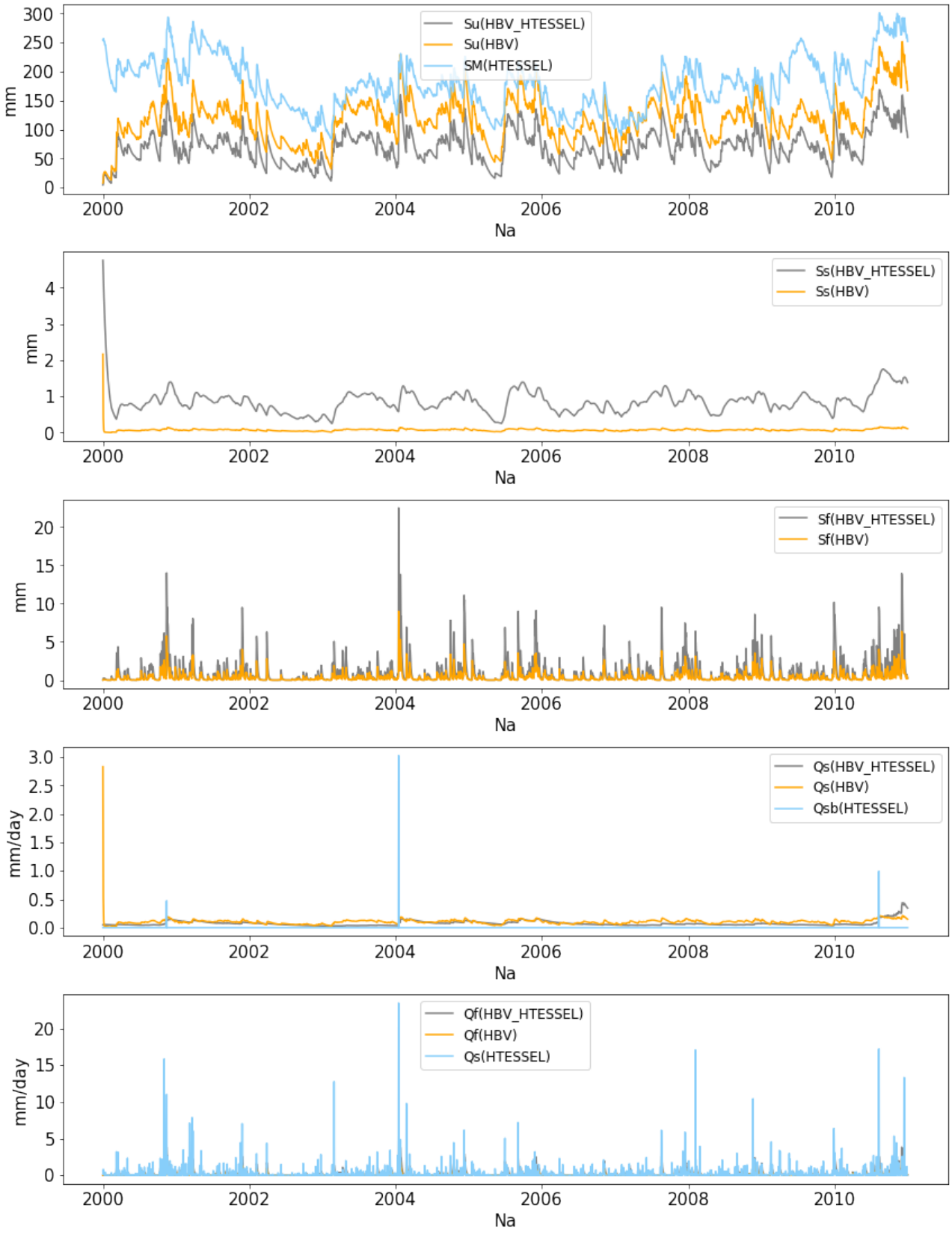
Su(HBV_HTESSEL)
Su(HBV)
SM(HTESSEL)
mm
Na
Ss(HBV_HTESSEL)
Ss(HBV)
mm
Na
Sf(HBV_HTESSEL)
Sf(HBV)
mm
Na
Qs(HBV_HTESSEL)
Qs(HBV)
Qsb(HTESSEL)
mm/day
Na
Qf(HBV_HTESSEL)
Qf(HBV)
Qs(HTESSEL)
mm/day
Na

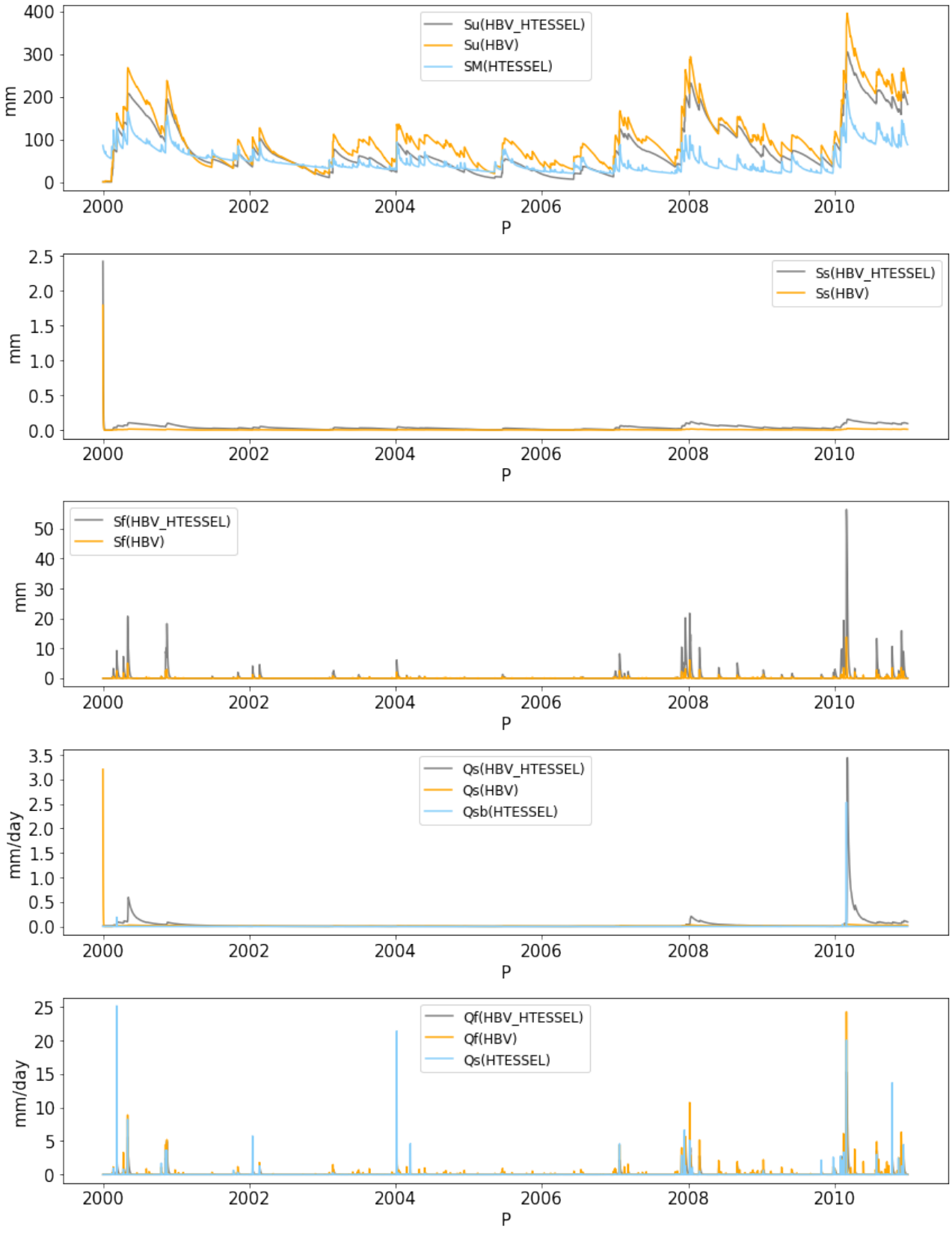
Su(HBV_HTESSEL)
Su(HBV)
SM(HTESSEL)
mm
P
Ss(HBV_HTESSEL)
Ss(HBV)
mm
P
Sf(HBV_HTESSEL)
Sf(HBV)
mm
P
Qs(HBV_HTESSEL)
Qs(HBV)
Qsb(HTESSEL)
mm/day
P
Qf(HBV_HTESSEL)
Qf(HBV)
Qs(HTESSEL)
mm/day
P

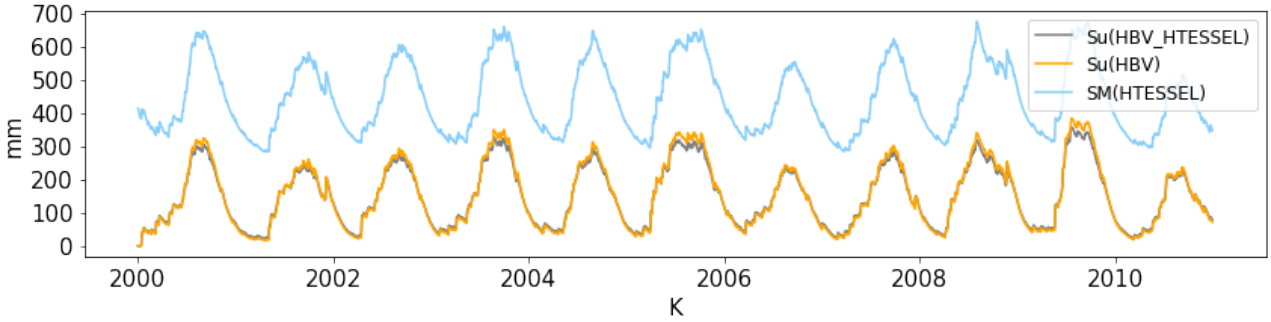
Su(HBV_HTESSEL)
Su(HBV)
SM(HTESSEL)
mm
K

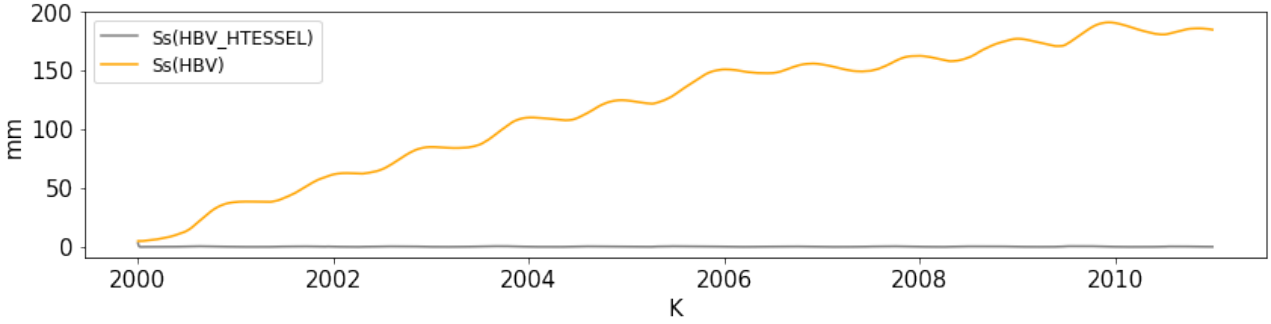
Ss(HBV_HTESSEL)
Ss(HBV)
mm
K

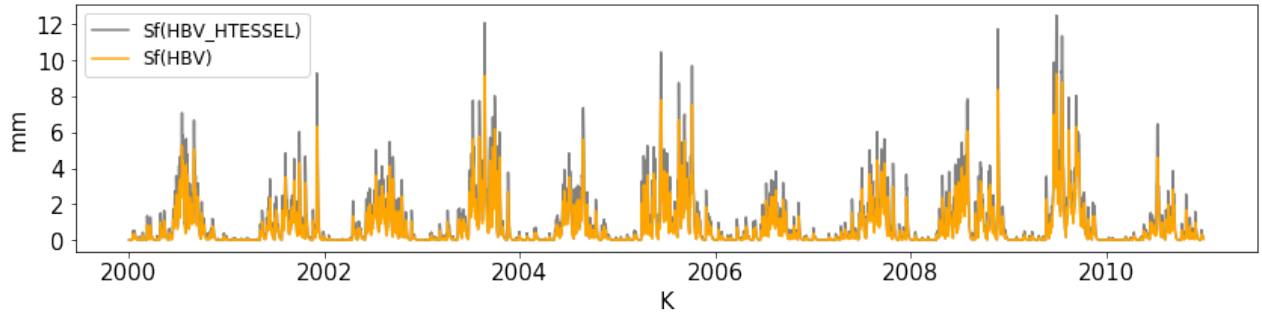
Sf(HBV_HTESSEL)
Sf(HBV)
mm
K

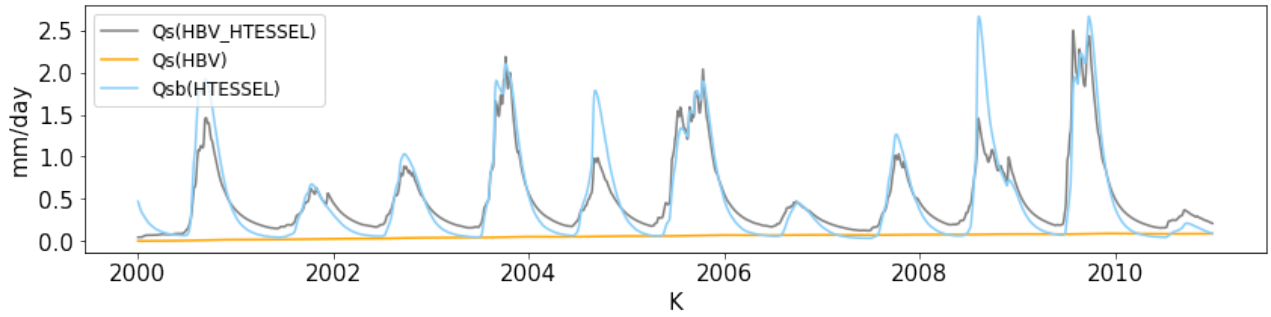
Qs(HBV_HTESSEL)
Qs(HBV)
Qsb(HTESSEL)
mm/day
K

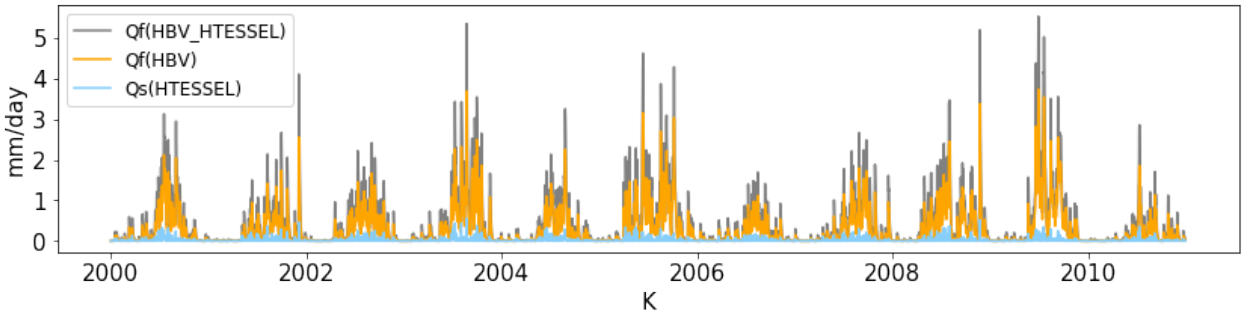
Qf(HBV_HTESSEL)
Qf(HBV)
Qs(HTESSEL)
mm/day
K

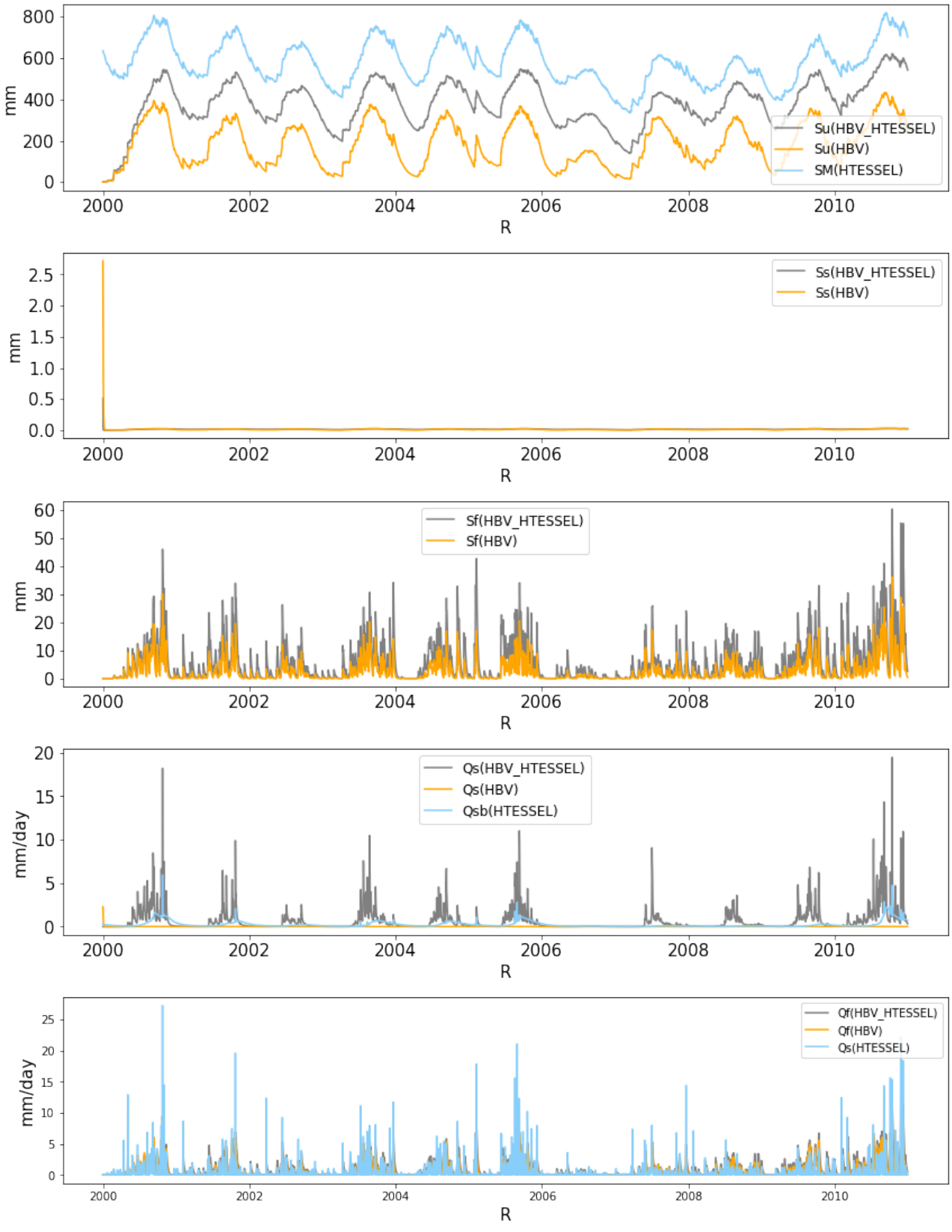
mm
R
Su(HBV_HTESSEL)
Su(HBV)
SM(HTESSEL)
Ss(HBV_HTESSEL)
Ss(HBV)
Sf(HBV_HTESSEL)
Sf(HBV)
mm/day
Qs(HBV_HTESSEL)
Qs(HBV)
Qsb(HTESSEL)
Qf(HBV_HTESSEL)
Qf(HBV)
Qs(HTESSEL)

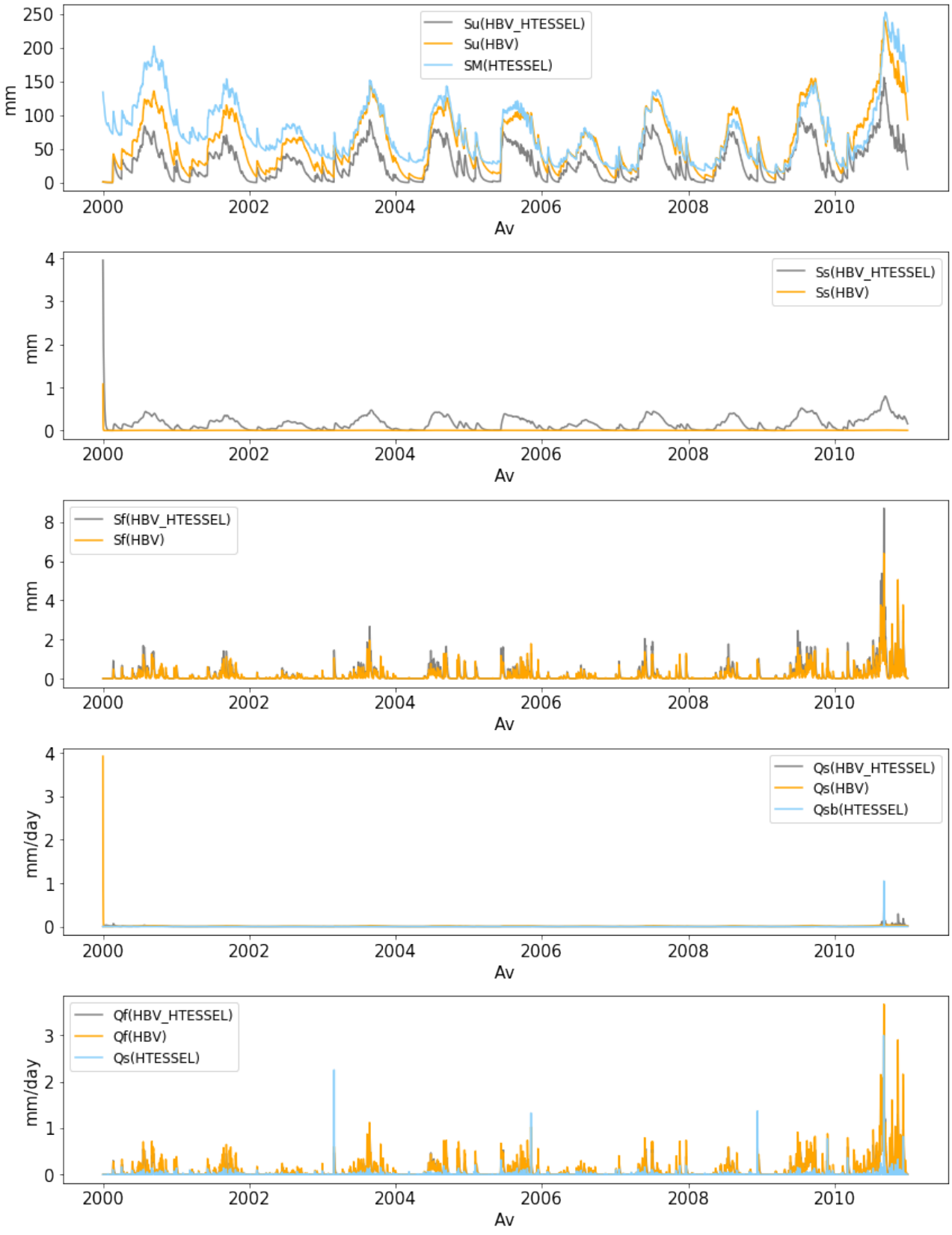
Su(HBV_HTESSEL)
Su(HBV)
SM(HTESSEL)
mm
Av
Ss(HBV_HTESSEL)
Ss(HBV)
mm
Av
Sf(HBV_HTESSEL)
Sf(HBV)
mm
Av
Qs(HBV_HTESSEL)
Qs(HBV)
Qsb(HTESSEL)
mm/day
Av
Qf(HBV_HTESSEL)
Qf(HBV)
Qs(HTESSEL)
mm/day
Av